Dissertation

submitted to the

Combined Faculties for the Natural Sciences and for Mathematics

of the Ruperto-Carola University of Heidelberg, Germany

for the degree of

Doctor of Natural Sciences

presented by

Diplom: Nidhi Gakhar

Born in New Delhi, India

Oral-examination: 15th December 2006

Regulation of neuronal differentiation by activity-induced calcium influx in striatal neural precursors

Referees:

Prof. Dr. Hilmar Bading

Prof. Dr. Klaus Unsicker

Table of Contents

List of Figures

List of Tables

Summary

Neuronal activity induces Ca^{2+} influx that regulates neurogenesis and distinct aspects of neuronal differentiation in the embryonic and adult brain. This thesis focusses on the regulation of neuronal differentiation in striatal neural precursors (NPCs) by activity-induced Ca^{2+} influx. Neurons arising from differentiating striatal NPCs show spontaneous Ca^{2+} transients, which are L-type VGCC-dependent. Neural activity increases the frequency of L-type VGCC-dependent Ca^{2+} transients. It also accelerates neuronal differentiation of striatal NPC-derived neurons by promoting GABA expression and neurite outgrowth that are essential steps in establishing neuronal identity and enabling neurons to form functional connections. Although excitatory activity activates CREB, its effects on neuronal differentiation are transcription and translation independent. Furthermore, regulation of GABA expression and neurite outgrowth by neural activity involve distinct signaling pathways. Neurite outgrowth is regulated by NMDAR-mediated localized Ca^{2+} influx that activates MAPK/CaMK and release of sAPP. On the other hand, GABA expression is regulated by PKA and PKC that are activated by VGCC-induced global rise in Ca^{2+}. Interestingly, a brief Ca^{2+} influx through VGCCs, induced by a short depolarizing stimuli, is sufficient to trigger an increase in GABA expression, whereas changes in neurite outgrowth require longer exposure to depolarization. Furthermore, neural activity accelerates GABA expression in neurons restricted to GABAergic fate, suggesting that these neurons express GABA synthesizing enzyme, GAD. Thus, it is conceivable that regulation of GABA expression by VGCC-induced Ca^{2} influx is achieved via phosphorylation/dephosphorylation of GAD by PKA and PKC. Thus, neural activity modulates NPC differentiation by inducing rapid responses

that are transcription independent and that may be important in timely functional integration of newly generated neurons in the mammalian brain.

Zusammenfassung

Die Regulation von Neurogenese und verschiedener neuraler Differenzierungsvorgänge im embryonalen und adulten Gehirn erfolgt durch den Einstrom von Kalziumionen, welcher durch neuronale Aktivitäten induziert wird. Gegenstand der vorliegenden Arbeit ist die Regulation der Differenzierung neuraler Vorläuferzellen (neural precursor cells, NPCs) des Striatums durch aktivitätsinduzierten Ca^{2+} Einstrom. NPCs des Striatums differenzieren zu Neuronen, welche spontane Ca^{2+} Signale aufzeigen. Diese Signale werden durch spannungsabhängige Kalziumkanäle (voltage gated calcium channels, VGCC) des L-Typs vermittelt, wobei die Frequenz der Ca^{2+}-Signale durch neurale Aktivität verstärkt wird. Diese verstärkt auch die neuronale Differenzierung durch Ausbildung von Neuriten und Expression von GABA, welche essentielle Schritte der Etablierung neuronaler Identität darstellen und Nervenzellen befähigen, funktionelle Verbindungen herzustellen.

Obwohl durch ekzitatorische Aktivitäten CREB (cAMP response element binding protein) aktiviert wird, ist der Einfluss auf neurale Differenzierung transkriptions- und translationsunabhängig. Darüber hinaus sind verschiedene Signaltransduktionskaskaden an der Regulation der Expression von GABA und der Ausbildung von Neuriten durch neurale Aktivität beteiligt. Dabei wird die Neuritenbildung durch NMDA-vermittelten Ca^{2+} Einstrom reguliert, welcher MAPK/CaMK aktiviert und sAPP freisetzt. Die Expression von GABA wird durch PKA und PKC, welche durch einen VGCC-induzierten allgemeinen Anstieg der Ca^{2+} Konzentration aktiviert werden, reguliert. Interessanterweise ist

ein durch kurze Depolarisierungsstimuli induzierter Einstrom von Ca^{2+} durch VGCCs ausreichend, um einen Anstieg der Expressionsrate von GABA hervorzurufen. Im Gegensatz dazu bedürfen Veränderungen des Neuritenwachstums längerer Depolarisationen.

Des Weiteren wird durch neurale Aktivitäten die Expression von GABA in GABAergen Neuronen verstärkt, was zu der Vermutung führt, das diese Neuronen das GABA-synthetisierende Enzym GAD exprimieren. Daher ist es vorstellbar, dass die Expression von GABA durch VGCC-vermittelten Ca^{2+} Einstrom durch eine Phosphorylierung/Dephosphorylierung von GAD durch PKA und PKC reguliert wird. Die Differenzierung von NPCs wird daher durch neurale Aktivitäten mittels Induktion schneller, transkriptionsunabhängiger Reaktionen gesteuert. Dieser Vorgang ist höchstwahrscheinlich entscheidend für die rechtzeitige Integration neuer Neuronen im Säugetiergehirn.

Articles from this PhD thesis

Transcription independent regulation of GABA expression by excitation-induced Ca^{2+} influx in striatal neural precursor-derived neurons.
Nidhi Gakhar, C. Peter Bengtson, Rosanna Parlato, Günther Schütz, and Francesca Ciccolini. To be submitted to: The Journal of Neuroscience.

Chapter 1 : Introduction

1.1: Ca^{2+} influx: the versatile messenger

Ca^{2+} is one of the most ubiquitous and versatile signaling messengers. Ca^{2+} homeostasis in different cell types of the body is maintained by the combined action of Ca^{2+} channels that allow influx of Ca^{2+}, Ca^{2+} binding proteins that buffer Ca^{2+} and Ca^{2+} pumps that remove Ca^{2+} from the cytoplasm by pumping it into the extracellular space or internal Ca^{2+} stores against a concentration gradient (Berridge MJ 2003). Ca^{2+} enters the cell in response to stimuli such as depolarization, stretch, extracellular agonists, intracellular messengers etc. via plasma membrane (PM) Ca^{2+} channels (discussed in section 1.1.1) (Berridge MJ 2003). Alternatively, secondary messengers such as inositol-1, 4, 5-triphosphate (Ins (1, 4, 5) P_3) generated in response to phospholipase C activation induce release of Ca^{2+} from internal stores of endoplasmic/sarcoplasmic reticulum, ER/SR through channels within the Ins (1, 4, 5) P_3R complex (Berridge MJ 2003) (Fig 1.1). Ca^{2+} entering through PM channels may also bind ryanodine receptors (RYRs) located on the ER/SR membrane and induce release of Ca^{2+} from the ER/SR internal stores, a phenomena referred to as Ca^{2+}-induced-Ca^{2+} release (Berridge MJ 2003). Elevation of Ca^{2+} lasts only briefly and acts as an intracellular signal that activates downstream signaling pathways controlling various intracellular and physiological processes such as fertilization, muscle contraction, cell proliferation and migration (Berridge MJ 1998; Berridge MJ 2003; Lledo PM 2006) (Fig 1.1). Most of the Ca^{2+} binds to buffers in the cytoplasm and only a small proportion binds to signaling molecules (effectors) (Fig 1.1). Intracellular Ca^{2+} concentration is brought to resting levels (30 to 200 nM) by the action of ATP dependent Ca^{2+} pump (PM Ca^{2+} ATP-ase, PMCA), a Na^{+}-Ca^{2+} exchanger (NCX) present in the PM, ATP-dependent Ca^{2+} pumps of

the ER (sarcoplasmic and endoplasmic reticulum ATP-ase, SERCA) and the mitochondria Ca^{2+} exchanger (Fig 1.1).

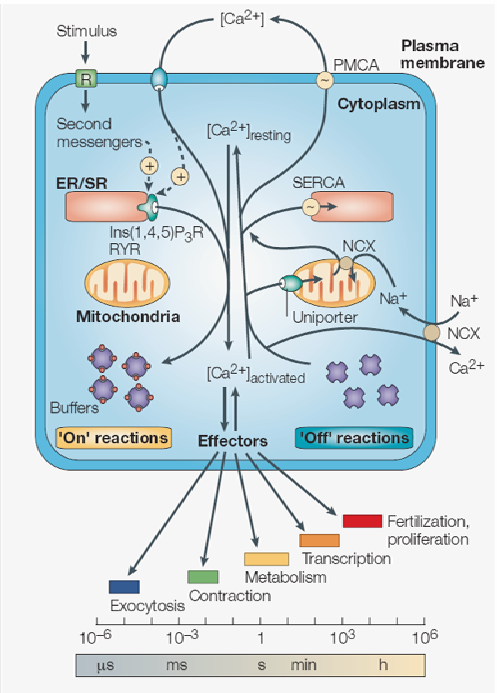

Figure 1.1: Calcium homeostasis

Various stimuli induce Ca^{2+} entry (''On reactions'') through plasma membrane Ca^{2+} channels. Alternatively, stimuli induce formation of secondary messengers that mediate Ca^{2+} release from ER/SR through Ins (1, 4, 5) P3Rs. Ca^{2+} entering through plasma membrane channels binds to and induces release of Ca^{2+} through RYRs located at the ER/SR membrane. This mechanism is referred to as Ca^{2+}-induced-Ca^{2+}-release. Most of the Ca^{2+} entering the cell binds to buffers in the cytoplasm, whereas a small proportion binds to effectors/signaling molecules that regulate various cellular processes over a wide temporal spectrum. Ca^{2+} is removed from the cytoplasm (''Off reactions'') by the action of NCX, PMCA and SERCA. This cartoon has been adapted from (Berridge MJ 2003).

1.1.1: Ca^{2+} channels

There are various Ca^{2+} entry sites located at the PM (Berridge MJ 2003; Lai HC 2006). Second-messenger-operated channels (SMOCs) open in response to

internal messengers, such as cyclic nucleotide gated channels that are found in the sensory system. Then there are channels belonging to transient-receptor-protein ion-channel family (TRP) that have low conductance and allow Ca^{2+} entry over a long period and hence control slow processes such as smooth-muscle contraction and cell proliferation (Lai HC 2006). Ca^{2+} channels that respond to membrane depolarization are called as the voltage-gated-Ca^{2+} channels (VGCCs) (discussed in section 1.1.1.1) (Lai HC 2006). Another category of Ca^{2+} channels are receptors that are activated upon ligand binding. These are called receptor operated Ca^{2+} channels (ROCCs). N-methyl-D-aspartate receptor, NMDAR, that opens in response to glutamate binding, is a classic example of both, receptor operated and voltage dependent channel, since along with glutamate binding, it also requires depolarization to remove Mg^{2+} ions from the channel pore to allow influx of Ca^{2+} (Lai HC 2006).

1.1.1.1: Voltage Gated Ca^{2+} Channels (VGCCs)

VGCCs, similar to voltage-gated K^+ and Na^+ channels, belong to the family of transmembrane ion channel proteins. They open in response to electrical activity and have been shown to regulate various intracellular processes like cell proliferation and differentiation, neurotransmission, migration and gene transcription (Lai HC 2006). VGCCs are multimers comprising various subunits (Fig 1.2). Pharmacological and biophysical behavior and the channel type are determined by the α subunit. To date, ten α_1 subunits have been cloned and are classified into 3 gene families Ca_v1, Ca_v2 and Ca_v3. Ca_v1 subunit is specific for L-type VGCC. N, P/Q and R-type channels have Ca_v2 subunit and T-type channels contain Ca_v3 subunits (Lai HC 2006). The α_1 is the largest subunit, and incorporates the conduction pore, the voltage sensor and gating apparatus; it is

also known to be the binding site for second messengers, drugs and toxins. It has 4 trans-membrane domains, each one having 6 trans-membrane helices (Fig 1.2). There are several auxiliary subunits that effect the channel function and expression: an intracellular β subunit that is responsible for some kinetic features like activation, inactivation, and voltage-dependent facilitation; a disulphide-linked $\alpha_2\delta$ complex and an occasional γ subunit which gives it a $\alpha_1\alpha_2\delta\beta\gamma$ channel composition (Lai HC 2006).

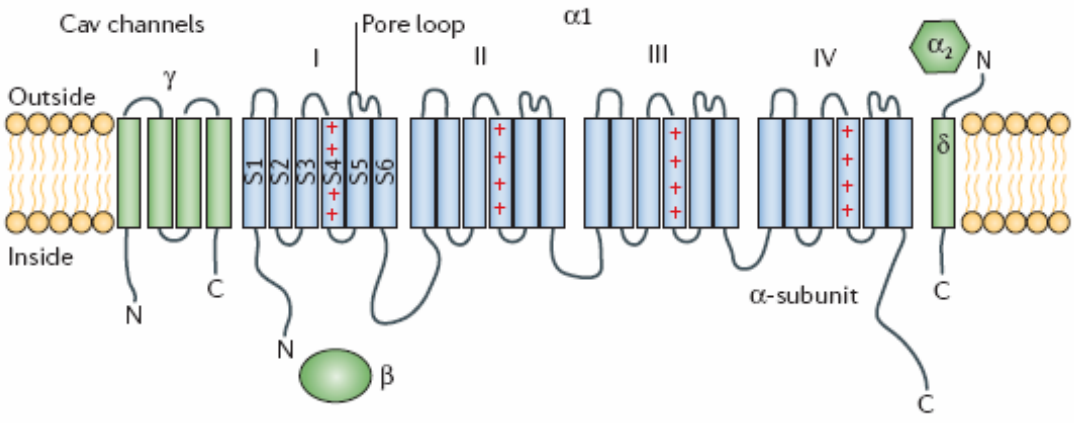

Figure 1.2: VGCCs: transmembrane heteromers

VGCCs comprise of $\alpha_1\alpha_2\delta\beta\gamma$ composition. α1 is the channel forming subunit with four transmembrane domains (blue). β is an intracellular subunit, α2δ form a disulphide-linked complex and γ is transmembrane subunit. This cartoon has been adapted from (Lai HC 2006).

L-type VGCCs are ubiquitous. They are expressed in neurons; cardiac, smooth, and skeletal muscle, as well as fibroblast and kidney cells. Their obvious function is to mediate Ca^{2+} entry in cells that contract or secrete in response to long or steady depolarization. They also are the source of Ca^{2+} entry for slow processes such as gene expression (Finkbeiner S 1998; Shaywitz AJ 1999). In pyramidal neurons, L-type VCGGs are especially localized to basal dendrites and cell soma where they are well positioned to transduce changes in cytosolic

Ca^{2+} to the nucleus (Catterall WA 2000). Ca^{2+} influx through L-type VGCCs has been shown to be coupled to gene transcription, CREB being one of their major targets (West AE 2001). L-type VGCCs show high sensitivity to 1, 4-dihydropyridines (DHPs), such as nifedipine and BAY K 8644 (Bean and Mintz 1994). Dihydropyridines can either activate or inactivate L-type VGCC. BAY K 8644 is an agonist whereas nifepidine is an antagonist. Non-L-type VGCCs are expressed primarily in neurons, where they seem to be involved in synaptic transmission. They are insensitive to DHPs, but selectively blocked by different neurotoxins.

1.2: Stem/Precursor Cells of the Central Nervous System

Stem cells are characterized by their ability to give rise to multiple cell types and self-renew. The first and truly totipotent cell of the body is a zygote that divides and gives rise to pluripotent and self-renewing embryonic stem cells found in the blastocyst (Fig 1.3). During development, as cells start to segregate into tissues, the ability of the stem cells to give rise to multiple cell types and self-renew gradually decreases as shown in Fig 1.3. In the embryonic and adult brain, stem cells have a restricted potential and only give rise to neural cells; neurons and glia. Thus neural stem/precursor cells (NPCs) are defined as uncommitted and immature precursor cells possessing the ability to self renew and give rise to multiple cell types of the CNS; astrocytes, oligodendrocytes and neurons (Temple S 2001).

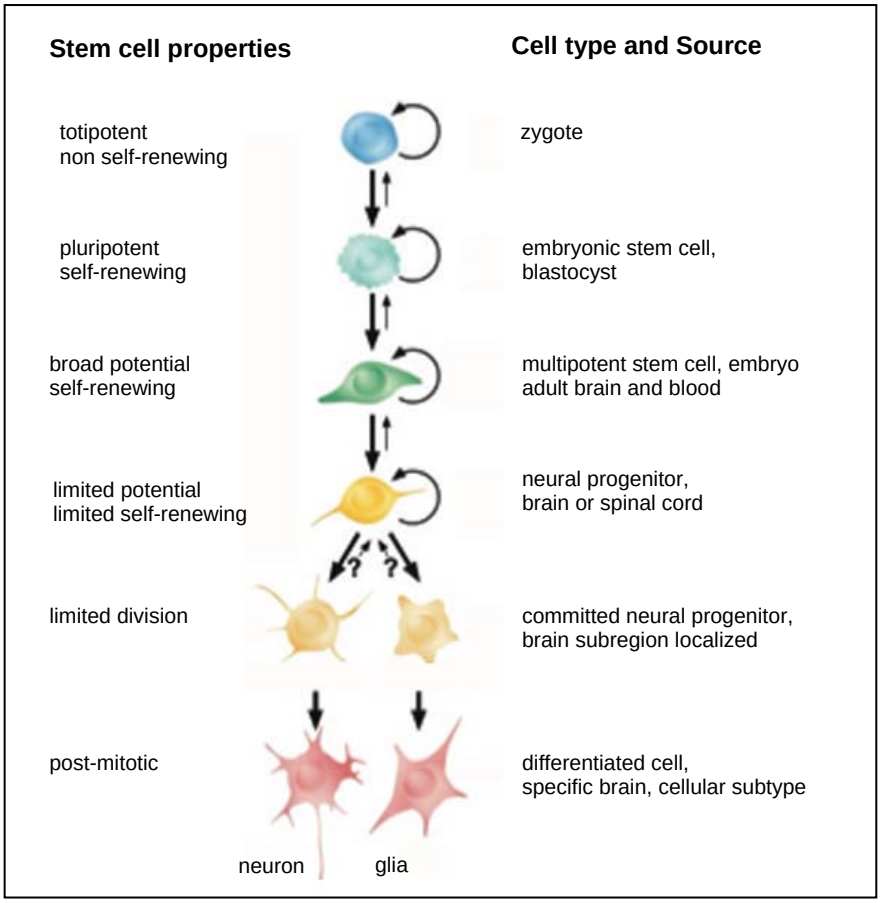

Figure 1.3: The hierarchy of stem cells

This cartoon depicts the hierarchy of stem cells from the most primitive and multi-potent to most restricted progenitors that give rise to differentiated cell types of the brain; neuron and glia. This cartoon has been adapted from (Gage FH 2000).

1.2.1: NPCs during development

During the embryonic development, neuroepithelial cells (NECs) of the neural tube act as NPCs and give rise to more differentiated cell types of the brain (Kintner 2002); (Alvarez-Buylla A 2001). Inductive signals generated in NECs cause the induction of patterning genes which form a concentration gradient across the dorso-ventral axis of the neural tube. This concentration gradient of patterning genes gives rise to germinal zones of NPCs that induce the

expression of specific bHLH transcription factor cascades which determine NPC differentiation into specific neural types. For example, hedgehog signaling induces a cascade involving proneural gene Olig 2 and Ngn 2 that promotes differentiation of ventral NECs into motor neurons (Mizuguchi R 2001; Novitch BG 2001).

Radial glia that arise during the development of the ventricular zone (VZ) of the lateral ventricle also show NPC characteristics. Radial glia have an elongated appearance with their soma in the VZ and a long process that extends towards the pial surface (Fig 1.4). Radial glia show many characteristics of NECs such as expression of intermediate filament nestin, forming contact with ventricle lumen and possessing a cilium with 9+0 microtubule organization that extends into the cerebrospinal fluid (Alvarez-Buylla A 2001). Although, earlier thought to serve a structural role as scaffolds for neuronal migration, they have now been shown to function as NPCs that give rise to glia and neurons *in vitro* (Malatesta P 2000) and *in vivo* (Noctor SC 2001). Figure 1.4 describes the alternative forms of radial glia divisions that generate neurons and astrocytes. Radial glia divide asymmetrically in the SVZ to self-renew and give rise to one neuron (Noctor SC 2004). Alternatively, radial glia may divide symmetrically in the VZ to self renew and generate a transit amplifying progenitor (Noctor SC 2004) (Fig 1.4). The transit amplifier then divides symmetrically into two neurons in the subventricular zone (SVZ). In either case, the daughter neuron extends into the cortex (towards the pial surface) along the process of the radial glia that acts as a scaffold (Fig 1.4). After neurogenic divisions, radial glia transforms into an astrocyte (Noctor SC 2002).

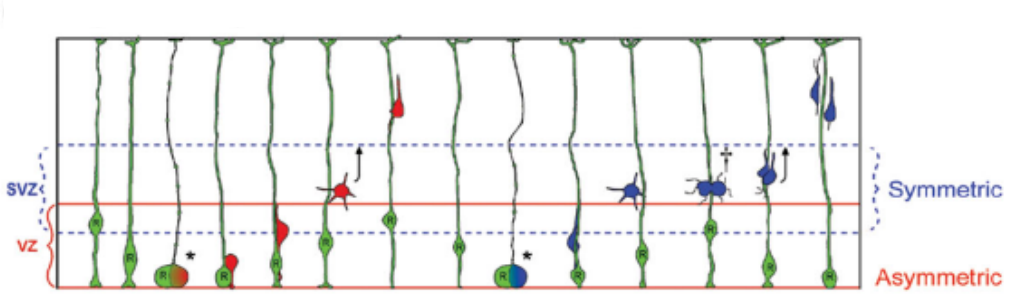

Figure 1.4: Radial glia as stem cells

The cartoon shows a radial glia cell (green) with its process towards the pial surface of the neocortex. The radial glia can undergo an asymmetric division in the ventricular zone (VZ) to self-renew and give rise to one neuron (red) that migrates along the radial glia process towards the cortical layers. Alternatively, radial glia self-renews and gives rise to a transitly amplifying progenitor (blue), that migrates to SVZ and divides symmetrically into two neurons (blue) that migrate along radial glia process towards the cortical layers. Rarely, transit progenitor divides symmetrically into two progenitors (not shown). The scheme has been adapted from (Noctor SC 2004).

1.2.2: Adult NPCs

In the adult mammalian brain, neurogenesis and presence of NPCs mainly exists in two brain regions; the SVZ of lateral ventricles and the subgranular zone (SGL) of hippocampal dentate gyrus (Gage FH 2000), Doestch). In contrast, postnatal neurogenesis in lower vertebrates like lizards is capable of recreating entire brain parts. Thus, there is a decrease in the adult neurogenesis with increasing brain complexity along the evolution (Kempermann G 2004). In the recent years, it has been shown that the adult NPCs possess properties of astrocytes (Doetsch F 1999). The type B cells that express astrocytic marker, GFAP, are the NPCs in the adult SVZ (Alvarez-Buylla A 2001). Type B cells show characteristics of NPCs such as expression of nestin, and presence of single cilium (9+0 arrangement of microtubules) that contacts ventricular space.

Type B cells give rise to transient amplifiers (type C cells) that in-turn divide into SVZ neuroblasts (type A cells) (Fig 1.5). Chains of type A cells ensheathed within type B cells migrate tangentially towards the olfactory bulb (OB) forming a rostral migratory stream (RMS) (Fig 1.5) (Alvarez-Buylla A 2001). Once in OB, these neuroblasts migrate radially and differentiate into OB interneurons, granule and periglomerular neurons (Lois C and Alvarez-Buylla 1994).

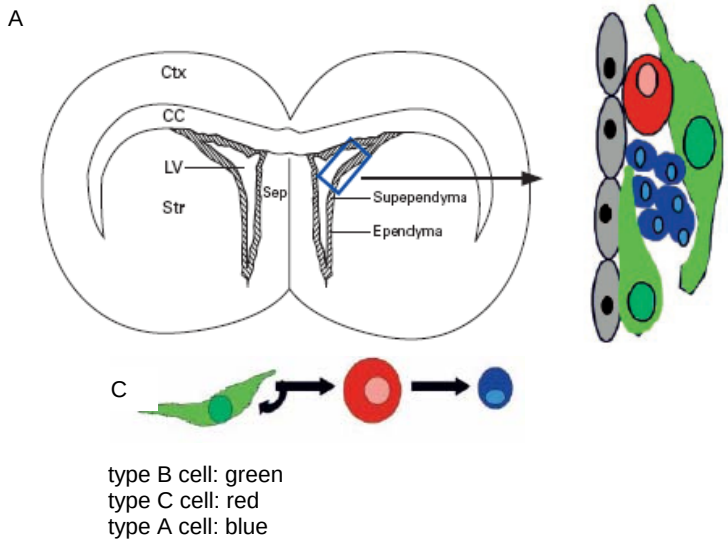

Figure 1.5: Adult SVZ NPCs

The blue box in A marks the SVZ lying next to the lateral ventricles in the adult brain. B is the enlargement of the section marked in A. Sheaths of type A neuroblasts (blue) surrounded by type B NPCs (green) and type C transitly amplifying progenitors (red) migrate tangentially towards the OB in RMS. In grey are endothelial cells. Type B cells are the stem cells that self-renew and give rise to type C transit amplifiers which divide to give rise to type A neuroblasts (C). The cartoon has been adapted and modified from (Morshead CM 2004).

1.3: Regulation of NPC differentiation by activity- induced Ca^{2+} influx

1.3.1: Spontaneous and activity-induced Ca^{2+} transients in NPCs

As in many other cellular processes such as fertilization, muscle contraction etc., spontaneous oscillations in the intracellular Ca^{2+} play an important role in the regulation of neurogenesis and neuronal differentiation of NPCs. Spontaneous Ca^{2+} transients occur in embryonic and postnatal cortical NPCs and regulate neurogenesis (Owens DF 1998; Pla AF 2005; D'Ascenzo M 2006). In murine neural crest progenitors, spontaneous Ca^{2+} transients are observed during neuronal differentiation and provide progenitors competence to differentiate into neurons (Carey MB 1999). Spontaneous Ca^{2+} influx through canonical transient receptor potential 1 (TRPC1) regulates rat NPC proliferation (Pla AF 2005). It has been previously shown that striatal NPCs show spontaneous Ca^{2+} transients during early stages of differentiation (Ciccolini F 2003). These spontaneous Ca^{2+} transients in striatal NPCs were more prominent during the early stages of differentiation and decreased with the on-going differentiation. When striatal NPCs were incubated in the absence of extracellular Ca^{2+}, neuronal differentiation was slowed down as the percentage of neurons expressing GABA neurotransmitter decreased, as did the neurite outgrowth This suggests that the spontaneous Ca^{2+} transients are important for timely differentiation of neurons arising from striatal NPCs (Ciccolini F 2003).

1.3.2: Regulation of neurogenesis by neural activity-induced Ca^{2+} influx

Neural activity, excitatory and inhibitory, is the means of communication in neural networks. Other than mediating communication in an established neural network, neural activity also regulates neurogenesis and neuronal

differentiation during development and adult brain. Neural activity and associated Ca^{2+} influx regulate various aspects of neurogenesis in the embryonic and adult brain. In the adult dentate gyrus, brief activation of NMDAR decreased proliferation and subsequent generation of neurons, whereas brief NMDAR blockade had an opposite effect *in vivo* (Cameron HA 1995; Gould E 2000). In contrast, a recent paper showed that activation of NMDAR (and L-type VGCCs) with depolarization enhanced neuron production (neurogenesis) without affecting proliferation, survival or apoptosis of NPCs in the adult dentate gyrus (Deisseroth K 2004). It is known that NMDAR antagonists can produce excitatory activity patterns in vivo by disinhibiting local circuits (Deisseroth K 2004). Such an increase in excitatory activity can enhance neurogenesis acting via L-type VGCCs and provide an explanation for the contradictory data. Neural activity has been shown to promote NPC differentiation in other brain regions as well. In post-natal cortical NPCs, L-type VGCC activation promoted neurogenesis by enhancing neuron production (D'Ascenzo M 2006). Previous study has shown that membrane depolarization accelerated neuronal differentiation of embryonic striatal NPCs by increasing GABA expression and neurite outgrowth in neurons arising from NPCs (Ciccolini F 2003). Depolarization also increased the frequency of global and local Ca^{2+} transients occurring spontaneously in differentiating striatal NPCs, thereby establishing a correlation between Ca^{2+} influx and neuronal differentiation (Ciccolini F 2003). Futhermore, the effect of depolarization on neurite outgrowth as well as on the frequency of local Ca^{2+} transients was found to be NMDAR dependent, whereas depolarization induced increase in the GABA expression and the frequency of global Ca^{2+} transients was NMDAR independent (Ciccolini F 2003). Thus, neural activity acting via distinct cell surface Ca^{2+} channels can activate distinct signaling cascades that regulate

different aspects of NPC proliferation and differentiation. Similarly, neurotransmitters such as GABA (which is excitatory during development) as well as glutamate induced depolarization led to VGCC-dependent Ca^{2+} elevation in embryonic cortical NPCs that is critical for their differentiation into neurons (LoTurco JJ 1995). In the hippocampus, GABAergic inputs from hippocampal circuitry depolarized type-2 transitly amplifying NPcs leading to Ca^{2+} influx that promoted their differentiation into neurons (Tozuka Y 2005).

One way by which neural activity and associated changes in Ca^{2+} influx, regulate neurogenesis is regulation of gene expression. In the adult hippocampal NPCs, neural activity-induced activation of L-type VGCC and NMDAR led to a downregulation of glial fate genes *Hes1* and *Id2* and upregulation of neural fate gene, *NeuroD,* thus favoring neurogenesis (Deisseroth K 2004). Similarly, GABAergic input from hippocampal circuitry also enhanced neurogenesis in adult hippocampal NPCs via upregulation of *NeuroD* (Tozuka Y 2005). Regulation at the level of gene transcription has also been shown to modulate the acquisition of neurotransmitter phenotype. For example, specific frequency of Ca^{2+} transients, spontaneous and evoked, modulates GABA neurotransmitter acquisition by regulation of glutamic acid decarboxylase (GAD) transcription in *Xenopus* spinal neurons (Gu X 1995; Watt SD 2000).

1.4: Mechanisms involved in the regulation of neuronal differentiation by activity-induced Ca^{2+} influx

1.4.1: Regulation of neurite outgrowth by Ca^{2+} dependent mechanisms

1.4.1.1: Ca^{2+} activated kinase cascades

Extension of neurites and establishment of synapses is a crucial step in the development of functional neural networks. Neural activity-induced Ca^{2+} influx has been shown to activate various downstream signaling cascades that regulate different cell processes by the modulation of gene transcription and/or by post-translational modifications such as phosphorylation/dephosphorylation of target proteins (Fig 1.6). Changes in dendritic outgrowth and arborization are regulated by signaling pathways described in Fig 1.6. For example, in cortical neurons, VGCC-mediated Ca^{2+} influx induced dendritic growth via the activation of Ca^{2+}-calmodulin dependent kinase IV, CaMKIV, that in-turn phosphorylated and activated cAMP-response element binding protein, CREB (Redmond L 2002). In the sympathetic neurons, however, activity-induced Ca^{2+} influx activates dendritic growth via the activation of CaMKII and extracellular-signal regulated kinase, ERK (Vaillant AR 2002). ERK is activated by various axon growth promoting signals including depolarization and regulates neurite outgrowth in many cell types such as retinal neurons and PC-12 cells (Perron JC 1999; Hansen TVO 2003). Similarly, CaMKI have also been shown to regulate neurite outgrowth of hippocampal neurons (Wayman GA 2004). Interestingly, it has been shown that localized increase in Ca^{2+} (Ca^{2+} waves) restricted to a small dendritic regions, rather than a global rise in cytosolic Ca^{2+}, regulates neurite outgrowth (Spitzer NC 2000; Ciccolini F 2003). Localized increase in Ca^{2+} through different Ca^{2+} channels activates signaling molecules localized in the vicinity of the channels that

allows localized activation of signaling cascades regulating different cellular processes (West AE 2001). Hence Ca^{2+} influx can regulate various cellular processes depending on source of entry and downstream signaling activated.

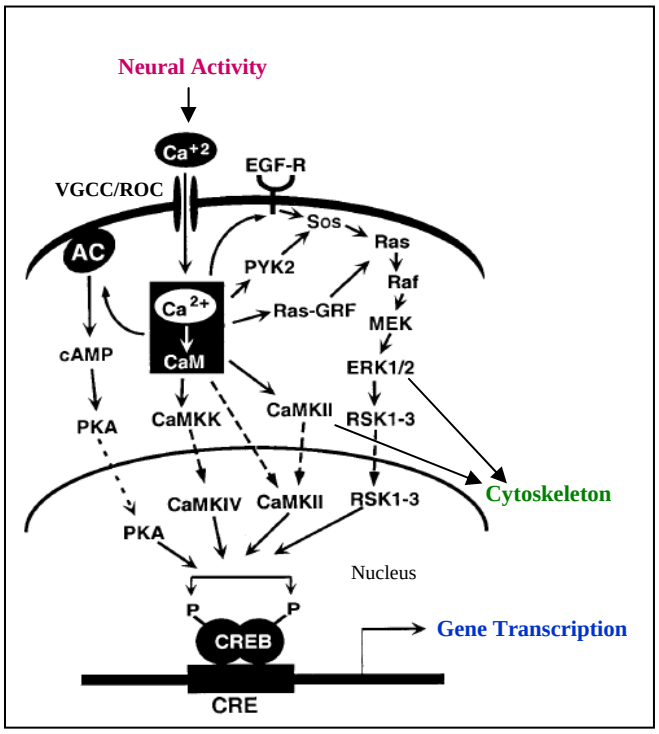

Figure 1.6: Signaling cascades activated by activity-induced Ca^{2+} influx

Neural activity induces Ca^{2+} influx through VGCCs that in-turn activates downstream signaling cascades. Binding of Ca^{2+} to CaM causes a conformational change in CaM and Ca^{2+}-CaM then activates CaMK pathway. Similarly, Ca^{2+} activates ERK pathway and adenylate cyclase (AC) causing increase in cAMP levels and activation of cAMP-dependent kinase (PKA). Activated kinases either modulate target proteins such as cytoskeletal proteins (actin) in the cytoplasm or enter the nucleus where they regulate gene transcription by activating transcription factors such as CREB. This cartoon has been adapted and modified from Greenberg, 2001.

One way of achieving changes in neurite growth and arborization is by modulation of cytoskeleton (Lankford KL and Letourneau PC 1989). For example, in the *Xenopus* spinal neurons, depolarization-evoked local Ca^{2+} waves activated a phosphatase, calcineurin, that inhibited neurite outgrowth by dephosphorylating actin filaments and destabilizing the cytoskeleton (Spitzer NC 2000). Alternatively, NMDAR-dependent Ca^{2+} influx led to the stabilization of actin cytoskeleton in dendritic spines of hippocampal neurons. Thus, it is conceivable that different cell types involve spatially localized Ca^{2+} signals that activate distinct signaling cascades for the regulation of neurite outgrowth.

1.4.1.2: Secreted amyloid precursor protein (sAPP) as a neurite outgrowth regulator

Amyloid precursor protein (APP) is known as the source of amyloid β peptide (Aβ), that forms characteristic fibrillar plaques of Alzheimer's disease. APP is a transmembrane protein with a single membrane-spanning domain. During development, APP expression parallels neuronal differentiation and neurite outgrowth (Hung AY 1992; Salbaum JM 1994). Three possible cleavage sites of APP are known. α-secretase cleaves between amino acids 612 and 613, β–secretase cleaves between 596 and 597 and by γ–secretase between 639 and 640. Aβ is released when APP undergoes two subsequent cleavages by β and γ secretases (Fig 1.7). α-secretase cleavage causes release of sAPPα and since it cleaves between Aβ sequence, it prevents release of the Aβ fragment. β–secretase cleavage releases sAPPβ and leaves behind a membrane bound COOH terminal which has intact Aβ peptide. A γ–secretase cleavage then releases Aβ and a C-terminal intracellular domain that regulates

gene transcription by translocating to the nucleus (Fig 1.7) (Leissring M). sAPPα has been shown to have various neuroprotective effects for example, promoting cell proliferation, neurite outgrowth, synaptogenesis and cell adhesion (Mattson, 1997).

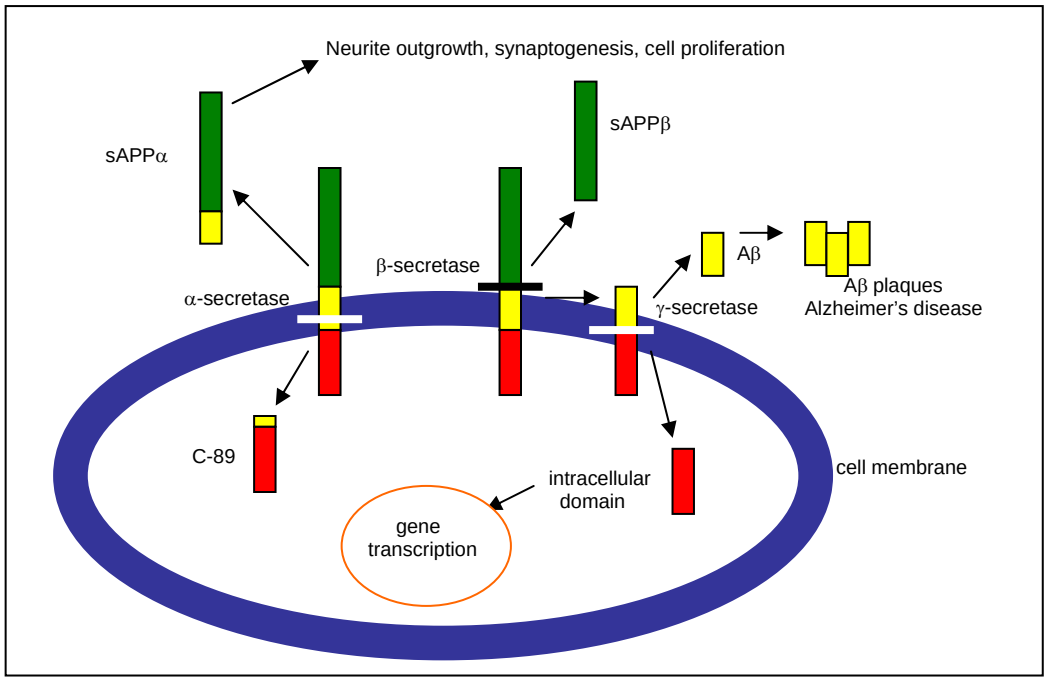

Figure 1.7: APP: soluble products and functional significance

Cartoon shows different soluble products generated from APP by 3 different secretases. α-secretase cleaves within the Aβ peptide (yellow) and releases sAPPα (green+yellow) into the extracellular space and C89 fragment intracellularly. sAPPα has various neuroprotective functions such as enhancing neurite outgrowth via its interaction with heparan sulfate proteoglycan. β-secretase releases sAPPβ (green) into the extracellular space. β-secretase cleavage is followed by γ-secretase cleavage that releases Aβ peptide into the extracellular space and intracellular domain (red) into the cytoplasm. Aβ is known to form senile plaques in Alzheimer's disease, whereas the intracellular domain translocates to the nucleus and regulates gene transcription.

sAPPα's neurite outgrowth promoting effect was shown to be mediated via its binding to heparan sulfate proteoglycan of the extracellular matrix in cultured chick sympathetic and mouse hippocampal neurons (Small D 1994). Moreover, its N-terminal domain possesses structural similarity to cystein-rich growth factors (Rossjohn J 1999). Furthermore, membrane depolarization (Nitsch R 1993) and activation of secondary messenger cascades enhance α-secretase cleavage of APP and hence, release of sAPPα. For example, activation of muscarinic and epidermal growth factor receptors enhances the production of sAPPα by pathways involving Ca^{2+} and phospholipid dependent kinase C (PKC), tyrosine kinases, and ERK (Mills J 1999).

Recent research has shown various functions of secreted forms of APP in regulating NPC proliferation, differentiation and migration. APPα has also been shown to enhance proliferation of NPCs from embryonic brain (Hayashi Y 1994) (Ohsawa I 1999). In the SVZ, sAPP was shown to bind EGFR positive NPCs and induces their proliferation (Caille I 2004). Secreted forms of APP, truncated at different sites (at 505 amino acid and at α cut) have been shown to increase human NPC (hNPC) differentiation into glia and neurons at low dosage and primarily favor glial fate selection at a higher dosage (Kwak YD 2006). In APP knockout mice, migration of hNPCs transplanted was reduced compared to the wild type mice, suggesting a role of secreted APP forms in NPC migration (Kwak YD 2006).

1.4.2: Regulation of GABA expression by Ca^{2+}-dependent mechanisms

GABA is one of the principal neurotransmitter of the mammalian central nervous system (CNS) where it mainly mediates inhibitory synaptic transmission. GABA is also involved in the regulation of several processes in the developing brain such as precursor proliferation, migration, and providing

trophic support for differentiating neurons (LoTurco JJ 1995; Behar TN 2000; Behar TN 2001; Owens DF and Kriegsteim AR 2002). It has been proposed that GABAergic neurons consist of two distinct pools of GABA: a cytoplasmic one and GABA found in the vesicles. Several lines of evidence support a scenario by which such a separation is achieved and maintained by the use of different routes of synthesis and transport systems (Waagepeterson HS 2001). Supporting the notion of separate pools of intracellular GABA is the existence of two different forms of the rate-limiting GABA synthesizing enzyme, glutamate decarboxylase (GAD), GAD 67 and GAD 65. GAD 67 is localized to the cytosplasm, active in its dephosphorylated state and is responsible for the maintenance of the metabolic pool of GABA, whereas GAD 65 is associated to the vesicular membrane, activated by phosphorylation and synthesizes vesicle-associated GABA involved in the synaptic transmission (Soghomonian J 1998; Waagepeterson HS 2001; Wei J 2004). Biochemical studies have shown that cAMP-dependent protein kinase, PKA and calcium and phospholipid-dependent protein kinase, PKC, and phosphatases such as PP1, PP2A and PP2B modulate the phosphorylation state of GAD 67 and GAD 65 (Wei J 2004).

During the embryonic development, neural activity can affect GABA expression by modulating the frequency of Ca^{2+} transients. It has been previously shown that neural activity and associated increase in the frequency of global Ca^{2+} transients correlated with the increase in GABA expression in striatal NPCs-derived neurons (Ciccolini F 2003). In embryonic *Xenopus* spinal neurons, the frequency of Ca^{2+} transients, spontaneous or evoked, effect GABA expression by regulating GAD transcription (Watt SD 2000). In this system, activity mediated changes in Ca^{2+} influx not only effected GABA expression, but indeed altered the type of neurotransmitter expressed (Borodinsky LN 2004). Lowering the frequency of Ca^{2+} transients increased the expression of

excitatory neurotransmitters, whereas increasing the frequency of Ca^{2+} transients caused the neurons to express inhibitory neurotransmitters without changing other parameters such as cell surface marker expression (Borodinsky LN 2004). This suggests that neural activity can induce changes that establish a state of homeostasis in the system (Borodinsky LN 2004). Alternatively, activity-induced Ca^{2+} influx has also been shown to regulate GABA expression by post-translational mechanisms. For example, in *Drosophila* neurons, activity-induced Ca^{2+} influx regulates GABA expression by post-translational mechanism downstream of GAD 67 and GAD 65 transcription (Küppers B 2003). A possible post-translational mechanism could be the regulation of GAD enzymatic activity (phosphorylation/dephosphorylation) by kinases such as PKA and PKC, and phosphatases such as PP1, PP2A and PP2B as shown by bio-chemical studies (Küppers B 2003; Wei J 2004).

1.5: Goals and outline of this study

The specific aim of this dissertation is to investigate the mechanisms underlying the effect of neural activity on neuronal differentiation of striatal NPC-derived neurons and if this regulation involves changes in Ca^{2+} signaling. It has been previously shown that embryonic striatal NPCs undergo spontaneous Ca^{2+} transients during differentiation that were defined either as global, when the elevations of intracellular Ca^{2+} encompassed the whole cell body, or local, when they were restricted to a small region of the cytoplasm (Ciccolini F 2003). Membrane depolarization increased the frequency of both types of Ca^{2+} transients and it effected neuronal differentiation by causing neurons to acquire GABA prematurely and by enhancing neurite outgrowth (Ciccolini F 2003). It was also found that changes in global Ca^{2+} transients

correlated with the early onset of GABA expression, whereas increased frequency of local Ca^{2+} transients correlated with neurite outgrowth, suggesting that global and local transients regulated distinct aspects of neuronal differentiation (Ciccolini F 2003). In this dissertation I have used the same experimental system of differentiating striatal NPCs and asked the following questions:

1) Which signaling pathways regulate GABA expression and neurite outgrowth in neurons differentiating from striatal NPCs downstream of neural activity?
2) Do neurons arising from striatal NPCs show spontaneous Ca^{2+} transients and if so, does neural activity induce changes in the frequency/kinetics of these Ca^{2+} transients?
3) Is there a direct link between spontaneous/evoked Ca^{2+} transients and GABA expression in neurons differentiating from striatal NPCs?
4) Do same signaling pathways regulate GABA expression in neurons under normal physiological and depolarizing conditions or does depolarization-induced regulation of GABA expression involve a different mechanism?

To this end, in the first part of the dissertation I quantified rate of neuronal differentiation and acquisition of GABA by neurons in striatal NPC cultures left in control or exposed to depolarizing stimuli. In the second part, I investigated the potential signaling cascades involved in the regulation of neurite outgrowth and GABA expression in neurons differentiating in the presence or absence of membrane depolarization. I also examined the involvement of gene expression on depolarization-induced changes in neuronal differentiation. This analysis showed that depolarization leads to changes in neurite length and GABA expression by activating distinct intracellular

pathways. In the third part, I performed Ca^{2+} imaging and retrospectively distinguished neurons from non-neurons in order to examine the involvement of Ca^{2+} signaling in activity-induced GABA expression. Due to the correlation between global Ca^{2+} transients and GABA expression, I analysed global Ca^{2+} transients in the neurons. To establish a direct link between Ca^{2+} influx and GABA expression, experiments in the absence of extracellular Ca^{2+} and antagonists of VGCCs were performed in the fourth section. In the last section, I focused on dissecting the signaling involved in the regulation of GABA expression in neurons undergoing normal differentiation and those in which differentiation is enhanced by depolarizing stimuli. I also tested the effect of depolarization in neurons arising from cortical NPCs to ascertain the specificity of depolarization-induced GABA expression.

The broader goal of this study was to understand the mechanism entailed in the differentiation of neural precursors into functional neurons in response to excitation stimuli. Insights obtained from this study could be used to establish in vivo models for manipulation of NPC proliferation and differentiation by neural activity. This could lead to generation of tools for modulating invasion, survival and formation of functional connections by NPCs following neurodegeneration occurring in stroke and ischemia.

Chapter 2 : Materials and Methods

2.1: Materials

2.1.1: General Reagents

Agarose	Invitrogen
Bromophenolblue	CHROMA
Chloroform	Fluka
GeneRuler 1 kb DNA ladder	Fermentas
DAPI	Boehringer
Ethidiumbromide	Serva
Ethanol	SIGMA
Isopropanol	Applichem
Milk powder	Frema/Reform
Prestained protein ladder	Fermentas
SDS	Serva
TEMED	Serva
Tris	Roth

Other general reagents and chemicals like $MgCl_2$, $CaCl_2$, NaCl etc. were purchased from SIGMA

2.1.2: Cell Signaling Modulators, Anta/agonists

Pharmacological agent (concentration used)

Actinomycin-D (10 μM)	SIGMA
AktI (10 μM)	Calbiochem
Anisomycin (10 μg/ml)	SIGMA
BDNF (20 ng/ml)	Chemicon
FK506 (1 μM)	Calbiochem

Forskolin (10 μM)	SIGMA
FPL 64176 (1 μM)	SIGMA
GM6001 (ilomastat) (10 μM)	SIGMA
KN-62 (10 μM)	Calbiochem
LY294002 (10 μM)	Calbiochem
Myristoylated PKC peptide inhibitor (1 μM)	Promega
Myristoylated PKA inhibitor amide 14-22 (1 μM)	Merck
Mibefradil dihydrochloride (1 μM)	SIGMA
Nifedipine (10 μM)	SIGMA
NT-3 (20 ng/ml)	R & D systems
NT-4 (20 ng/ml)	R & D systems
OAG (25 μM)	Tocris
UO106 (10 μM)	Calbiochem
ω- Conotoxin MVIIC (1 μM)	Tocris

2.1.3: Total RNA isolation, cDNA synthesis reagents and RT-PCR

5X Buffer Transcription Buffer	Fermentas
DEPC water	Fermentas
dNTPs	Fermentas
First strand buffer	Promega
M-MLV Reverse Transcriptase	Promega
Proteinase K	Roche
PCR-mix 2X	Applied Biosystems
Rnasin Plus RNase inhibitor	Fermentas
RQ1 DNAse (RNAse free)	Invitrogen

Random Hexamer Primers	Promega
TRIzol	Gibco
Taq DNA polymerase	Fermentas

GAPDH, GAD 67 and GAD 65 TaqMan gene expression assays were from Applied Biosystems

2.1.4: Buffers and Solutions

For the preparation of aqueous solutions desalted water from a "MilliQ Water Purification System" (Millipore) was used.

DNA Loading buffer	For 10 ml final volume
	9.5 ml formamide
	5 mg bromophenolblue
	5 mg xylencyanol
	0.5 mg of 0.5 M EDTA
5X Protein Sample buffer	For 100 ml final volume
	15 g SDS
	15.6 ml Tris 2 M, pH 6.8
	57.5 g of 87% glycerol
	16.6 ml β-mercaptoethanol
TE (Tris-EDTA)	10 mM Tris/HCl pH 8,0
	1 mM EDTA
10X TBE (Tris-Boric acid-EDTA)	For 1000 ml final volume
	108 gm trisbase
	55 gm boric acid
	0.74 gm EDTA

SDS/Running Buffer	25 mM Tris 192 mM Glycine 0.1% SDS
10X Western blot transfer buffer	For 1000 ml final volume 1.5 M glycine 0.2 M Tris 50 ml of 20% SDS During 1X preparation, add 20% methanol

2.1.5: Cell Culture Reagents, Media and Equipment

B-27	Gibco
DME/F-12 medium	Gibco
Euromed-N medium	Euroclone
FCS	BioWhittaker
Human recombinant EGF	Peprotech
Human recombinant FGF2	Peprotech
L-Glutamine	Gibco
Leibovitz medium	Gibco
Penicillin/Streptomycin	SIGMA
PLO	SIGMA
PI	SIGMA
CELLocate graded cover slips	Eppendorf
Photoetched cover slips	Bellco glass Inc. from Dunn labor-technik

2.1.6: Primary Antibodies

Mouse anti-Tuj1 (1:400)	SIGMA
Mouse anti-APP A4 (MAB348) (1:200 for western blot) (1:100 for cell culture)	Chemicon
Mouse IgG (1:100)	SIGMA
Rabbit anti-GABA (1:2000)	SIGMA
Rabbit anti-glutamate (1:1000)	SIGMA
Rabbit anti-CREB (1:1000)	From Prof.Schütz's lab, described in (Mantamadiotis T 2002)
Rabbit anti-pCREB (1:1000)	Upstate

2.1.7: Secondary Antibodies Antigens

Anti-rabbit IgG PE (1:200) against rabbit anti-GABA	Molecular Probes
Anti-mouse Alexa 488 (1:1000) against mouse anti-Tuj1	Molecular Probes
Anti-rabbit Alexa 555 (1:1000) against rabbit anti-glutamate	Molecular Probes
Anti-rabbit biotin (1:200) +Strepavidin -Cy3 (1:500) against rabbit anti-pCREB	Molecular Probes
Anti-mouse tubulin (1:50,000) against mouse anti-tubulin	SIGMA

2.1.8: Fluorescent calcium indicators

Fluo-3 cell permeant (AM ester) was from Molecular Probes

2.2: Methods

2.2.1: Primary striatal neural precursor cell (NPC) culture

Neural precursor cells (NPCs) were obtained from dissecting striata (and/or cortex where specified) of embryonic day 14 (E 14) CD1 albino mice embryos (plug day=1.0) (Charles River). Tissue was transferred into ice cold Euromed-N basal serum free culture medium consisting of, Penicillin-Streptomycin (100 U/ml), glutamine (2 mM) and 2 % B27 supplement and gently triturated with a fire-polished Pasteur pipette. Human recombinant EGF and human recombinant FGF-2 were added at a concentration of 20 ng/ml and 10 ng/ml, respectively (hereafter referred to as culture medium). Following dissociation, 10^6 cells were plated at a density of 2 x 10^5 cells/ml in Nunc culture flasks in the culture medium. Cells were fed with 1/2 the volume of fresh culture medium every four days. NPCs were kept in a suspension culture for a week, during which they proliferate and expand to form heterogeneous cell clusters, neurospheres, consisting of NPCs and differentiated cells.

2.2.2: Differentiation of neurosphere-derived precursors

Following one week in culture, neurospheres were centrifuged at 800 rpm for 3 min to obtain cell pellet. The medium was discarded and the pellet was re-suspended in 3 ml of ice-cold PBS containing 0.6% of glucose and kept on ice for 5 min. During this step, cell-cell adhesion weakens in the absence of medium enriched with ions and proteins and a single cell suspension can be obtained with mild trituration. Neurospheres were then centrifuged at 800 rpm for 3 minutes and the pellet was re-suspended in 200 µl of culture medium and mechanically triturated through a fire-polished Pasteur pipette. Differentiation was promoted by reducing the growth factor concentration (no EGF was added

and FGF-2 was reduced to 2 ng/ml from 20 ng/ml under proliferating conditions) and addition of FCS (hereon referred to as differentiation medium). $2x10^5$ cells/well were plated onto PLO-coated chamber-slide or 25 mm glass cover-slip in 200 μl differentiation medium and returned to the incubator. Cells were left in differentiating conditions for upto 7 days. Neuronal phenotype was determined immunocytochemically at different days after plating (DAP) using antibodies against type III tubulin (Tuj1), γ-amino butyric acid (GABA) and glutamate (Glu).

2.2.3: Modulation of NPC differentiation

In certain experiment, differentiating NPCs were treated with differentiation medium containing 50 mM KCl (referred as high KCl medium hereafter). High KCl medium was prepared by adding 3 ml Euro-med medium to 1.25 ml depolarizing solution (170 mM KCl, 2 mM $CaCl_2$, 1 mM $MgCl_2$, 10 mM HEPES) to obtain 50 mM KCl concentration. Penicillin-Streptomycin, glutamine, B27 supplement and FGF2 were added at the same concentration as for the differentiation medium. To test the modulation of NPC differentiation with depolarization, NPCs were exposed to high KCl medium for either on one or two day/s after plating (referred to as DAP 1 or DAP 2 and so on) for varying time periods. In other experiments, (as mentioned in the Results section), differentiating NPCs were treated with pharmacological agents, agonists and antagonists, in order to activate or inhibit specific signaling molecules. In experiments where pharmacological agents being tested were suspended in DMSO or any other buffer solution, cultures containing similar concentration of these solutions without the pharmacological agents were included as appropriate controls. Certain experiments were performed in Ca^{2+} free

differentiation medium. For this purpose, DME-F12 Ca^{2+} free medium from Gibco was used. 0.2% heparin (1:500) was added to the medium. Penicillin-Streptomycin, glutamine, B27 supplement and FGF2 were added at the same concentration as normal differentiation medium. To compensate for Ca^{2+} ions, Mg^{2+} was added at the concentration of 1mM to the medium. Ca^{2+} free-high KCl medium was prepared by combining 3 ml of Ca^{2+} free-DME-F12 medium and 1.25 ml of Ca^{2+} free-depolarization solution (Ca^{2+} was replaced by Mg^{2+} :170 mM KCl, 3 mM $MgCl_2$, 10 mM HEPES). Concentrations of all added factors were kept same as the normal high-KCl medium.

2.2.4: Immunocytochemistry

To perform immunocytochemistry, the cells were first fixed with 3% paraformaldehyde (PFA) in PBS containing 4% sucrose for 10 minutes and rinsed several times in PBS at room temperature. Cells were permeabilized with NP-40 (0.5% in PBS) for 5 minutes. After permeabilization, cells were incubated with primary antibodies overnight at 4°C. Next day, cells were washed with PBS, 2X5 min, to washout extra primary antibody and then incubated with fluorescently labelled secondary antibodies for 45 min-1 hour. Cells were washed 2X5 min with PBS and rinsed with water to remove PBS. Excess water was removed by gently tilting and tapping the chamber-slide or coverslip on a tissue paper. 5 µls of moviol was placed on each well of a chamber-slide and a glass coverslip was gently placed on top it. Chamber-slides or coverslips were stored in dark to preserve fluorescence (at 4°C).

2.2.5: Transgenic animals

For some experiments, NPCs were derived from the tissues of transgenic mice described below:

1. *Creb knock-out mouse line* on Crem knock-out background ($Creb^{Nescre}Crem^{-/-}$ mice) was generated in the lab of Prof. G. Schütz as previously described in (Mantamadiotis T 2002).

In the case of Creb knock-out mice, embryos were genotyped using the primers described in (Mantamadiotis T 2002) and results were confirmed by 10% SDS-PAGE and western blot analysis (see section 2.5). Neurospheres prepared from wild type ($Crem^{-/+}$ $Creb^{+/+}$, WT), single mutant ($Crem^{-/-}$ $Creb^{+/+}$, $M^{-/-}B^{+/+}$) and double mutant ($Crem^{-/-}$ $Creb^{-/-}$, $M^{-/-}B^{-/-}$) embryos were plated on PLO-coated chamber slides and were used for further experiments.

2. *TauEGFP knock-in mice* were generated in the lab of Dr. K. Tucker as described in (Tucker KL 2001). These mice express tau and EGFP as a fusion protein under the tau promoter. $EGFP^{+/+}$ males were mated with wild type C57BL/6 females to obtain $EGFP^{+/-}$ embryos. These heterozygous E14 embryos were used for striatal neurosphere cultures and further experiments.

3. *TrkB knock-out mice* was generated in the lab of Prof. K. Unsicker as described in (Schober A 1997). $TrkB^{+/-}$ males were mated with $TrkB^{+/-}$ females to obtain embryos of various genotypes. On E14, the mother was sacrificed and embryo tail biopsies were used for genomic DNA extraction, followed by genotyping as described in (Schober A 1997). Neurospheres from $TrkB^{+/+}$, $TrkB^{-/-}$ and $TrkB^{+/-}$ embryos were used for further experiments.

2.2.6: Western blot

SDS-PAGE and western blot were performed for testing secretion of secreted form of amyloid precursor protein, sAPP by differentiating NPCs under unstimulated and depolarizing conditions. 500,000 neurosphere-derived NPCs were plated on PLO-coated 12 well plate on DAP 0. On DAP 1, medium change was performed using normal differentiation medium in one set of cultures and high KCl medium in another set of cultures. Cell lysates and media were collected from both, unstimulated and stimulated, cultures either after 1 hour of medium change or after 24 hours of medium change. To lyse the cells, 50 µl of 1X protein sample buffer was added and samples were heated to 95° C for 2 min. For the medium, 12.5 µl of 5X protein sample buffer was added to 50 µl of medium and samples were heated to 95° C for 2 min. 30 µl of each sample was loaded on 7.5% SDS-PAGE (prepared according to the standard procedures) and run at 35 mA till the gel front reached the bottom of the gel. Following this, the gel was transferred on to Protran nitrocellulose filter (Schleicher & Schuell) using semi-dry western blot apparatus. To identify the sAPP bands, nitrocellulose was first blocked with 5% milk in PBST (PBS with 0.2 % Tween) for an hour, washed 2X5 min with PBST and incubated with MAB348 anti-APP at 1:500 dilution overnight. As a loading control, the blot was counterstained for anti-α tubulin (1:50,000). Next day, primary antibodies were removed and nitrocellulose was washed 5X5 min with PBST and incubated with secondary-mouse horse radish peroxidase (HRP) antibody (1:5000) for an hour, followed by 5X5 min washing steps with PBST. Chemiluminescence reaction was performed by exposing the nitrocellulose for a min to HRP substrate, 1:1 mixture of detection reagent I and detection reagent 2 of Amersham ECL western blotting detection kit.

A similar procedure was repeated for the analysis of CREB knockout mice. For this, neurospheres from wild type ($Crem^{-/+}$ $Creb^{+/+}$, WT), single mutant ($Crem^{-/-}$ $Creb^{+/+}$, $M^{-/-}B^{+/+}$) and double mutant ($Crem^{-/-}$ $Creb^{-/-}$, $M^{-/-}B^{-/-}$) embryos, proliferating in culture medium for a week were triturated and 1 million cells were resuspended in 50 µl of 1X protein sample buffer and heated to 95° C for 2 min. Samples were run on 10% SDS-PAGE followed by western blot analysis as mentioned above. CREB bands were identified with rabbit polyclonal anti-CREB (1:1000) and secondary-rabbit horse radish peroxidase (1:5000) antibodies. Chemiluminescence was performed as mentioned above.

2.2.7: Ca^{2+} imaging

NPCs for Ca^{2+} imaging were plated on CELLocate graded coverslips or Bellco graded coverslips. Calcium recording was performed on differentiating NPCs at DAP 1. The cells were loaded with cell permeable Fluo3-AM (2.5 nM, dissolved in pluronic acid with 0.05% DMSO) for 30 minutes at room temperature (20-22ºC) in Ringers solution containing: NaCl (140 mM), KCl (3 mM), $MgCl_2$(1 mM), $CaCl_2$ (2 mM), Hepes (10 mM) and glucose (10 mM). In certain experiments cells were pre-treated with high KCl medium and/or L-type VGCC antagonist, nifedipine, for 6 hours on DAP 1. For cultures exposed to high KCl medium, Ringers solution with 50 mM KCl, referred to as high KCl-Ringers solution, [NaCl (93 mM), KCl (50 mM), $MgCl_2$ (1 mM), $CaCl_2$ (2 mM), Hepes (10 mM) and glucose (10 mM)] was used during Fluo-3 AM loading and Ca^{2+} imaging. Ca^{2+} imaging was performed through a 20x (N.A. 0.9) objective on an upright fluorescent microscope (Olympus BX51WI, Hamburg, Germany), equipped with a CCD camera (Photometrics Coolsnap HQ, Roper Scientific, Ottobrunn, Germany) connected through a software

interface (Metafluor, Molecular Devices, Downington PA, USA) to a computer monitor. Image were acquired at a size of 347x260 pixels corresponding to 340 x 260 μm and at an acquisition rate of 1 frame/sec. Excitation light was generated by a monochromator coupled to a xenon light source (Optoscan and Optosource, Cairn, Faversham, UK) and passed through a 470-490nm filter (Olympus). Emission light was passed through a 510-550nm filter (Olympus). Following imaging, cells were fixed with 3% paraformaldehyde (PFA) containing 4% sucrose and immunocytochemistry for neuronal marker Tuj1 was performed to identify neurons. Ca^{2+} imaging analysis was then performed for neurons and non-neurons (all other cells).

2.2.8: Measurement of Ca^{2+} recording parameters

Active neurons were quantified as the percentage of neurons showing Ca^{2+} transients during a 15 min recording. Ca^{2+} transients were defined as an increase in Ca^{2+} signal of more than 10% above baseline fluorescence (after background subtraction). The frequency of Ca^{2+} transients was measured as the number of Ca^{2+} transients during 15 minutes recording. Amplitude, given as F/F°, was quantified as the ratio between the highest fluorescence value reached at the peak (F) and the basal fluorescence level of the Ca^{2+} trace (F°). Ca^{2+} influx following acute application of high KCl medium (acute KCl response) was quantified as $F^{KCl}/F°$, where F^{KCl} was the maximum fluorescence obtained immediately after KCl treatment and F° the baseline fluorescence level before stimulation. The duration of the Ca^{2+} transient was measured as the time elapsed between its onset and the time at which the Ca^{2+} signal returned to baseline levels. Area under curve was quantified by Origin graphing software as the integral of the Ca^{2+} signal (fluorescence intensity after background

deduction) relative to the baseline for the duration of the Ca^{2+} transient (fluorescence intensity.sec). The calibration for basal cytosolic Ca^{2+} level was calculated as ($F°-F_{min}/F_{max}-F°$) where F° was the baseline fluorescence, F_{max} was the maximum fluorescence following treatment with ionomycin (50 μM) and F_{min} was the minimum fluorescence achieved by the subsequent treatment of cells with saturated manganese solution (1:200).

2.2.9: Fluorescence microscopy

Chamber-slides immunostained with fluorescently labelled antibodies were analysed using Xeis-Axiophot microscope. Cell counting was performed using cell-counter manually. For measurement of neurite length, Image J software was used. The longest neurite of the neuron was selected for measurement.

2.2.10: Fluorescence activated cell sorting (FACS)

Neurosphere cultures and differentiation for TauEGFP knock-in mice were performed as described above. $5x10^6$ NPCs were plated on PLO-coated 6 cm cell culture dishes from Nunc. On DAP 1, differentiating NPCs were treated with high KCl medium for 24 hours. On DAP 2, NPCs were detached from the culture dish using 2 ml of Papain per culture dish and left at 37°C for 5 minutes following which, 4 ml of sorting medium (containing Euromed/Leibovitz medium (1:1), 2% B27, 10% FCS, 10 ng/ml human recombinant FGF2). 10% FCS was added to the sorting medium to block Papain activity. NPC suspension was centrifuged at 1000 rpm for 5 min and the pellet was resuspended in PBS containing 0.6% glucose and 10% FCS after mild trituration at the concentration of $5x10^6$ cells/0.5 ml and passed through cell strainer cap of polypropylene round-bottom tube with cell strainer cap. Viable cells were revealed by

propidium iodide, PI, (1μg/ml) exclusion. Sorting gates were set to collect cells having strongest EGFP fluorescence, (representing 3-6% of the viable cells, $EGFP^{+/-}$) and the cells displaying lower EGFP fluorescence (70-75%, $EGFP^{-/-}$). Cells were sorted using a FACSVantage (Becton Dickinson) directly into PBS-0.6% glucose containing 10% FCS and later centrifuged and resuspended in 100 μl TRIzol and frozen at -20° C.

2.2.11: Total RNA isolation and RT-PCR

Sorted $EGFP^{+/-}$ and $EGFP^{-/-}$ cells lysed in TRIzol from at least 5 independent experiments were pooled to obtain approximately 0.5-1X10^6 cells of each population and total RNA isolation was performed according to the instructions recommended by the manufacturer. In brief, 2 μg of total RNA (in 20 μl volume) was treated with 0.5 μl of RQ1 RNase-free DNase and 1 μl of RQ1 RNase-free DNase 10X Reaction Buffer as per manufacturer's instructions (Invitrogen). 1 μl of RNasin plus RNase inhibitor was added to the reaction mixture to inhibit RNase activity. To this, 2 μl M-MLV reverse transcriptase (200 u/μl), 8 μl first strand buffer (5X), 2 μl random hexamer primers (500u/ml), 4 μl dNTPs (total 40mM, each nucleotide 10mM) and 3 μl of DEPC water, were added for cDNA synthesis and samples were incubated for 2 hours at 37°C and then for 5 min at 90°C, followed by cooling on ice and storing at -20°C.

TaqMan gene expression assays for genes of interest, GAD67 (assay ID: Mm00725661_s1) and GAD65 (assay ID: Mm00484623_m1) and house keeping gene, GAPDH (assay ID: Mm99999915_g1) were purchased from Applied Biosystems. For all 4 cDNAs; from $EGFP^{+/-}$ & $EGFP^{-/-}$ from control cultures and $EGFP^{+/-}$ & $EGFP^{-/-}$ from KCl treated cultures; real time-PCR was performed for all three genes; genes of interest (GOI), GAD1 and GAD2, and house keeping

gene (HOI), GAPDH;. 3µl of 1:10 diluted cDNA was pippeted into 96 well plates. To this, 15µl of PCR-mix 2X, 1.5µl gene assay mix 20X, and 10.5 µl of DEPC water were added. Following pippeting of all the reagents, 96 well plate was sealed with the plastic foil and centrifuged for a minute to bring all solutions to the bottom of the well and to eliminate air bubbles. The RT-PCR was run in 7300 Real Time PCR system from Applied Biosystems for 45 cycles using standard programme. Ct values were obtained from the amplification plot between normalized fluorescence of Fam reporter dye of TaqMan MGB probe and cycle numbers for the PCR. Since reactions were run in triplicates, average Ct value was calculated from the three values obtained. ΔCt values were calculated as the difference between Ct value of GOI and Ct value of HKG for each cDNA. This was used to calculate relative mRNA expression of KCl treated sample vs. control sample as $2^{-(\Delta CtKCl - \Delta CtControl)}$ using Comparative Ct method (as described in the Technical bulletin on RT-PCR Basics from Ambion).

Chapter 3 : Results

3.1: Membrane depolarization regulates neuronal differentiation of striatal neural precursor cells (NPCs)

3.1.1: Generation and differentiation of neurons in striatal NPCs

E14 striatal neural precursors (NPCs) cultured in the presence of growth factors, EGF and FGF-2, form neurospheres (Reynolds BA 1992; Ciccolini F 1998; Ciccolini F 2003). Neurospheres represent a heterogeneous cell population, consisting of multipotent NPCs, developmentally more restricted progenitor cells and post-mitotic differentiated cells. Under these proliferative conditions, NPCs self-renew and also give rise to multiple cell types of the CNS (Reynolds BA 1996). Thus, neurosphere culture provides an *in-vitro* system for studying properties of NPCs.

Using this experimental approach, I have here investigated the pattern of neurogenesis and neuronal differentiation in neurons arising from striatal NPCs. To this end, one week old neurosphere-derived neural precursors were plated on poly-ornithine (PLO) coated chamber slides (day after plating 0; DAP 0) with the addition of FCS and withdrawal of growth factors. These conditions promote differentiation of NPCs into glial cells and neurons. In order to follow neurogenesis and neuronal differentiation, neurons were stained for a neuronal marker, type-III tubulin (Tuj1). One day after induction of differentiation (DAP 1), the percentage of cells that were immunopositive for Tuj1 in differentiating striatal NPC culture was 0.40±0.05% and increased to 3.57±0.19% at DAP 2 (Fig 3.1B). With time in culture, neurogenesis continued and at DAP 4 and DAP 7, the percentage of neurons was 5.28±0.49% and 8.57±0.38%, respectively. Thus, between DAP 1 and DAP 2, the percentage of neurons increases almost 10 times signifying massive neurogenesis during this time window. As newly

generated neurons attain functional maturity, they start to express neurotransmitter. Since GABA is the major neurotransmitter expressed in the ventral brain, I quantified GABA immunopositive neurons in differentiating NPCs at different stages of differentiation (Fig 3.1A). At DAP 1, the percentage of neurons (Tuj1 immunopositive) that were immunopositive for GABA was 59.53±3.49%, which decreased to 36.50±2.75% at DAP 2 (Fig 3.1C). This decrease in GABA positive neurons can be explained in the view of on-going neurogenesis between DAP 1 and DAP 2. Since there was a 10 fold increase in the number of neurons from DAP 1 to DAP 2, these newly born neurons must have expressed Tuj1, but not GABA, which is acquired at a later stage of differentiation. Hence from DAP 1 to DAP 2, the number of neurons increased whereas the number of GABA positive neurons decreased. As neurogenesis continued, the percentage of GABA positive neurons increased to 45.33±5.42% at DAP 4 and 57.63±3.60% at DAP 7 (Fig 3.1B).

Thus, in differentiating striatal NPCs, the percentage of neurons increased gradually with differentiation and represented 10% of the striatal NPC population at DAP 7. GABA expression followed Tuj1 expression in newly born neurons with a prevalence reaching 60% of neurons on DAP 7.

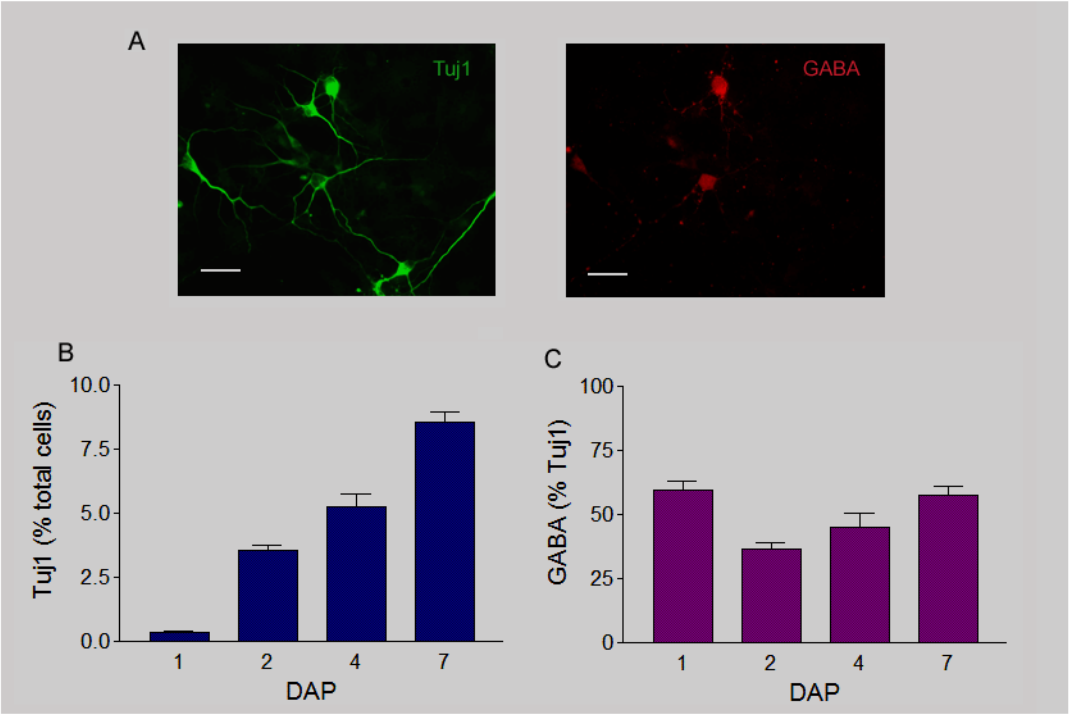

Figure 3.1: Generation and differentiation of neurons in the striatal NPCs

Panel A shows double immunopositive cells for Tuj1 (green) and GABA (red) in striatal NPCs on day after plating 2 (DAP 2). In graph B is the percentage of neurons ($Tuj1^+$) and graph C shows the percentage of GABA immunopositive neurons ($Tuj1^+$ / $GABA^+$) in striatal NPC culture on DAP 1, 2, 4 and 7. The data shown represent the mean ± SEM of at least three independent experiments. A minimum of 150 cells were analysed for each condition in each experiment.

3.1.2: Membrane depolarization regulates neuronal differentiation of striatal NPCs

In excitable cells such as muscle cells and neurons, depolarization of the membrane by action potential activates and open VGCCs to induce Ca^{2+} influx that regulates various processes such as neurotransmitter release and gene transcription (West AE 2001; Lai HC 2006). It has been previously shown that

mimicking membrane depolarization *in vitro* with 50 mM KCl induced changes in neurons differentiating from striatal NPCs. Specifically, 24 hours high KCl treatment caused pre-mature GABA acquisition and promoted neurite outgrowth (Ciccolini F 2003). To determine the minimum duration of KCl exposure required to induce changes in neuronal differentiation, I treated the NPC cultures with either high KCl medium for varying time periods (1, 3 and 6 hours) or normal differentiation medium (control; for 6 hours) on DAP 1, after which cultures were fixed and immunostained for Tuj1 and GABA. These experiments showed that the percentage of cells that were immunopositive for Tuj1 did not change following high KCl treatment (Fig 3.2A). Interestingly, high KCl treatment for 3 or 6 hours was enough to significantly increase the percentage of GABA immunopositive neurons. The percentage of neurons that were immunopositive for GABA was 74.69±12.47% for 1 hour of high KCl exposure, 82.27±6.40% for 3 hours of KCl exposure and 88.24±1.04% for 6 hours of high KCl exposure compared to 53.69±2.50% for control neurons (Fig 3.2B). Neurite length measurement showed that high KCl exposure for 6 hours led to a significant increase in neurite length, 548.97±22.71 (arbitrary units), compared to control neurons, 412.9±2.90 (Fig 3.2C). 1 and 3 hours of high KCl exposure did not induce a significant change in the neurite length.

It has been recently shown that neural activity can be directly sensed by the hippocampal NPCs via their cell surface VGCCs that open in response to depolarization (Deisseroth K 2004; Tozuka Y 2005). Thus, I tested whether activation of VGCCs acts on the level of neural precursors or differentiated neurons (Tuj1 positive cells) in differentiating striatal NPCs. To this end, parallel sets of cultures were treated with high KCl medium or normal differentiation medium (control) for different times (within a range of 3 and 24 hours) on DAP 1 and analysed at DAP 2 or DAP 4. I found that the percentage

of neurons in the cultures did not change with high KCl treatment in either cultures fixed on DAP 2 and DAP 4 (Fig 3.2D and 3.2G). This indicates that KCl did not promote selective differentiation of precursors towards a neuronal fate in preference to a glial fate. More so, no change in the percentage of neurons upon KCl treatment suggests that KCl had no effect on proliferation or the viability of the neurons. In the cultures fixed on DAP 2, high KCl treatment for 6 and 24 hours induced significant increases in the percentage of neurons that were immunopositive for GABA (46.38±4.70% and 87.47±2.54%, respectively) compared to the control neurons (30.58±2.38%) (Fig 3.2E). With respect to the neurite length, a significant increase over the control was seen only in the cultures treated with KCl for 24 hours (1091.08±60.50 arbitrary units) compared to the control neurons (768±34.33 arbitrary units) (Fig 3.2F). In contrast, no significant effect on GABA acquisition was observed when cells were fixed on DAP 4 (Fig 3.2H). By DAP 4, the neurons had acquired such long neurites which were so spread across the chamber slide and were so entangled with one another, that neurite length measurement could not be performed.

These data show that the effect of depolarization (both, percentage of GABA positive neurons and increased neurite outgrowth) is more pronounced in the cultures fixed immediately after depolarizing stimuli and decreases with increasing incubation time after the removal of depolarization. In the light of ongoing neurogenesis (section 3.1.1), the phenotypic effects of depolarization were observed in the neurons that were exposed to depolarization and not in the neurons that were born from NPCs after the removal of depolarization. Thus, depolarization directly acts on the cells that have acquired neuronal identity, and not on the NPCs, to elicit changes in GABA expression and neurite outgrowth.

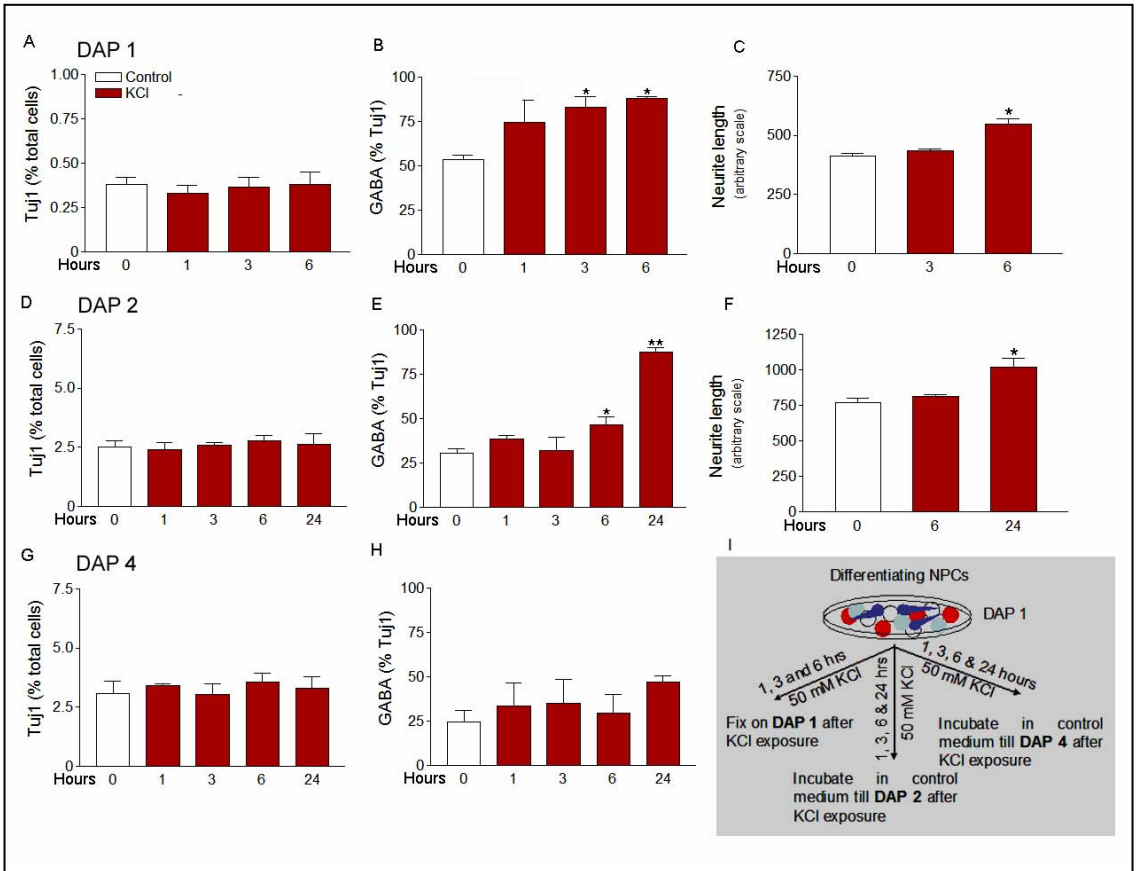

Figure 3.2: Membrane depolarization regulates neuronal differentiation of striatal NPCs

The following graphs show the percentage of neurons (Tuj1$^+$) (A, D & G), the percentage of GABA immunopositive neurons (Tuj1$^+$/ GABA$^+$) (B, E & H) and the quantification of neurite length (arbitrary units) (C & F) at DAP 1 (upper row), DAP 2 (middle row) and DAP 4 (lower row). I show a schematic representation of the experimental procedures (see materials and methods section 2.2.3 for details). The data shown represent the mean ± SEM of at least three independent experiments. A minimum of 150 cells were analysed for each condition in each experiment. Statistical analysis was done with one-way ANOVA and Newman-Keuls test. * and ** denote significantly different from control ($P< 0.05$) and ($P< 0.01$), respectively. The longest neurite of the neuron was used for neurite length measurement which was determined using ImageJ software.

3.2: Signaling involved in the regulation of neuronal differentiation by depolarization

3.2.1: Mitogen-activated protein kinase (MAPK) and Ca^{2+}-calmodulin dependent kinase (CaMK) pathways regulate depolarization-induced neurite outgrowth

It has been previously shown that along with promoting GABA expression and neurite outgrowth of striatal NPC-derived neurons, depolarization also increases the frequency of Ca^{2+} transients occurring during early stages of neuronal differentiation, thus establishing a correlation between depolarization, neuronal differentiation and Ca^{2+} transients (Ciccolini F 2003). Furthermore, the effect of depolarization on neurite outgrowth was shown to be N-methyl-D-aspartic acid receptor (NMDAR) dependent, whereas the changes in GABA expression were NMDAR independent (Ciccolini F 2003). A similar link between depolarization, neuronal differentiation and Ca^{2+} transients has been observed in other systems. For example in the *Xenopus* spinal neurons, KCl-induced Ca^{2+} transients activate calcineurin, a phosphatase that inhibits neurite outgrowth by dephosphorylating actin filaments and there-by destabilizing the cytoskeleton (Spitzer NC 2000). Increase in intracellular Ca^{2+} activates several signaling cascades discussed in section 1.4. In order to investigate the signaling molecules activated by the KCl-induced Ca^{2+} influx that mediate changes in neuronal differentiation of striatal NPCs, I used pharmacological agents to block or activate specific kinases/phosphatases that are known to be activated by Ca^{2+}. Cultures were treated on DAP 1 with high KCl medium or normal differentiation medium (control) for 24 hours, in the presence or absence of the following pharmacological agents: CaMK inhibitor, KN-62; p38 kinase inhibitor, SB203580; ERK 1 & 2 inhibitor, UO126; Akt

inhibitor, Akt I; calcineurin inhibitor, FK506; PI3kinase inhibitor, LY294002 followed by quantification for GABA expression and neurite outgrowth (Fig 3.3). Some of the inhibitors tested such as PKA inhibitors, H89 and PKI 14-22 amide and PKC inhibitor, myristoylated PKC peptide inhibitor, had cytotoxic effects on striatal NPCs and hence could not be used. Other agents were not toxic and their effects were further analysed. Analysis of GABA immunoreactivity showed that KCl-induced GABA expression was not affected by the latter group of pharmacological agents, suggesting that KCl upregulation of GABA expression does not involve these signaling pathways (Fig 3.3B). However, blockers of ERK1 and 2, UO126; p38 kinase, SB203580 and CaMKs (CaMKII, CaMKIV and CaMKI), KN-62, almost completely blocked KCl-induced increase in the neurite outgrowth (Fig 3.3A and 3.3C), suggesting that KCl-induced neurite outgrowth is mediated by MAPK (ERKs and p38 are MAPK subtypes) and CaMK pathways.

These results are consistent with the previous findings that GABA expression and neurite outgrowth are regulated by spatially distinct Ca^{2+} transients that activate distinct signaling cascades (Gu X 1995; Spitzer NC 2000; Ciccolini F 2003). Collectively, these results indicate that KCl-induced local Ca^{2+} transients, require NMDAR activity (Ciccolini F 2003) and activate MAPK and CaMK pathways leading to changes in neurite outgrowth. On the other hand, KCl-induced global Ca^{2+} transients do not require NMDAR activation and MAPK/CaMK to promote GABA expression.

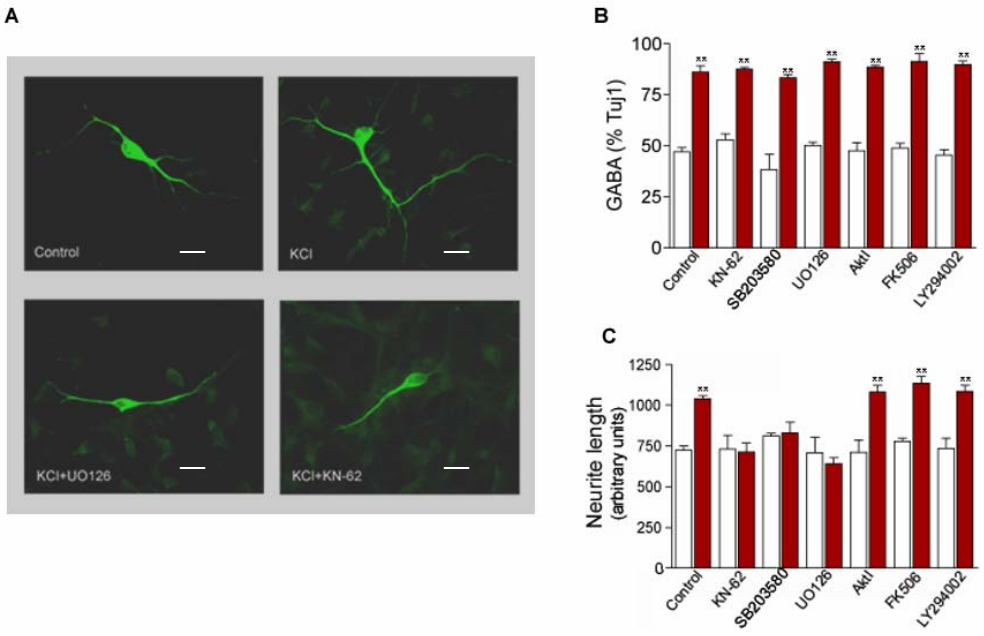

Figure 3.3: MAPK and CaMK pathways regulate depolarization-induced neurite outgrowth but not GABA expression

Panel A shows examples of neurons in striatal NPCs treated with differentiation medium or high KCl medium in the absence or presence of CaMK inhibitor, KN-62 (10 μM) and ERK 1 & 2 inhibitor, UO126 (10 μM) on DAP 1 for 24 hours (images are on same scale, white bars). Graphs B and C show the percentage of GABA immunopositive neurons ($Tuj1^+/GABA^+$) and neurite length quantification respectively, for striatal NPCs that were exposed to differentiation medium or high KCl medium on DAP 1 for 24 hours with the addition of or without the following pharmacological agents: CaMK II inhibitor, KN-62 (10 μM); p38 kinase inhibitor, SB203580 (10 μM); ERK 1 & 2 inhibitor, UO126 (10 μM); Akt inhibitor, Akt I (10 μM); calcineurin inhibitor, FK506 (1 μM); PI3kinase inhibitor, LY294002 (10 μM). The data shown represent the mean ± SEM of at least 3 independent experiments. 100-150 cells were analysed for each condition in every experiment. Statistical analysis was done with one-way ANOVA and Newman-Keuls test. * and ** denote significantly different from control ($P< 0.05$) and ($P< 0.01$), respectively. The longest neurite of the neuron was used for neurite length measurements which were made using ImageJ software.

3.2.2: Soluble amyloid precursor protein (sAPP) is involved in depolarization-induced neurite outgrowth

The amyloid precursor protein (APP) is the source of amyloid-β (Aβ) peptide that is implicated in the Alzheimer's disease. APP can be cleaved at different sites leading to the release of distinct soluble products (see section 1.4.1.2). α-secretase releases sAPPα and β-secretase releases sAPPβ into the extracellular space. Secreted forms of APP (sAPP) have been shown to have various neuroprotective functions such as enhancing neurite outgrowth of embryonic hippocampal neurons and neuroblatoma cells (Mattson MP 1997; Mattson MP 2004). Interestingly, sAPPα has been shown to bind EGFR positive neural precursor cells in SVZ and promotes their proliferation (Caille I 2004). Neural activity has been shown to enhance α-secretase activity and hence, release of sAPPα.

Due to this evidence of its effects on NPC proliferation and differentiation and neurite outgrowth under physiological conditions and upon depolarization, I tested whether sAPP modulates proliferation and differentiation of neurons arising from striatal NPCs. For this, NPC cultures were treated with high KCl medium and differentiation medium (control) for 24 hours on DAP 1, in the presence or absence of antibody against N-terminus of APP, which binds also α and β sAPP (MAB348). In parallel sets of cultures treated with differentiation medium and high KCl medium, unspecific mouse IgG fraction was added as a control for anti-APP addition. GABA positive neurons and neurite outgrowth were quantified on DAP 2. Addition of the blocking antibody did not have any effect on the percentage of neurons that were positive for GABA, but abolished KCl-induced increase in the neurite outgrowth (Fig 3.4A, 3.4C and 3.4D), without altering the percentage of neurons in culture (Fig 3.4B). I next blocked

sAPP production with GM6001 that inhibits metallo-proteinsases, α and β secretases. Consistent with the data obtained with blocking antibodies, the addition of GM6001 to striatal NPCs exposed to high KCl medium on DAP 1 for 24 hours blocked the effect of KCl on neurite length (Fig 3.5A).

Since sAPPs are known to be secreted from almost all cell types under normal physiological conditions (Mattson MP 1997), I next checked whether differentiating striatal NPCs secrete sAPPα and sAPPβ. I also asked whether neural activity promotes α-secretase cleavage of APP and therefore, increases secretion of sAPPα as shown previously (Nitsch R 1993). To this end, NPCs were plated on PLO-coated 6 well plates. On DAP 1, cultures were exposed to high KCl medium or differentiation medium. Media and cell lysates were collected either 1 hour or 24 hours after the medium change. The collected samples were analysed by SDS-PAGE, followed by western blot and ECL reaction (using MAB348 antibody recognizing N-terminus APP) to visualize sAPP bands. I found that sAPP (110 KD) bands were stronger in the medium collected from the culture that was incubated for 24 hours with either control or KCl treatment as compared to the medium from corresponding treatment for 1 hour (Fig 3.5B). In contrast, the bands in the cell lysates collected after 1 hour and 24 hour samples were not different (Fig 3.4C). This shows that sAPP is accumulated in the media during 24 hours incubation period (Fig 3.5B). Due to the fact that sAPPα and sAPPβ differ in size by only 16 amino acids, this type of analysis is only suitable for qualitative but not for a quantitative assessment. Thus, a shift from β to α cleavage could not be quantified.

Taken together these data suggest that inhibiting sAPP with the blocking antibody or α and β–secretase, blocks depolarization-induced increase in the neurite outgrowth. This suggests that depolarization promotes the cleavage and release of sAPP by α and/or β-secretase. Alternatively, depolarization

might also enhance the interaction of sAPPα with its unknown receptor (Caille I 2004).

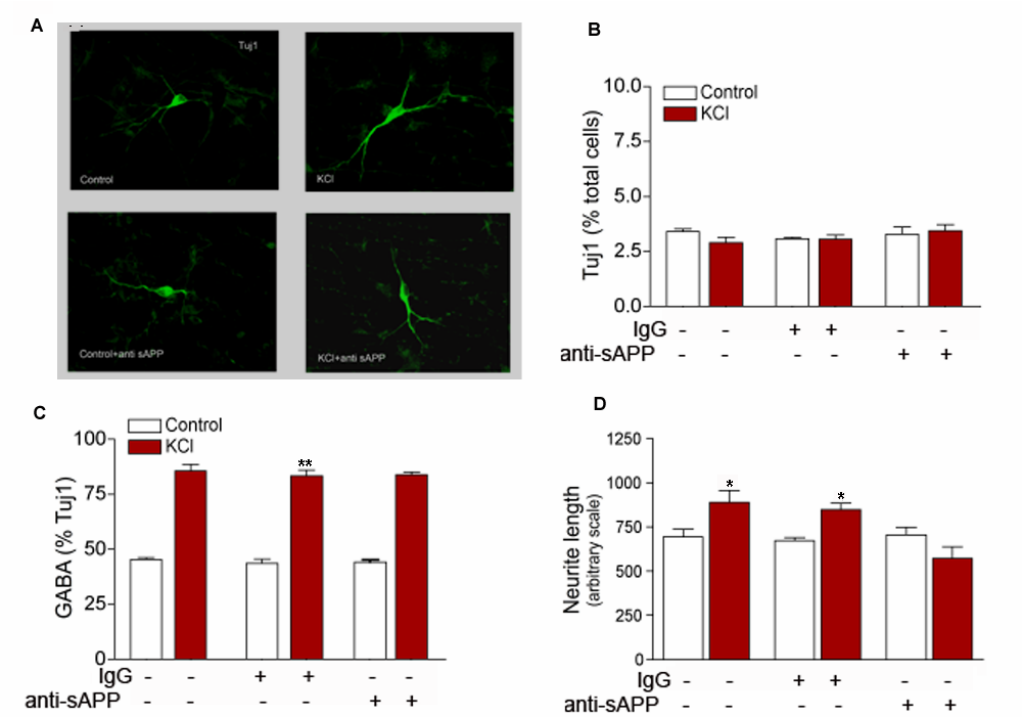

Figure 3.4: anti-APP inhibits depolarization-induced neurite outgrowth

Panel A shows examples of neurons differentiating from striatal NPCs. The NPCs were exposed to differentiation medium or high KCl medium with or without addition of anti-APP for 24 hours on DAP 1 (images are on same scale). Unspecific mouse IgG antisera was added to parallel cultures as a control for anti-APP addition. Graphs B, C and D show the percentage of Tuj1 immunopositive cells, the percentage of GABA immunopositive neurons and neurite length respectively, in cultures exposed to differentiation medium or high KCl with addition of anti-APP or human-IgG fraction as shown in panel A. The data shown represent the mean ± SEM of at least three independent experiments. A minimum of 75-100 cells were analysed for each condition in each experiment. Statistical analysis was done with one-way ANOVA and Newman-Keuls test. * and ** denote significantly different from control ($P< 0.05$) and ($P< 0.01$), respectively. The longest neurite of a neuron was considered for neurite length measurement using ImageJ software.

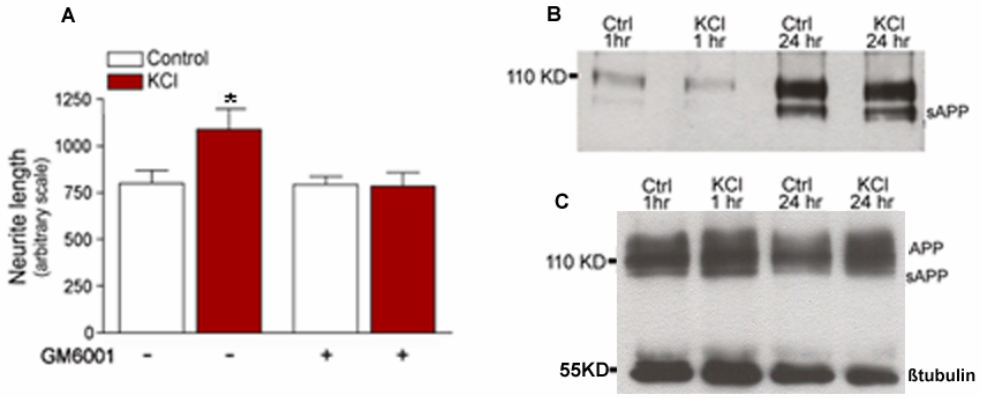

Figure 3.5: The secretase inhibitor, GM6001, blocks depolarization-induced neurite outgrowth

Graph A shows quantification of neurite length in striatal NPCs exposed to high KCl medium or differentiation medium with or without the addition of α and β-secretase inhibitor, GM6001, on DAP 1 for 24 hours. Panel B and C show western blot analyses of media (B) and cell lysates (C) of striatal NPCs incubated with differentiation medium or high KCl medium. Media and the cell lysates were collected either after 1 hour or 24 hours. The data shown represents the mean ± SEM of at least three independent experiments. A minimum of 75-100 cells were analysed for each condition in each experiment. Statistical analysis was done with one-way ANOVA and Newman-Keuls test. * denotes significantly different from control ($P < 0.05$). The longest neurite of the neuron was considered for neurite length measurement using ImageJ software.

3.2.3: Transcription and translation are not required for depolarization-induced changes in neuronal differentiation

As discussed in the previous section, depolarization-induced global Ca^{2+} transients regulate GABA expression during neuronal differentiation of striatal NPCs (Ciccolini F 2003). In *Xenopus* spinal neurons, the frequency of global Ca^{2+} transients (spontaneous and evoked) regulates GABA expression by modulating the transcription of glutamic acid decarboxylase (GAD: the GABA

forming enzyme) (Watt SD 2000). Moreover, in the nervous system many activity-dependent changes are mediated by regulation of gene transcription by Ca^{2+} (Bading H 2000). Thus, I next analyzed the involvement of gene transcription and translation in KCl-induced changes in neuronal differentiation. The CREB family of transcription factors is one of the major targets of Ca^{2+} signaling and upon Ca^{2+} influx is activated by phosphorylation on serine 133 (pCREB) (Xing J). To test whether CREB is activated following KCl exposure, differentiating striatal NPCs were treated with high medium KCl on DAP 1 for varying times (10 and 30 minutes, 1, 3 and 6 hours) or with differentiation medium for 6 hours. Within 10 minutes, KCl induced a significant increase in the percentage of neurons immunopositive for pCREB (73.3±12.02% compared to 13.87±8.53% in control neurons) (Fig 3.6A and 3.6B). This increase showed a bell shaped curve that started to return to baseline after 3 hours of KCl exposure (Fig 3.6A and 3.6B). To directly test whether pCREB is involved in KCl-stimulated GABA expression, I analyzed CREB knock out mice with a $Crem^{-/-}$ background ($Creb^{Nescre}Crem^{-/-}$ mice) (Mantamadiotis T 2002). CREB and CREM are the two main CREB family members expressed in the brain and CREM has been shown to compensate for the loss of CREB (Mantamadiotis T 2002). Hence, I used double knock-out for my experiments. NPCs were derived from wild type ($Crem^{-/+}$ $Creb^{+/+}$, WT), single mutant ($Crem^{-/-}$ $Creb^{+/+}$, $M^{-/-}B^{+/+}$) and double mutant ($Crem^{-/-}$ $Creb^{-/-}$, $M^{-/-}B^{-/-}$) mice. Loss of CREB was confirmed by western blot analysis (Fig 3.6C). I found that the absence of CREB (and/or CREM) did not prevent the effect of depolarization on GABA expression and neurite length (Fig 3.6D, 3.6E). Thus, although KCl promotes CREB activation specifically in neurons, it is not involved in depolarization-induced GABA expression and neurite outgrowth.

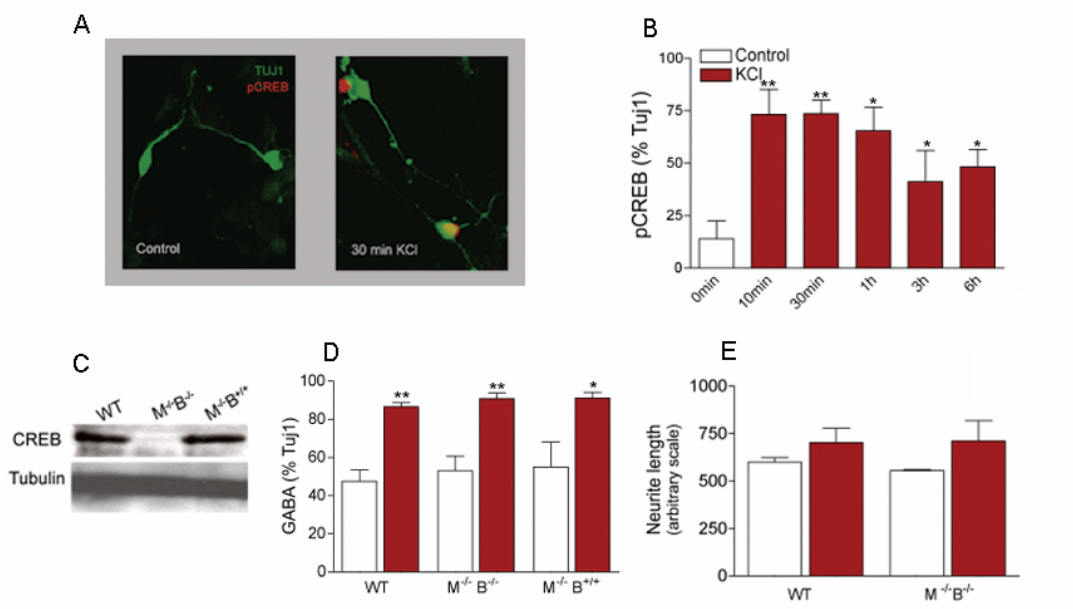

Figure 3.6: CREB is not involved in regulation of depolarization-induced GABA expression and neurite outgrowth

Panel A shows double immunopositive cells for Tuj1 and pCREB in striatal NPCs exposed to differentiation medium or high KCl medium for 30 min on DAP 1. Graph B shows the percentage of neurons showing pCREB immunopositivity ($Tuj1^{+}/pCREB^{+}$) in striatal NPCs exposed to differentiation medium or high KCl medium on DAP 1 for different time periods; 10 min, 30 min, 1 hour, 3 hours and 6 hours. In C is the western blot analysis of CREB knockout embryos. Wild type, $Crem^{-/+}$ $Creb^{+/+}$ (WT); double mutant, $Crem^{-/-}$ $Creb^{-/-}$ ($M^{-/-}B^{-/-}$) and single mutant, $Crem^{-/-}$ $Creb^{+/+}$ ($M^{-/-}B^{+/+}$) are the genotypes tested here. In graphs D and E are the percentage of GABA immunopositive neurons ($Tuj1^{+}/GABA^{+}$) and quantification of neurite length respectively, for striatal NPCs from WT, $M^{-/-}B^{-/-}$ and $M^{-/-}B^{+/+}$ embryos. NPC cultures with these genetic backgrounds were exposed to differentiation medium or high KCl medium for 24 hours on DAP 1. The data shown represent the mean ± SEM of at least three independent experiments. A minimum of 75-100 cells were analysed for each condition in each experiment. Statistical analysis was done with one-way ANOVA and Newman-Keuls test. * and ** denote significantly different from control ($P< 0.05$) and ($P< 0.01$), respectively. The longest neurite of a neuron was considered for neurite length measurement using ImageJ software.

Next I tested whether KCl exposure increases GABA expression by modulating GAD transcription. GAD 67 and GAD 65 are two isoforms of GAD that have different cell localization, GAD 67 being cytosolic and GAD 65 being membrane associated (Wei J 2004). To test whether depolarization modulates GAD transcription, I performed real time PCR to compare levels of GAD 65 and 67 mRNAs in neurons that had been exposed to KCl compared to the un-stimulated neurons. For these experiments, I took advantage of the transgenic mice expressing EGFP specifically in neurons under the control of the tau promoter (Tucker KL 2001). One week old NPC cultures were plated on PLO-coated 6 well plates. On DAP 1, the cultures were exposed to high KCl medium or differentiation medium for 24 hours. The cultures were processed for the isolation of EGFP positive neurons from EGFP negative non-neurons (representing precursors) by fluorescence activated cell sorting (FACS) on DAP 2 (Fig 3.7A), followed by total RNA isolation, cDNA synthesis and RT-PCR. Using this approach I found that the relative increase in mRNA expression (in KCl treated cultures compared to unstimulated cultures) for GAD 67 in neurons was 2.05±0.21% and in non-neurons was 2.32±0.49% (Fig 3.7, Table 3.1). Similarly, for GAD 65 the relative mRNA expression was 1.87±0.56% in neurons and 1.03±0.06% in non-neurons. Thus, the increase in the mRNA expression with KCl treatment in both, neurons and non-neurons, for GAD 67 and GAD 65 was around 2 fold (not significant). Hence, KCl treatment does not have a significant effect on GAD transcription and KCl promotion of GABA expression is mediated by another mechanism independent of GAD transcription.

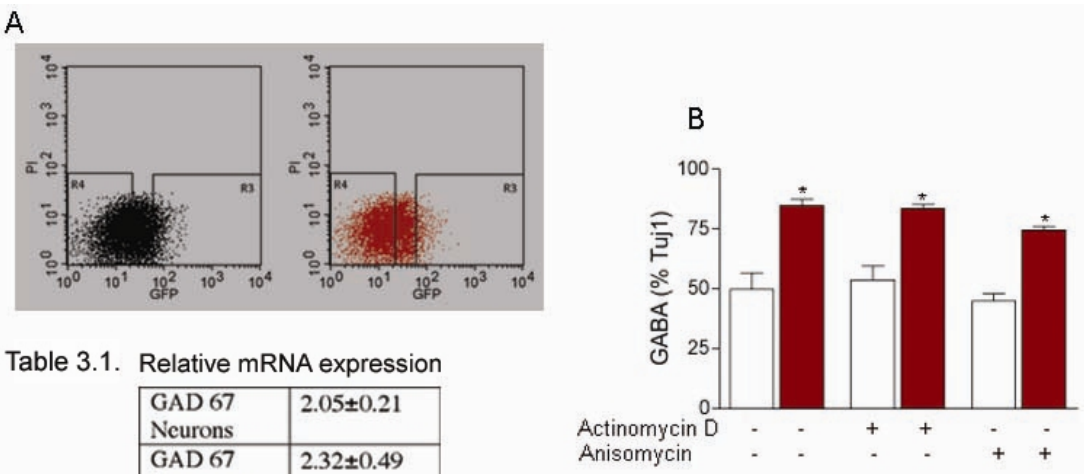

Table 3.1. Relative mRNA expression

GAD 67 Neurons	2.05±0.21
GAD 67 Non-neurons	2.32±0.49
GAD 65 Neurons	1.87±0.56
GAD 65 Non-neuons	1.03±0.06

Figure 3.7: Transcription and translation are not required for depolarization-induced changes in neuronal differentiation

Panel A shows FACS plots of striatal NPCs from tau-EGFP embryos ($EGFP^{+/-}$). The cultures were either exposed to differentiation medium (black) or high KCl medium (red) for 24 hours on DAP 1. R3 gate shows $EGFP^{+/-}$ neurons and R4 gate shows $EGFP^{-/-}$ non-neurons. Table 3.1 shows relative mRNA expression of GAD 67 and GAD 65 mRNA in $EGFP^{+/-}$ neurons and $EGFP^{-/-}$ non-neurons. The relative mRNA expression in KCl treated cultures compared to control cultures was calculated as $2^{-(\Delta CtKCl\ -\ \Delta CtControl)}$ using comparative Ct method. In graph B is the percentage of GABA immunopositive neurons ($Tuj1^{+}/GABA^{+}$) in striatal NPC cultures that were exposed to differentiation medium or high KCl medium, with or without the addition of transcription blocker, actinomycin D (10 μM) and translation blocker, anisomycin (10 μg/ml), on DAP 2 for 6 hours. The data shown represent the mean ± SEM of at least three independent experiments. A minimum of 75-100 cells were analysed for each condition in each experiment. Statistical analysis was done with one-way ANOVA and Newman-Keuls test. * denotes significantly different from control ($P< 0.05$).

I next tested whether KCl induced changes in neuronal differentiation required transcriptional or translational regulation of any genes other than GAD. To do so, NPCs were treated with high KCl medium or differentiation medium in the

presence or absence of transcription blocker, actinomycin D, and translation blocker, anisomycin, for 6 hours on DAP 2. Incubation of NPC cultures for more than 6 hours with these blockers showed cytotoxic effects. Therefore, cultures were exposed to transcription and translation blocker only for 6 hours on DAP 2. Even with 6 hours exposure, these blockers had minor cytotoxic effects and therefore, neurite length measurements were not performed. Quantification of the percentage of neurons immunopositive for GABA showed that KCl induced a similar increase in GABA acquisition in the presence of actinomycin D and anisomycin as in the absence of any drug (Fig 3.7B). Taken together these data show that the KCl-induced changes in neuronal differentiation are independent of gene transcription and translation and therefore, involve a post-translational mechanism.

3.3: Spontaneous and depolarization-evoked Ca^{2+} transients in neurons and precursors of striatal NPCs

3.3.1: Spontaneous and KCl-evoked global Ca^{2+} transients in neurons and non-neurons in differentiating striatal NPCs

As discussed above, a correlation between Ca^{2+} transients and neuronal differentiation has been shown previously (Ciccolini F 2003). In this previous work, Ca^{2+} transients were analysed in the entire differentiating NPC population and not specifically in the neurons. Therefore, the relationship between Ca^{2+} transients, membrane depolarization and neuronal differentiation was not clarified. In this dissertation, I have instead analysed global Ca^{2+} transients specifically in neurons differentiating in the presence or absence of depolarization. If global Ca^{2+} transients, spontaneous or depolarization-induced, are able to modulate the acquisition of a GABA phenotype, then Ca^{2+}

transients must precede GABA expression. For this reason, I performed Ca^{2+} imaging experiments on DAP 1 instead of DAP 2 when neuronal phenotype (GABA expression and neurite length) is analysed in previous experiments. To do so, one week old neurosphere-derived striatal NPCs were plated on PLO-coated graded cover slips to allow retrospective cell identification following Ca^{2+} imaging. On DAP 1, the medium was changed to Ringers solution and the NPCs were loaded with Fluo-3 AM. Ca^{2+} imaging was recorded for 15 minutes using an Olympus upright microscope. After imaging cells were fixed and immunostained for Tuj1 to identify neurons (Fig 3.8A). All the cells identified as neurons showed spontaneous global Ca^{2+} transients in fifteen minutes of imaging (Fig 3.8B). These transients in Tuj1 positive cells showed amplitude of 1.31±0.07 (F/F°), a frequency of 3.55±0.69 transients/neuron/15 min recording and a duration of 0.66±0.07 minutes (Table 3.2 and Fig 3.9A). To better represent the kinetics of the spontaneous variation of intracellular Ca^{2+} concentrations, I also measured the area between the line marking the resting fluorescence level and the one describing the fluorescence increase over time (area under curve) calculated as the integral of the Ca^{2+} signal during the transient (Table 3.2). The area under curve for global Ca^{2+} transients in neurons was 185±53.00 fluorescence intensity.sec (Table 3.2).

To investigate the effect of depolarization on Ca^{2+} transients in such neurons differentiating from striatal NPCs, similar experiments were performed on NPC cultures that were pre-incubated in high KCl medium for 6 hours on DAP 1. Cells were incubated in high KCl-Ringers solution during Fluo-3 AM loading as well as during Ca^{2+} imaging. As observed in neurons imaged under control conditions, all neurons exposed to KCl displayed Ca^{2+} transients (Fig 3.8C). KCl treatment did not significantly change the amplitude and duration compared to control neurons (Table 3.2). However, KCl treated neurons showed more than

two-fold increase in the frequency of Ca^{2+} transients and the area under curve. The frequency of Ca^{2+} transients in KCl treated neurons was 8.57±1.03 transients/neuron/15 min compared to 3.55±0.69 transients/neuron/15 min in unstimulated neurons (Table 3.2 and Fig 3.9A). The area under curve in KCl treated neurons was 419.41±71.00 fluorescence intensity.sec compared to 185±53.00 fluorescence intensity.sec in unstimulated neurons (Table 3.2).

Ca^{2+} transients were also observed in Tuj1 negative cells that represented striatal precursors and glial cells. I found that 37.14% of the non-neurons showed Ca^{2+} transients under control conditions (Table 3.3). More so, 6 hours KCl exposure led to an increase in the percentage of active non-neurons from 37.14% to 56.00% (Table 3.3). Interestingly, as observed in neurons, KCl treatment increased the frequency of Ca^{2+} transients in non-neuronal cells to more than two fold of unstimulated non-neuronal cells (Table 3.3). The frequency of Ca^{2+} transients in unstimulated non-neurons was 3.43±0.49 transients/neuron/15 min whereas it was 6.13±0.94 transients/neuron/15 min in KCl-treated non-neurons (Table 3.3). To test whether there is a change in basal intracellular Ca^{2+} concentration upon depolarization, I calibrated the basal fluorescence of striatal NPCs incubated in differentiation and high KCl medium for 6 hours. The calibration involved treating striatal NPC cultures with the ionophore, ionomycin and the quencher of Fluo-3 fluorescence, manganese, during imaging. Thus, the cells were damaged after treatment with these reagents and could not be stained for Tuj1 following Ca^{2+} imaging. For this reason, neurons could not be identified among heterogeneous NPCs and calibrated calcium levels were calculated for entire NPC populations. I found that the calibrated Ca^{2+} levels in KCl treated cultures (0.22±0.04) was not significantly different from unstimulated cultures (0.26±0.01) (Table 3.4).

These data show that spontaneous Ca^{2+} transients occur in differentiating neurons and non-neurons and that membrane depolarization increases the frequency of Ca^{2+} transients of both neuronal and non-neuronal precursors. However, whereas 100% of the neurons analysed showed Ca^{2+} transients under both control and depolarization conditions, only 56.00% of the non-neurons showed Ca^{2+} transients.

Treatment	Active neurons	Frequency (transients/neuron per15 min)	Area Under Curve (intensity.sec)	Amplitude (F/F°)	Acute KCl response (% of neurons)	Acute KCl response (F^{KCl}/F°)	Duration (min)
Ctrl	100%	3.55±069	185±53.00	1.31±0.07	100%	2.53±0.29	0.66±0.07
KCl	100%	8.57±1.03	419.41±71.0	1.15±.02			0.56±0.05
Ctrl+Nif	42.86%	1.86±1.10	48.2±18.80	1.13±.02	100%	1.60±0.34	0.90±0.19
KCl+Nif	71.43%	2.73±1.09	145±51.30	1.20±.05			0.64±0.11

Table 3.2: Characterization of spontaneous and depolarization-induced Ca^{2+} transients in neurons

Table 3.2 shows various parameters analysed for spontaneous and KCl-induced Ca^{2+} transients in neurons differentiating from striatal NPC cultures that were exposed to differentiation medium (Ctrl) or high KCl medium (KCl) for 6 hours, with or without the addition of L-type VGCC blocker, nifedipine (10 μM) on DAP 1. The data shown represent the mean ± SEM of at least three independent experiments. A minimum of 10-15 neurons were analysed for each condition.

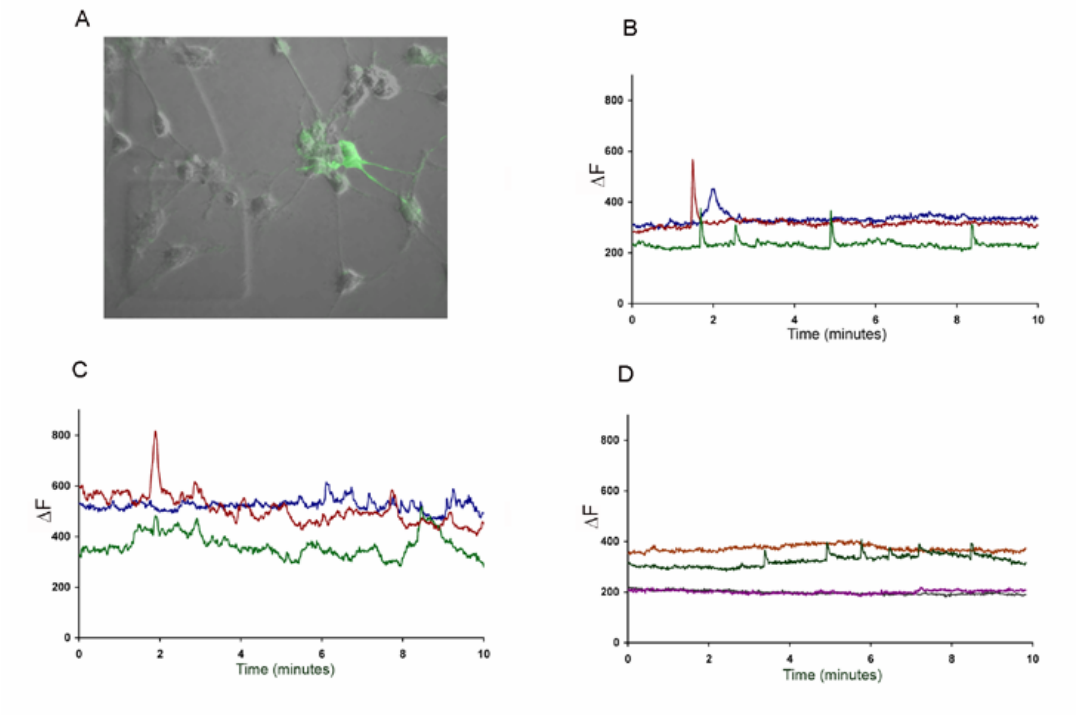

Figure 3.8: Spontaneous and depolarization-induced Ca^{2+} transients in neurons differentiating from striatal NPCs

Panel A shows a merge of DIC (grey) and Tuj1 immunostaining for neurons (green) in striatal NPC culture on DAP 1. The traces show the time course of Ca^{2+} transients in neurons that were exposed to differentiation medium (B) or high KCl medium (C) or incubated with L-type VGCC blocker, nifedipine (10 μM)(D), in the differentiation medium for 6 hours on DAP 1. ΔF represents the fluorescence intensity after background reduction.

Treatment	Active non-neurons	Frequency (transients/neuron per15 min)	Amplitude (F/F°)	Acute KCl response (% cells)	Acute KCl response ($F^{KCl}/F°$)	Duration (min)
Ctrl	37.14%	3.43±0.49	1.22±0.03	80%	1.52±0.29	1.13±0.15
KCl	56.00%	6.13±0.94	1.18±0.04			0.74±0.08
Ctrl+Nif	31.00%	3.36±0.64	1.18±0.05	16%	1.06±0.01	1.95±0.21
KCl+Nif	26.00%	3.39±0.50	1.33±0.14			0.63±0.07

Table 3.3: Characterization of spontaneous and depolarization-induced Ca^{2+} transients in non-neurons

Table 3.3 shows various parameters analysed for spontaneous and KCl-induced Ca^{2+} transients in non-neurons in striatal NPC cultures that were exposed to differentiation medium (Ctrl) or high KCl medium (KCl) for 6 hours, with or without the addition of L-type VGCC blocker, nifedipine (10 μM) on DAP 1. The data shown represent the mean ± SEM of at least two independent experiments where minimum of 20-25 non-neurons were analysed for each condition in each experiment.

Table 3.4: Calibration for cytosolic Ca^{2+} level

Treatment	Calibrated Ca^{2+} level
Ctrl	0.26±0.01
KCl	0.22±0.04
Ctrl+Nif	0.28±0.08
KCl+Nif	0.26±0.33

Table 3.4 shows calibrated Ca^{2+} levels ((Fmax-F)/(F-Fmin)) in striatal NPC cultures that were exposed to differentiation medium (Ctrl) or high KCl medium (KCl) for 6 hours, with or without the addition of L-type VGCC blocker, nifedipine (10 μM) on DAP 1. The data shown represent the mean ± SEM of at least three independent experiments where minimum of 20-25 cells were analysed for each condition in each experiment.

3.3.2: Involvement of L-type VGCC in spontaneous and KCl-evoked global Ca^{2+} events

During Ca^{2+} transients, Ca^{2+} can enter the cells through various cell-surface Ca^{2+} channels (section 1.1). In particular, Ca^{2+} entry from L-type VGCCs may be crucial for neuronal differentiation of NPCs (Deisseroth K 2004; D'Ascenzo M

2006). In order to investigate the role of L-type VGCCs in spontaneous and KCl-induced global Ca^{2+} transients, I performed pharmacological modulation of L-type VGCCs with specific antagonists and agonists. One week old neurospheres were plated on PLO-coated graded cover slips. On DAP 1, differentiating NPCs were pre-incubated with differentiation medium or high KCl medium for 6 hours, in the presence or absence of L-type VGCC antagonist, nifedipine. In the cultures exposed to nifedipine for 6 hours, nifedipine was added also during Fluo-3 AM loading and Ca^{2+} imaging. In the presence of nifedipine, the percentage of active neurons was reduced in both, unstimulated (from 100% to 42.86%) and KCl-treated (from 100% to 71.43%) NPCs (Table 3.2) Nifedipine also reduced the frequency of Ca^{2+} transients in unstimulated neurons, from 3.55±0.69 transients/neuron/15 min to 1.86±1.10 transients/neuron/15 min, and in KCl treated neurons, from 8.57±1.03 transients/neuron/15 min to 2.73±1.09 transients/neuron/15 min (Fig 3.9A and Table 3.2). The area under curve was also reduced in the presence of nifedipine in unstimulated neurons, from 185.00±53.00 fluorescence intensity.sec to 48.22±18.80 fluorescence intensity.sec, as well as in KCl treated neurons, from 419.41±71.00 fluorescence intensity.sec to 145.00±51.30 fluorescence intensity.sec (Table 3.2). In contrast, the duration, amplitude, and calibrated Ca^{2+} level were not significantly affected by nifedipine in neurons (Table 3.2 and Table 3.4).

In the non-neurons, nifedipine caused a reduction in the percentage of active cells in the KCl treated NPCs (from 56% in KCl treated cultures to 26% in KCl and nifedipine treated cultures) (Table 3.3), whereas it did not significantly effect the percentage of active cells in control NPC cultures. The duration, amplitude, and calibrated Ca^{2+} level were not significantly affected by nifedipine in non-neurons (Table 3.3 and Table 3.4).

To quantify the proportion of Ca^{2+} influx mediated by L-type VGCCs upon high KCl exposure, I measured Ca^{2+} influx occurring in response to acute high KCl treatment (acute KCl response) during Ca^{2+} imaging in NPC cultures pre-incubated with nifedipine for 6 hours (control+nif) or left untreated (control). All neurons analysed, whether control or nifedipine treated, showed Ca^{2+} influx in response to acute KCl perfusion (Table 3.2). The acute KCl response, given as $F^{KCl}/F°$, was 2.53±0.29 in control neurons and was 1.60±0.34 in control+nif neurons, representing a 36.60% smaller response (Fig 3.9B, Table 3.2). In contrast, nifedipine decreased the percentage of non-neurons that showed Ca^{2+} influx in response to acute KCl treatment drastically. Whereas 80.00% of non-neurons responded to acute KCl under control conditions, only 16.00% of control+nif non-neurons responded to acute KCl application. However, the amplitude of the acute KCl response was not significantly different in control and nifedipine treated non-neurons (1.52±0.29 for control non-neurons and 1.06±0.01 for those pre-incubated with nifedipine) (Table 3.3). Interestingly, acute KCl response was significantly larger in neurons (2.53±0.29) than in non-neurons (1.52±0.29) (Table 3.2 and 3.3).

These results demonstrate that a major fraction of global spontaneous Ca^{2+} transients in neurons are L-type VGCC-dependent, whereas global spontaneous Ca^{2+} transients in non-neurons are not L-type VGCC mediated. However, depolarization induces L-type VGCC-dependent global Ca^{2+} transients in neurons as well as non-neurons. Interestingly, L-type VGCCs account for only one-third of KCl-induced Ca^{2+} influx in neurons, the remainder presumably being mediated by nifedipine insensitive VGCCs. In contrast, most of the depolarization-induced Ca^{2+} influx in non-neurons is L-type VGCC-dependent.

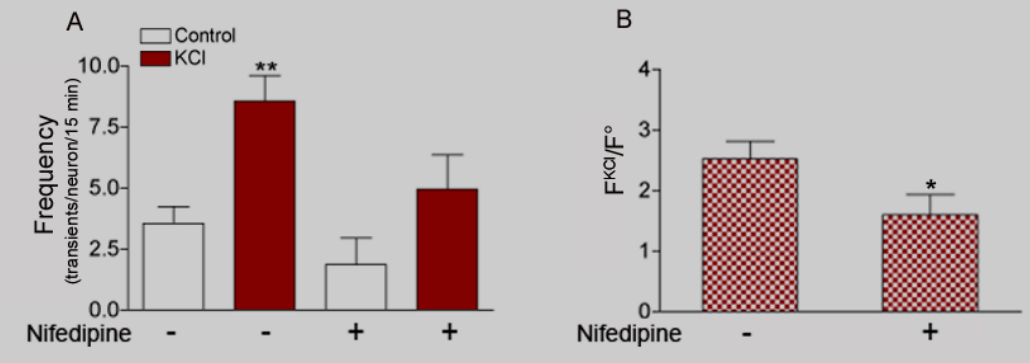

Figure 3.9: L-type VGCCs contribute to spontaneous and depolarization-induced Ca^{2+} transients in NPC derived-neurons

Graph A shows the frequency of Ca^{2+} transients (transients/neuron/15 min) in striatal NPC-derived neurons that were exposed to differentiation medium or high KCl medium, in the presence or absence of L-type VGCC blocker, nifedipine (10 μM), on DAP 1 for 6 hours. In the cultures treated with nifedipine, nifedipine was included in all solutions during Fluo-3 AM loading and Ca^{2+} imaging. Graph B shows the measurement of Ca^{2+} influx induced by acute application of high KCl-Ringers solution in striatal NPC-derived neurons during Ca^{2+} imaging on DAP 1. F^{KCl} is the highest fluorescence reached upon KCl application and F° is the basal cytosolic fluorescence. The data shown represents the mean ± SEM of at least three independent experiments with an average of 10-15 neurons analysed for each condition. Statistical analysis was done with one-way ANOVA and Newman-Keuls test. * and ** denote significantly different from control ($P< 0.05$) and ($P< 0.01$), respectively.

3.4: Regulation of GABA expression by depolarization-induced Ca^{2+} influx in neurons differentiating from striatal NPCs

3.4.1: Depolarization-induced changes in GABA expression are dependent on extracellular Ca^{2+}

As discussed above, depolarization promotes acquisition of GABA phenotype (section 3.1.2 and (Ciccolini F 2003)) and also increases the frequency of Ca^{2+} transients in striatal NPCs-derived neurons (section 3.3.1). Since there is a correlation between the effect of depolarization on GABA and increase in the frequency of Ca^{2+} transients, it is conceivable that depolarization-induced Ca^{2+} influx modulates GABA expression. To test this hypothesis I exposed differentiating striatal NPCs to KCl in the absence of extracellular Ca^{2+} to block KCl-induced Ca^{2+} influx. A week old neurospheres were plated on PLO-coated chamber slides in differentiation medium with 2 mM Ca^{2+} concentration. On DAP 2, cultures were washed with Ca^{2+} -free DME-F12 medium. Control cultures were washed with the differentiation medium with 2 mM Ca^{2+}. The cultures were then exposed to high KCl medium without Ca^{2+} or high KCl medium with 2 mM Ca^{2+} for 6 hours. I found that KCl exposure in the absence of extracellular Ca^{2+} failed to induce GABA expression showing that the effects of KCl on neuronal differentiation require extracellular Ca^{2+} (the percentage of GABA positive neurons was 28.02±3.02 in KCl treated cultures compared to 21.62±2.38 in unstimulated cultures) (Fig 3.10A). Moreover, the percentage of GABA immunopositive neurons was lower in the unstimulated cultures incubated in the absence of Ca^{2+} (21.62±2.38) than those incubated in the presence of Ca^{2+} (34.89±2.50) (Fig 3.10A), suggesting that extracellular Ca^{2+} is essential for normal GABA expression during the differentiation of striatal NPCs.

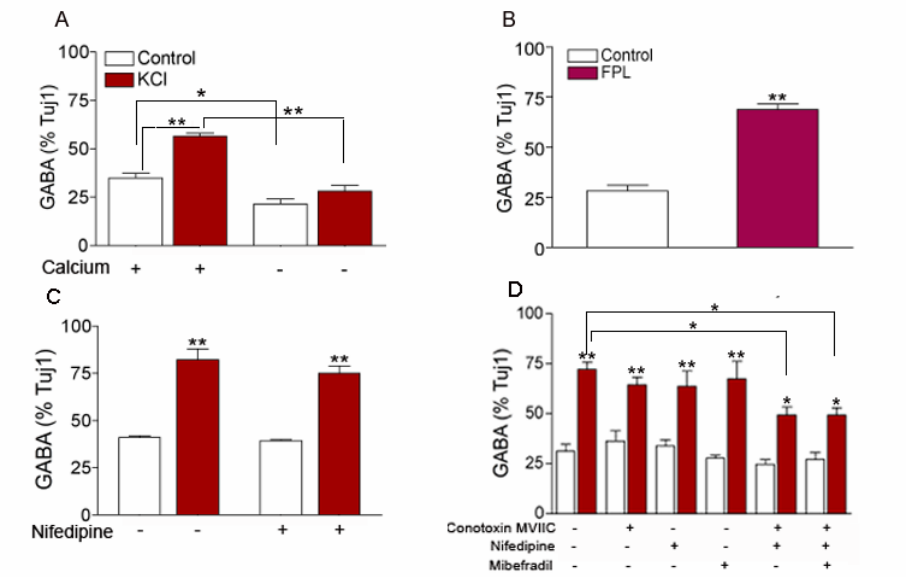

Figure 3.10: Ca^{2+} influx is crucial for depolarization- induced GABA expression

Graph A shows the percentage of GABA immunopositive neurons ($GABA^+/Tuj1^+$) in striatal NPCs in which medium change was performed to Ca^{2+} free or normal differentiation medium and the cultures were exposed to differentiation medium or high KCl medium containing Ca^{2+} or without Ca^{2+} for 6 hours on DAP 2. Graph B shows the percentage of $GABA^+/Tuj1^+$ neurons in striatal NPCs incubated in the absence or presence of L-type VGCC agonist, FPL 64176 (1 μM), 24 hours on DAP 1. Graph C shows the percentage of $GABA^+/Tuj1^+$ neurons in striatal NPCs pre-incubated with L-type VGCC antagonist, nifedipine (10 μM), for 1 hour before treatment with high KCl or differentiation medium (with the readdition of nifedipine) on DAP 1 for 24 hours. Graph D shows the percentage of $GABA^+/Tuj1^+$ neurons in striatal NPCs incubated with 1 or more VGCC antagonists on DAP 1: N and P/Q type VGCC blocker, ω-conotoxin MVIIC (1 μM); T-type VGCC blocker, mibefradil hydrochloride (1 μM) and nifedipine (10 μM). The cultures were then exposed to high KCl medium or differentiation medium with the readdition of same concentration of VGCC antagonists and incubated for 24 hours. The data shown represents the mean ± SEM of at least 3 independent experiments with an average of 75-100 cells analysed for each condition in every experiment. Statistical analysis was done with one-way ANOVA and Newman-Keuls test. * and ** denote significantly different from control ($P< 0.05$) and ($P< 0.01$), respectively.

3.4.2: A brief VGCC-dependent Ca^{2+} influx is sufficient to trigger changes in GABA expression

Having established a direct relation between KCl-induced Ca^{2+} influx and KCl-induced GABA expression (section 3.4.1), I next tested the role of L-type VGCC in mediating KCl-induced changes in GABA expression because of their role in mediating spontaneous and KCl-induced Ca^{2+} transients. To this end, I incubated differentiating NPCs with the L-type VGCC agonist, FPL 64176, on DAP 1 for 24 hours. A parallel culture was washed with unstimulated medium on DAP 1 and incubated for 24 hours. I found that FPL 64176 treatment increased the percentage of GABA immunopositive neurons, similar to the effect of KCl (Fig 3.10B). The percentage of GABA immunopositive neurons in FPL 64176 treated cultures was 68.87±2.79% compared to 28.25±2.75% in control cultures. Next, I repeated the same experiment but with nifedipine addition instead of FPL 64176. Differentiating striatal NPCs were pre-incubated with nifedipine for 1 hour or left-untreated and then exposed to high KCl medium or differentiation medium (with or without nifedipine) on DAP 1 for 24 hours. Surprisingly, the blockade of L-type VGCC with nifedipine did not inhibit or decrease the KCl-induced increase in GABA (Fig 3.10C). Since 63.4% of the acute KCl-induced Ca^{2+} influx occurs through nifedipine insensitive VGCCs (section 3.3.2), it is conceivable that KCl-induced Ca^{2+} influx through nifedipine insensitive VGCCs is sufficient to induce early GABA acquisition. To test this, I used pharmacological antagonists of other VGCCs; N and P/Q type VGCC antagonist, ω-conotoxin MVIIC and T-type VGCC antagonist in combination with nifedipine. Differentiating NPCs were pre-incubated with VGCC antagonists for 1 hour or left untreated prior to KCl exposure (or differentiation medium) for 6 hours in the presence or absence of VGCC antagonists on DAP

2. KCl exposure induced a significant increase in GABA expression in all cultures treated with a single VGCC antagonist (ω-conotoxin MVIIC, nifedipine or mibefradil hydrochloride, Fig 3.10D). However, the increase in GABA expression with depolarization was reduced in the cultures pre-incubated with more than one VGCC antagonist (Fig 3.10D). The percentage of GABA immunopositive neurons in cultures exposed to depolarization in the presence of ω-conotoxin MVIIC + nifedipine and ω-conotoxin MVIIC + nifedipine + mibefradil hydrochloride were 49.37±4.04 and 49.40±3.73 respectively, compared to 72.46±3.40 in the cultures exposed to depolarization in absence of any drugs (Fig 3.10D). These results suggest that the insensitivity of GABA expression to VGCC antagonists may have been due to a slow leakage of Ca^{2+} through unblocked channels during prolonged exposure to depolarization. Thus, I tested the effect of depolarization for a shorter duration on GABA expression, in the absence and presence of VGCC blockers. To test this hypothesis, differentiating NPCs were exposed to KCl pulses, short exposure to high KCl medium for 2-3 minutes at an interval of 1 hour (to mimic the specific frequency of Ca^{2+} transients), on DAP 2. Cultures were fixed either immediately after a single KCl pulse or returned to the incubator in control medium for 15 min, 30 min, 1 hour, 3 hours or 6 hours (Fig 3.11A and 3.11B). Interestingly, I found that a single KCl pulse was sufficient to increase the percentage of GABA positive neurons significantly (60.10±2.41) compared to unstimulated cultures (33.73±1.45), although such an increase occurred only if cultures were incubated at least for one hour after the KCl pulse (Fig 3.11A), suggesting that a short exposure to depolarization that leads to a single event of voltage-induced Ca^{2+} influx is sufficient to trigger GABA expression in the neurons.

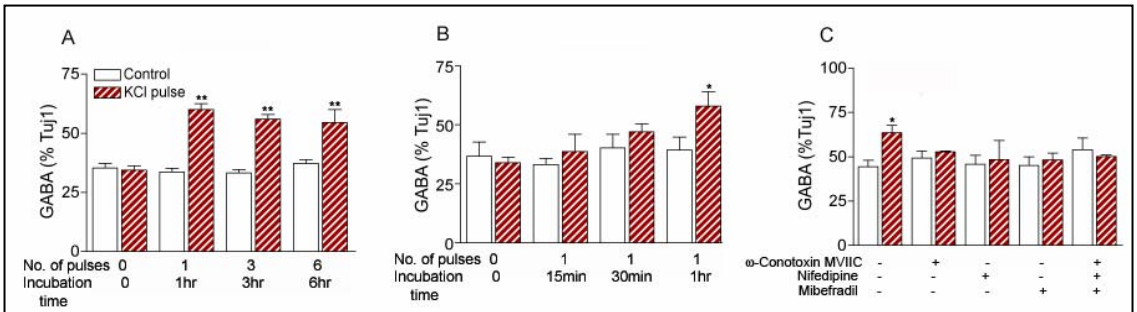

Figure 3.11: A single event of depolarization-induced Ca^{2+} influx is sufficient to promote GABA expression

Graph A and B show the percentage of GABA immunopositive neurons in striatal NPC cultures exposed to pulses of high KCl medium or differentiation medium (exposure for 2-3 minutes followed by incubation in differentiation medium) at the interval of 1 hour on DAP 2. Cultures were given multiple pulses (1 per hour) and fixed after 1, 3 or 6 hours (A) or fixed after short durations: 15 minutes, 30 minutes and 1 hour after a single pulse (B). Incubation time is the time elapsed between the first pulse and fixation. Graph C shows the percentage of GABA immunopositive neurons in striatal NPC cultures incubated with one or with a combination of VGCC antagonists on DAP 2: N and P/Q type VGCC blocker, ω-conotoxin MVIIC (1 μM); T-type VGCC blocker, mibefradil hydrochloride (1 μM) and L-type VGCC blocker, nifedipine (10 μM). After one hour pre-incubation with VGCC antagonists, cultures were exposed to a single pulse of high KCl medium or differentiation medium with the readdition of the same concentration/s of VGCC antagonists and incubated for 1 hour before fixation. Note that a single KCl pulse with a minimum incubation time of 1 hour increases GABA expression significantly (A and B), an effect that is blocked by inhibiting VGCCs (C). The data shown represents the mean ± SEM of at least three independent experiments with an average of 75-100 cells analysed for each condition in each imaging experiment. Statistical analysis was done with one-way ANOVA and Newman-Keuls test. * and ** denote significantly different from control ($P< 0.05$) and ($P< 0.01$), respectively.

Next, I used the KCl-pulse paradigm to test the effect of VGCC blockade on GABA expression. Differentiating NPCs were pre-incubated for 1 hour with VGCC antagonists; ω-conotoxin MVIIC, mibefradil hydrochloride and nifedipine to block N and P/Q type, T-type and L-type VGCCs, respectively, followed by a single KCl pulse or differentiation medium pulse (with or without VGCC antagonist addition), followed by incubation for 1 hour in differentiation medium with or without VGCC antagonists. I found that cultures treated with VGCC antagonists, whether applied individually or in combination, prevented the KCl pulse from promoting GABA expression (Fig 3.11C). The percentage of GABA positive neurons increased from 44.42±3.58 in unstimulated cultures to 63.65±4.11 in those exposed to KCl pulse. In cultures treated with all three VGCC antagonists, the percentage of GABA positive neurons after KCl pulse was 50.23±0.77, not different from 54.09±6.61 in unstimulated cultures. These results suggest that a single event of depolarization mediates Ca^{2+} influx via VGCCs which is sufficient to drive GABA expression. During prolonged KCl exposure of 6 hours, however, VGCC antagonists are unable to completely prevent depolarization induced GABA expression, an effect most likely due to minimal Ca^{2+} influx through unblocked VGCCs over a prolonged period.

3.4.3: Effect of other modulators of Ca^{2+} influx on GABA expression: neurotransmitters and neuromodulators

Various signaling molecules, such as neurotransmitters (GABA, glutamate) (LoTurco JJ 1995; Tozuka Y 2005) and neurotrophins (BDNF, NT-3 and NT-4) (Mizoguchi Y 2003; Yang B 2005) influence Ca^{2+} influx upon binding to their cell surface receptors that are either Ca^{2+} channels themselves or activate signaling

that leads to Ca^{2+} influx. It has been previously shown that glutamate application induces Ca^{2+} influx in striatal NPCs (Ciccolini F 2003). Similarly, canonical transient receptor potential channels (TRPCs) have also been shown to induce VGCC-dependent Ca^{2+} influx (Li Y 2005; Wang GX 2005). Since, neurotransmitters, neurotrophins and TRPCs are known to induce Ca^{2+} influx; I tested whether they effect GABA expression in striatal NPC-derived neurons. To do so, I treated differentiating NPCs with neurotransmitters, GABA and glutamate; a GABAR blocker, bicucculine, or a diacylglycerol analogue, OAG, which activates a subset of TRP channel isoforms. Differentiating NPCs were exposed to high KCl medium or differentiation medium with the addition6 of GABA, glutamate, bicucculine and OAG or without addition of any drugs on DAP1 for 24 hours. Treatment with any of these did not have any effect on the percentage of neurons immunopositive for GABA in unstimulated or stimulated cultures (Fig 3.12A). Thus, GABA, glutamate and TRP channels do not effect GABA expression in normal physiological conditions or under depolarizing conditions. Similarly, I tested the involvement of neurotrophins, by exposing NPCs to differentiation medium and high KCl medium with the addition or without the addition of BDNF, NT-3 and NT-4 on DAP 1 for 24 hours. Quantification of the percentage of neurons immunopositive for GABA showed that BDNF, but not NT-3 and NT-4, treatment increased GABA positive neurons significantly (54.57±4.12% compared to 34.00±1.30% in control neurons) (Fig 3.12B). In order to determine whether KCl induces GABA expression in striatal NPCs via BDNF release and TrkB receptor activation, mice lacking TrkB were used to abolish BDNF signaling. Striatal NPC cultures were derived from $TrkB^{-/-}$, $TrkB^{+/-}$ and $TrkB^{+/+}$ (wild type) embryos. On DAP 1, differentiating striatal NPCs was treated with high KCl medium for 24 hours or with differentiation medium. Analysis of the percentage of neurons

immunopositive for GABA showed that the TrkB$^{-/-}$ and TrkB$^{+/-}$ striatal neurons had KCl-induced early GABA acquisition similar to that of wild type neurons (Fig 3.12C), suggesting that BDNF signaling is not involved in KCl-induced neuronal differentiation.

Taken together these results suggest that depolarization and BDNF promote GABA expression in neurons arising from differentiating NPCs. However, depolarization and BDNF involve different mechanisms to promote GABA expression.

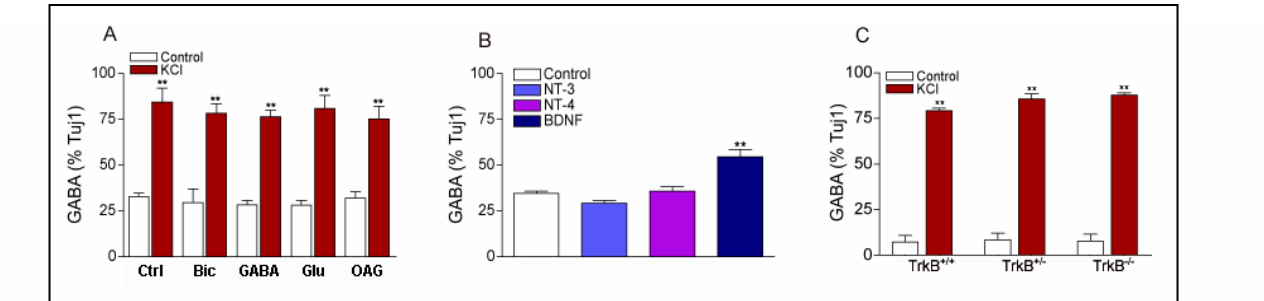

Figure 3.12: Neurotransmitters, neurotrophins and TRP channels do not contribute to VGCC-induced GABA expression

Graph A shows the percentage of GABA immunopositive neurons (GABA$^+$/Tuj1$^+$) in striatal NPCs that were exposed to high KCl medium or differentiation medium on DAP 1 for 24 hours, with or without the addition of the following: neurotransmitters, GABA (10 μM) and glutamate (100 μM); GABAR antagonist, bicucculine (10 μM); and the diacylglycerol analog known to activate some TRP channels, OAG (25 μl). Graph B shows the percentage of GABA$^+$/Tuj1$^+$ neurons in striatal NPCs incubated with neurotrophins, NT-3 (20 ng/ml, blue), NT-4 (20 ng/ml, purple) and BDNF (20 ng/ml, dark blue) on DAP 1 for 24 hours. Graph C shows the percentage of GABA$^+$/Tuj1$^+$ neurons in striatal NPCs from TrkB$^{+/+}$, TrkB$^{+/-}$ and TrkB$^{-/-}$ embryos. Cultures were exposed to high KCl medium or differentiation medium on DAP 1 for 24 hours. The data shown represent the mean ± SEM of at least three independent experiments with an average of 75-100 cells analysed for each condition in each experiment. Statistical analysis was done with one-way ANOVA and Newman-Keuls test. * and ** denote significantly different from control ($P< 0.05$) and ($P< 0.01$), respectively.

3.5: Specificity and mechanism of KCl-induced GABA expression

3.5.1: Opposing effect of PKA and PKC in activity-dependent and activity-independent regulation of GABA expression

As discussed in the previous sections, the effect of depolarization on GABA acquisition is independent of transcription/translation (section 3.2.3) and can be triggered by a single event of KCl-induced Ca^{2+} influx (section 3.4.2). These results suggest that depolarization triggers a rapid post-translational mechanism that in-turn modulates GABA acquisition. In *drosophila* neurons, depolarization modulates GABA expression by post-translational regulation of GAD enzymatic activity (Küppers B 2003). Moreover, it is known that GAD 67 and GAD 65 activity is regulated by phosphorylation and dephosphorylation (Wei J 2004). GAD 67 is active in its dephosphorylated state, whereas GAD 65 is active when it is phosphorylated. PKA and PKC are the two candidates that have been shown to phosphorylate GAD 67 and GAD 65 (Wei J 2004). Similarly, phosphatases like PP1, PP2A and PP2B dephosphorylate GAD 67 and GAD 65 (Wei J 2004). Thus, I hypothesized that depolarization-induced regulation of GABA acquisition is achieved by regulation of GAD activity. To test this hypothesis, I analysed the effect of PKA and PKC antagonists on NPC cultures. As stated in section 3.2.1, 24 hours treatment with these pharmacological agents had cytotoxic effects. Therefore I used a single KCl-pulse paradigm to test the involvement of PKA and PKC. To this end, differentiating striatal NPC cultures were pre-incubated with the PKA inhibiting peptide, PKI 14-22 amide (PKAI), and/or the PKC inhibiting peptide, myristoylated PKC peptide inhibitor (PKCI), for one hour on DAP 2, prior to a 2-3 min pulse with high KCl medium or differentiation medium pulse with the addition of or without PKAI and/or PKCI, followed by one hour incubation in

differentiation medium with the addition of or without PKAI and/or PKCI. As a control, parallel set of culture was exposed to a high KCl pulse or differentiation medium pulse without addition of the inhibitors. Analysis of the percentage of neurons that were immunopositive for GABA showed that the inhibition of PKA and/or PKC led to an increase in GABA positive neurons (Fig 3.13A). The percentage of neurons immunopositive for GABA was 37.83±2.94 in unstimulated cultures, 49.25±3.33 in PKAI treated unstimulated cultures, 49.39±1.85 in PKCI treated unstimulated cultures and 61.90±4.04 in PKAI and PKCI treated unstimulated cultures. Interestingly, in the cultures exposed to a KCl pulse, PKA and/or PKC antagonists blocked the KCl-induced increase in GABA acquisition (Fig 3.13A). The percentage of neurons immunopositive for GABA was 53.86±2.52 in KCl treated cultures, 37.32±2.05 in KCl+PKAI treated cultures, 41.70±5.42 in KCl+PKCI treated cultures and 42.49±5.29 in KCl+PKAI+PKCI treated cultures.

I also tested the effect of forskolin that stimulates adenylate cyclase to increase cAMP levels which in-turn activates PKA. On DAP 1, striatal NPC cultures were treated with forskolin for one hour followed by a pulse with high KCl medium or differentiation medium and subsequent incubation in differentiation medium for one hour. I found that forskolin treatment increased the percentage of neurons that were immunopositive for GABA under unstimulated conditions (39.65±1.72 in forskolin treated compared to 34.60±1.11 in without forskolin) (Fig 3.13B). The percentage of GABA positive neurons in forskolin and KCl treated cultures was similar to KCl treated cultures without forskolin addition (Fig 3.13B). This suggests that forskolin enhances GABA expression in striatal NPCs as does depolarization.

These results show that PKA and PKC regulate GABA expression in control and depolarizing conditions by acting on distinct targets. Under normal

physiological conditions, basal PKA and PKC activity keeps GABA expression low. The increase in active PKA and PKC achieved by forskolin or depolarization leads to a shift in their target which increases GABA expression in neurons differentiating from striatal NPCs.

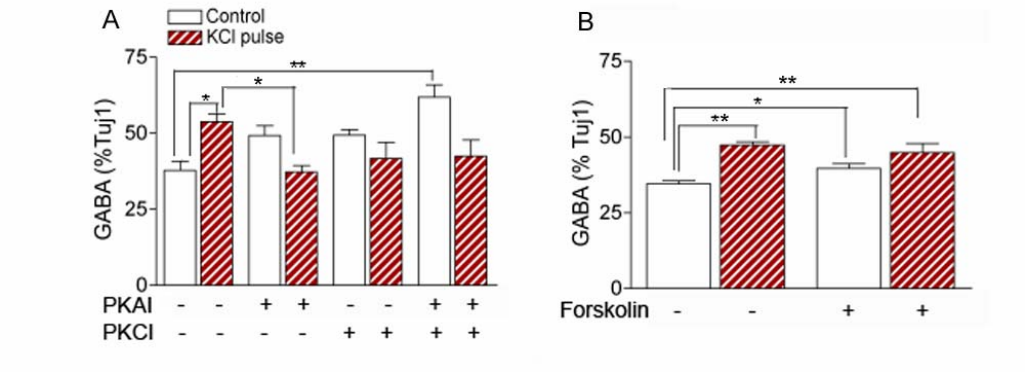

Figure 3.13: PKA and PKC regulate GABA expression

Graphs A and B show the percentage of GABA immunopositive neurons in striatal NPC cultures incubated with PKA inhibitory peptide, myristoylated PKA inhibitor amide 14-22 (PKAI, 1 μM) and PKC inhibitory peptide, myristoylated PKC peptide inhibitor (PKCI, 1 μM) or both (1 μM each) (A) and adenylate cyclase activator, forskolin (10 μM) (B), for 1 hour on DAP 1, followed by a pulse of high KCl medium or differentiation medium with the same concentration of the pharmacological agents. This was followed by 1 hour incubation in differentiation medium including the same pharmacological agents. The data shown represents the mean ± SEM of at least three independent experiments with an average of 75-100 cells analysed for each condition in each imaging experiment. Statistical analysis was done with one-way ANOVA and Newman-Keuls test. * and ** denote significantly different from control ($P< 0.05$) and ($P< 0.01$), respectively.

3.5.2: Depolarization effects neurons committed to GABAergic fate

Throughout this thesis I have analysed the effect of depolarization on neurons differentiating from striatal NPCs, of which the majority express GABA neurotransmitter (section 3.1.1). It has been shown that modulation of transcription by neural activity mediates changes in the fate and functionality

of the neurons by altering the type of neurotransmitter expressed (Borodinsky LN 2004). My results, however, show that KCl increases GABA expression in a transcription-independent manner (section 3.2.3) and may act by modulation of the phosphorylation state of target proteins by PKA and PKC (section 3.5.1). Thus, I predicted that in striatal NPCs, depolarization might promote GABA expression only in neurons that are restricted to become GABAergic, for example by the expression of GAD, but does not promote GABA expression in neurons that normally do not express GAD. To test this hypothesis I analysed the effect of KCl treatment in NPCs originating from the embryonic cortex that mainly give rise to glutamatergic neurons. One week old neurospheres from striatum and cortex were plated on PLO-coated chamber slides. On DAP 1, differentiating NPCs were exposed to high KCl medium or differentiation medium for 24 hours. As seen in previous sections, KCl exposure led to a dramatic increase in the percentage of neurons that were immunopositive for GABA (Fig 3.14B), from 29.44±3.72% to 84.19±6.59% in striatal cultures, whereas there was no significant increase in glutamate positive neurons (Fig 3.14B). In contrast, in cortical cultures KCl promoted a more modest increase in the number of GABAergic neurons, from 11.97±6.52% to 35.13±8.94% (Fig 3.14C) without altering the number of glutamatergic neurons (Fig 3.14C). Since I found that albeit small, a subset of cortical neurons does express GABA following KCl treatment, I next asked whether these neurons are committed to become GABAergic. I therefore analysed the expression of the two major neurotransmitters, GABA and glutamate, in neurons derived from cortical and striatal NPCs at various steps during *in vitro* differentiation. On DAP 2, striatal cultures had 33.00±1.53% of GABA positive neurons and 62.55±6.55% glutamatergic neurons (Fig 3.14D). On DAP 4, GABA positive neurons represented 54.00±3.80% of the neurons in striatal cultures, whereas glutamate

was expressed by 55.75±5.75% of the neuronal cells Fig 3.14D). At DAP 7 the number of GABA positive neurons remained constant (51.90±3.90%) whereas the number glutamatergic neurons increased slightly (73.83±1.17%) (Fig 3.14D and 3.14A). Thus, at later days of differentiations a sub-population of striatal neurons showed co-expression of both GABA and glutamate. Alternatively, in cortical cultures the majority of neurons (> 80%) expressed glutamate at every time-point analysed, whereas GABA expression was limited at a small neuronal subset (Fig 3.14E). On DAP 2, cortical cultures contained 11.97±6.52% GABA positive neurons and 70.78±5.22% glutamate positive neurons (Fig 3.14E). A similar situation in terms of GABAergic (14.4±0.60%) and glutamatergic neurons (67.75±5.75%) was found at DAP 4. On DAP 7, 28.64±6.60% were GABA positive and 83.25±2.90% expressed glutamate (Fig 3.14E and 3.14A). Thus, upto 30% of cortical NPC-derived neurons express GABA, at DAP 7 during normal differentiation and at DAP 2 when differentiation is accelerated by depolarization.

These data show that depolarization promotes GABA expression in striatal and cortical NPC-derived neurons. However, the effect of depolarization is restricted to neurons committed to become GABAergic and does not alter the number of glutamate expressing neurons. Thus, depolarization acts specifically to accelerate GABA expression and does not change the neuronal fate from glutamatergic to GABAergic or vice versa.

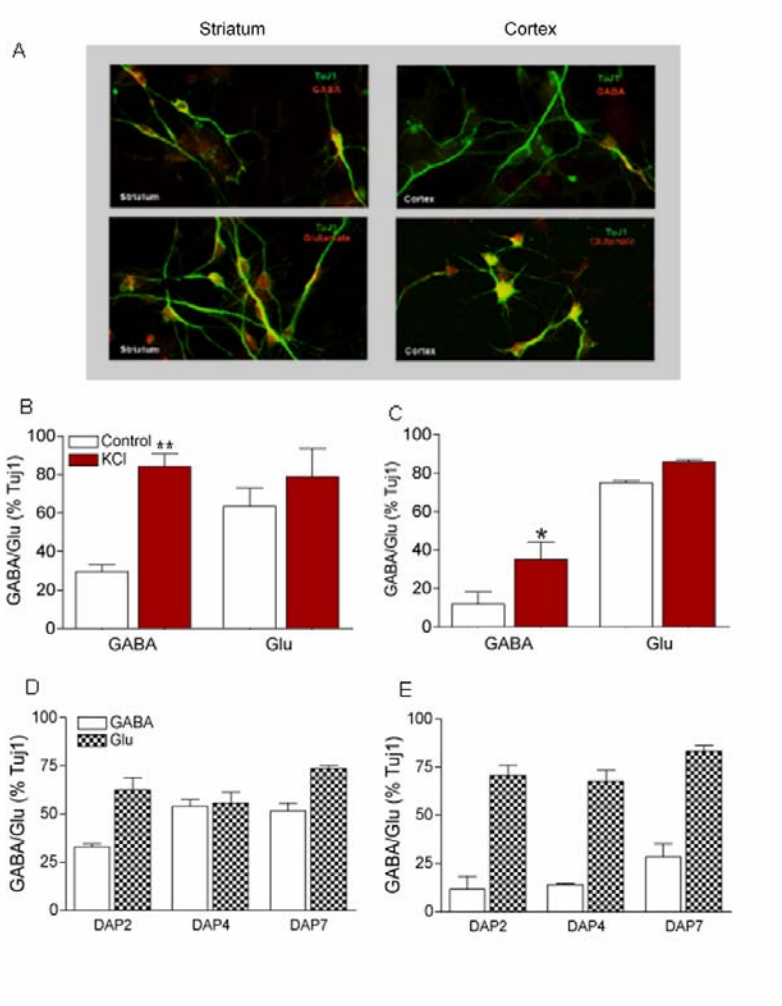

Figure 3.14: Depolarization increases GABA expression only in neurons committed to GABAergic fate

Panel A shows double immunostaining for GABA and Tuj1 or glutamate and Tuj1 in striatal and cortical NPCs on DAP 7. Graphs B and C shows the percentage of GABA and glutamate immunopositive neurons in striatal (B) and cortical (C) NPCs exposed to high KCl medium or differentiation medium on DAP 1 for 24 hours. Graph D and E show the percentage GABA and glutamate immunopositive neurons in striatal (D) and cortical (E) NPCs on DAP 2, 4 and 7. The data shown represent the mean ± SEM of at least 3 independent experiments with an average of 75-100 cells analysed for each condition in every experiment. Statistical analysis was done with one-way ANOVA and Newman-Keuls test. * and ** denote significantly different from control ($P< 0.05$) and ($P< 0.01$), respectively.

Chapter 4 : Discussion

4.1: Spontaneous and depolarization-evoked Ca^{2+} transients in neurons and precursors in differentiating striatal NPCs

4.1.1: Neurons show L-type VGCC-mediated spontaneous and depolarization-evoked Ca^{2+} transients, whereas precursors show only depolarization-evoked Ca^{2+} transients through L-type VGCCs

Spontaneous Ca^{2+} transients have been observed at several stages of development and in different neural lineages. I found that neurons arising from embryonic striatal NPCs show global Ca^{2+} transients during differentiation, similar to those shown previously in heterogeneous striatal NPCs (Ciccolini F 2003). All the neurons analysed showed Ca^{2+} transients. In contrast only one-third of non-neurons (Tuj1 negative cells representing neural precursors) showed spontaneous Ca^{2+} transients. Thus, neurons have higher spontaneous activity compared to precursors. Exposing differentiating striatal NPCs to depolarization increased the frequency of Ca^{2+} transients by more than two fold in both, neurons and non-neurons, without altering other parameters such as the amplitude and duration of Ca^{2+} transients. Depolarization also increased the percentage of active non-neurons from 37.14% to 56.0%. Calibrated basal Ca^{2+} levels were not different in cultures exposed to depolarization for 6 hours compared to unstimulated cultures. Since, calibration involved treating the cells with an ionophore, ionomycin, the culture could not be stained for neuronal marker following calibration. Hence, calibrated Ca^{2+} levels, which reflect the Ca^{2+} concentration, were common to the whole NPC population and were not different between neurons and non-neurons. Interestingly, the amplitude of Ca^{2+} influx in response to acute depolarization was higher in neurons than in non-neurons. Larger amplitude of Ca^{2+} influx could result from

two possibilities; higher expression of VGCCs on the cell surface of neurons compared to non-neurons or enhanced amplification of the cytosolic Ca^{2+} in neurons by Ca^{2+}-induced-Ca^{2+}-release that involves release of Ca^{2+} from the internal stores following depolarization.

Experiments aimed at exploring the role of L-type VGCCs in spontaneous Ca^{2+} transients showed that inhibition of L-type VGCCs reduced the percentage of active neurons significantly. The percentage of active neurons decreased from 100% to 42.86% with nifedipine treatment. Similar, L-type VGCC-mediated Ca^{2+} transients occur in neurons arising from post-natal cortical progenitors and regulate their neurogenesis (D'Ascenzo M 2006). The role of these transients in neurogenesis of striatal NPCs remains to be tested. Striatal NPC-derived neurons are not synaptically connected, thus release of secreted factors such as neurotransmitters could induce generation of spontaneous L-type-mediated Ca^{2+} transients. For example, glutamate and GABA have been shown depolarize the NPCs leading to VGCC-mediated Ca^{2+} influx that regulated neurogenesis of NPCs (LoTurco JJ 1995; Ciccolini F 2003; Tozuka Y 2005). Ca^{2+} influx through Ca^{2+} channels belonging to the canonical transient receptor potential family (TRPC) could also depolarize the neuron sufficient to activate VGCCs (Li Y 2005; Wang GX 2005). Another possible source of depolarizing signals is through cell-cell interactions. For example, in the developing CNS Ca^{2+} elevation in cohorts of radial glial cells spreads through intercellular connections (gap junctions) and regulates embryonic cortical neurogenesis (Weissman TA 2004). In my imaging experiments I seldom observed Ca^{2+} waves spreading across groups of cells, however from these experiments I cannot exclude that intercellular communication is involved in the generation of spontaneous Ca^{2+} transients. Blockade of L-type VGCCs also decreased the percentage of active neurons in the NPCs exposed to depolarization from 100%

to 71.43% as well as it prevented depolarization from increasing the frequency of L-type VGCC-mediated Ca^{2+} transients. In the non-neurons, inhibition of L-type VGCCs did not affect the percentage of active cells significantly in unstimulated NPCs, but caused a reduction in active NPCs exposed to depolarization from 56% to 26%. Thus, most of the spontaneous Ca^{2+} transients in neurons, but not in the non-neurons, are generated by Ca^{2+} influx through L-type VGCCs. However, as for the neurons, inhibition of L-type VGCCs blocked the depolarization-induced increase in the frequency of Ca^{2+} transients in non-neurons, suggesting that depolarization induces L-type VGCC-mediated Ca^{2+} transients in neurons as well as non-neurons. Furthermore, L-type VGCC blockade decreased the amplitude of depolarization-induced Ca^{2+} influx by one-third in neurons (although 100% of the neurons responded) suggesting that two-third of depolarization-induced Ca^{2+} influx takes place through non-L-type VGCCs. In contrast, L-type VGCC blockade decreased the percentage of non-neurons that showed Ca^{2+} influx in response to depolarization from 80% to 16%, although the amplitude of Ca^{2+} influx was not changed. This shows that L-type VGCCs are the major entry source of Ca^{2+} following depolarization in the non-neurons, blockade of which drastically reduces the number of precursors that show Ca^{2+} influx in response to depolarization. Thus, neurons express different VGCCs that open in response to depolarization, whereas non-neurons primarily contain L-type VGCCs that mediate Ca^{2+} influx in response to depolarization.

4.2: Regulation of neuronal differentiation of striatal neural precursor cells (NPCs) by membrane depolarization

4.2.1: Depolarization regulates neuronal differentiation of striatal NPCs

Neurogenesis in differentiating striatal NPCs proceeds gradually over several days in culture. Following neurogenesis up to 7 days in culture, I saw that maximum neurogenesis occurs between DAP 1 and 2. Maturation and differentiation of neurons was followed by expression of the neurotransmitter GABA as most of the striatal neurons are GABAergic. Interestingly, there was a decrease in GABA positive neurons from DAP 1 to DAP 2, although the percentage of cells which were neurons on DAP 2 was ten fold higher than seen on DAP 1. Thus, GABA expression follows commitment to the neuronal lineage.

Exposing differentiating striatal NPCs to depolarization promoted GABA expression and enhanced neurite outgrowth, thus accelerating neuronal differentiation. Interestingly, cells that had acquired neuronal identity, and not the neural precursors, were the ones to respond to depolarizing stimuli and showed enhanced neuronal differentiation. In experiments where cultures were fixed immediately after KCl exposure, GABA expression and neurite outgrowth were increased significantly (Fig 4.1A). In contrast, the cultures that were incubated for one or two days after KCl washout showed smaller increases in GABA expression and neurite outgrowth (Fig 4.1B and 4.1C). If KCl was acting on precursors, neuronal precursors that differentiated into neurons after KCl washout should have also shown an increase in GABA expression and neurite outgrowth irrespective of the time of fixation. However, my results show that the effect of KCl is diluted after KCl washout. Hence, only

the neurons present in the culture at the time of KCl exposure showed an increase in GABA expression and neurite outgrowth. I have focused on the effect of depolarization on the differentiation of neurons arising from striatal NPCs in the short time window analysed in my experiments. Previous studies in the literature have looked at the effect of depolarization on neurogenesis of NPCs. For example, depolarization was found to increase the rate of neurogenesis in hippocampal and cortical NPCs in long term experiments (Deisseroth K 2004; D'Ascenzo M 2006). To summarize my results in the context of previous literature, it is conceivable that depolarization has distinct effects at different stages of NPC development. Neuronal activity *in-vivo* may act on proliferating neural precursors to enhance their likelihood of becoming neurons (neurogenesis), whereas at later stages neural activity may act on young neurons to enhance their differentiation and allow them to become functional (neuronal differentiation).

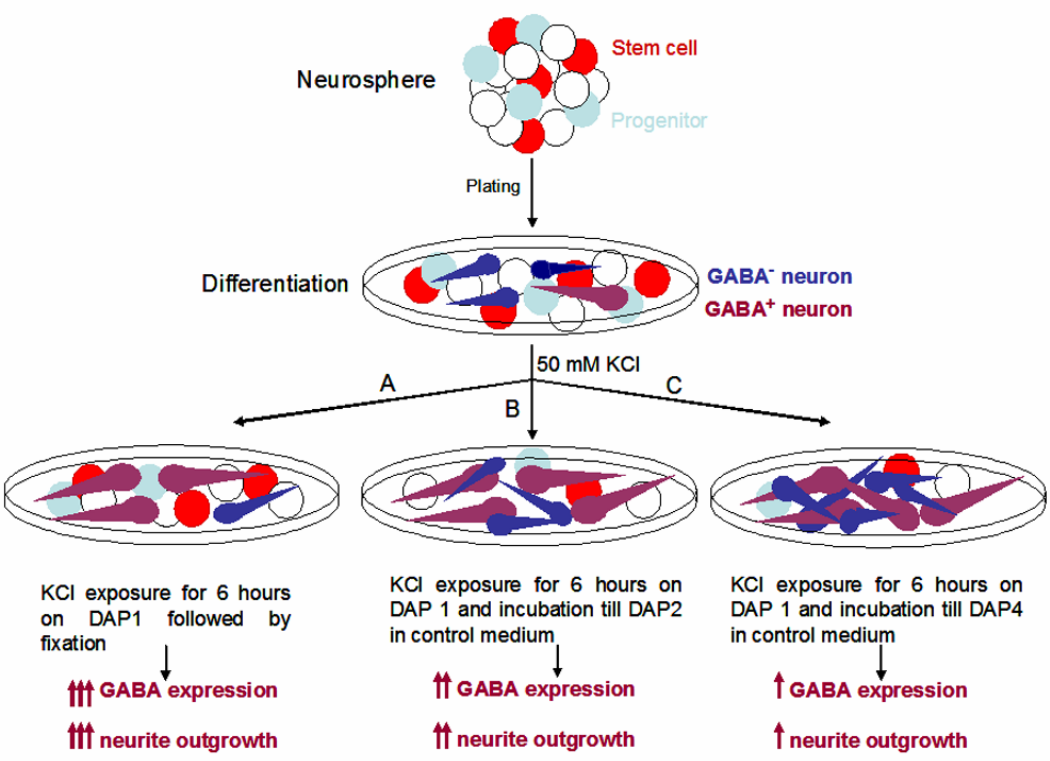

Figure 4.1: Depolarization acts directly on neurons in striatal NPCs

This cartoon summarizes the effect of KCl on neuronal differentiation in striatal NPCs. Neurospheres were plated on day after plating 0 (DAP 0) and differentiation was promoted by removal of growth factors and addition of FCS. On DAP 1, parallel cultures were exposed to KCl for 6 hours time period. One set of cultures was fixed immediately thereafter (A), whereas the other two sets of cultures were incubated in differentiation medium after KCl washout and fixed on DAP 2 (B) or on DAP 4. The effect of KCl in enhancing GABA expression (percentage of GABA immunopositive neurons) and neurite outgrowth (average length of the longest neurite of a neuron) was most significant in A and was diluted with increase in incubation time after KCl washout. This shows that neurons that are exposed to KCl are the ones to express GABA earlier and have longer neurites and neurons differentiating from precursors after KCl washout were not affected by KCl.

4.3: Distinct signaling molecules regulate distinct aspects of depolarization-induced neuronal differentiation

4.3.1: Activation of MAPK and CaMK pathway/s and the release/activation of sAPP by depolarization mediates enhanced neurite outgrowth, but not GABA expression

Analysis of the signaling cascades that regulate depolarization–induced neuronal differentiation showed that depolarization promotes GABA acquisition and neurite outgrowth by distinct mechanisms. These results strengthen the previous findings that GABA expression is regulated via global Ca^{2+} transients, whereas NMDAR-dependent local Ca^{2+} transients regulate neurite outgrowth (Ciccolini F 2003). Similar phenomena have been reported in the literature. For example in *Xenopus* neurons, GABA expression is regulated by global Ca^{2+} transients that promote GAD transcription, whereas neurite outgrowth is regulated by local Ca^{2+} transients that involve modulation of the phosphorylation state of cytoskeletal proteins (Spitzer NC 2000).

Inhibition of ERK, p38 kinase and CaMK with specific antagonists blocked depolarization-induced neurite outgrowth, whereas it failed to affect depolarization-induced GABA acquisition. ERK and CaMK pathways have been shown to regulate axonal outgrowth in neurons derived from different brain regions. For example, ERK is activated by various axon growth promoting signals including depolarization and regulates neurite outgrowth in many cell types such as retinal neurons and PC-12 cells (Perron JC 1999; Hansen TVO 2003). In sympathetic neurons, activity-induced Ca^{2+} influx activates dendritic growth via activation of CaMKII and ERK (Vaillant AR 2002). Similarly, CaMKI has also been shown to regulate neurite outgrowth of hippocampal neurons (Wayman GA 2004). Consistent with these data from the

literature, my results also show involvement of ERK and CaMK pathways in depolarization-induced neurite outgrowth in neurons differentiating from striatal NPCs.

The experiments with anti-APP and α and β-secretase inhibitor showed that these reagents completely blocked the effect of depolarization in promoting neurite outgrowth without affecting depolarization-induced GABA acquisition. Thus, depolarization requires sAPP to promote neurite outgrowth. Depolarization either increases sAPP release or stabilizes the interaction of sAPP with its unknown receptor. Due to a small size difference between sAPPα and sAPPβ, the western blot analysis did not reveal the nature of sAPP secreted by striatal NPCs. However, it is probable that sAPPα is involved in neurite outgrowth promoting effect in striatal NPC-derived neurons since it has been reported to have neurite outgrowth promoting effects in many other cell types. For example, sAPPα has been shown to promote neurite outgrowth in chick sympathetic and mouse hippocampal neurons via its interaction with heparan sulfate proteoglycan of the extracellular matrix (Small D 1994; Mattson MP 1997). Interestingly, neural activity and the activation of the ERK pathway increase sAPPα production (Nitsch R 1993; Mattson MP 1997).

My results show that MAPK (ERK and p38) and/or CaMK pathway and sAPP act downstream of neural activity to induce neurite outgrowth. Whether MAPK and/or CaMK are upstream of sAPP or downstream remains to be elucidated. These results together with the previous finding of my lab that depolarization-induced neurite outgrowth is NMDAR dependent lead to a possible pathway linking depolarization to changes in neurite outgrowth in differentiating striatal NPCs (Fig 4.2). The scheme suggests that neural activity activates NMDARs leading to Ca^{2+} influx (1) that activates the ERK/p38/CaMK pathway/s (2) which in-turn enhances sAPPα production by α-secretase (3).

sAPPα then induces changes in neurite outgrowth via its interaction with heparan sulfate proteoglycan of the extracellular matrix (4) as shown previously (Small D 1994). Alternatively, it is also conceivable that sAPPα might bind to its unknown receptor (5) and activate signaling that acts on the cytoskeleton to promote neurite outgrowth (6).

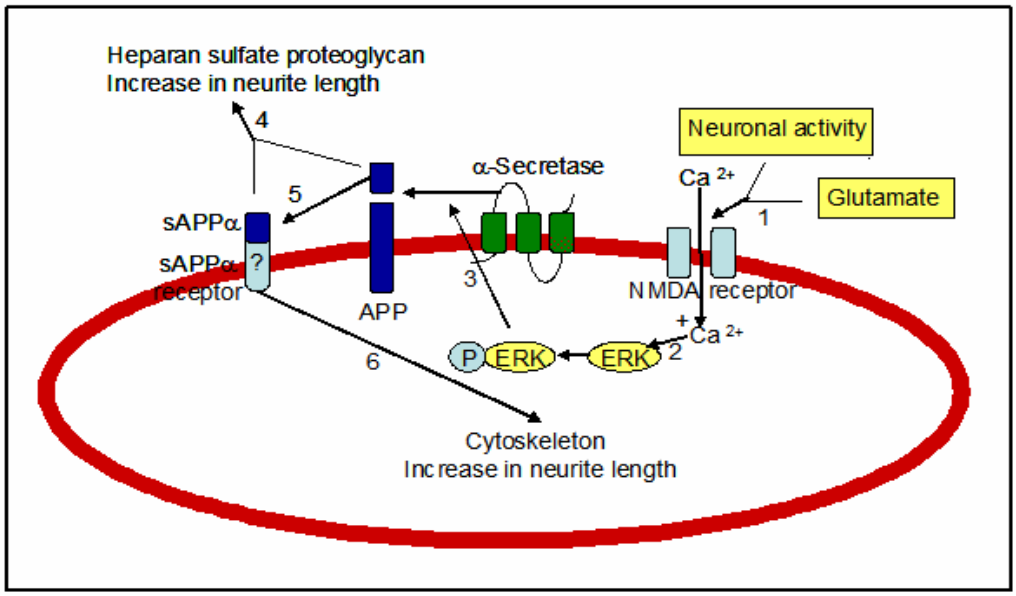

Figure 4.2: Depolarization regulates neurite outgrowth of neurons differentiating from striatal NPC cultures via activation of MAPK/CaMK signaling and involves sAPP

The cartoon depicts the mechanism of depolarization-induced neurite outgrowth in neurons differentiating from striatal NPC culture. Neural activity/glutamate induces Ca^{2+} influx through NMDAR (1) which then activates kinases such as ERK, p38 and/or CaMK (2). Kinases then promote APP cleavage by α-secretase leading to increase in sAPPα generation. sAPPα secreted into the extracellular space might interact with heparan sulfate proteoglycans of the extracellular matrix (4) and there-by regulate neurite outgrowth or it may interact with its unknown receptor on the cell surface (5) and activate downstream signaling leading to changes in cytoskeleton and neurite outgrowth (6).

4.3.2: Depolarization-induced neuronal differentiation involves transcription and translation independent mechanism/s

Many of the downstream effects of excitatory activity are mediated by modulation of gene transcription (West AE 2001). For example, in the *Xenopus* spinal neurons specific frequency of Ca^{2+} transients have been shown to regulate GAD transcription. Increasing the frequency of Ca^{2+} transients with depolarization upregulated GAD transcription and GABA expression (Watt SD 2000). CREB transcription factor is a major target of voltage-dependent Ca^{2+} influx and upregulates gene transcription of target genes (Bading H 2000). I found that CREB is activated following depolarization and that the pCREB immunopositivity was restricted to neurons arising from striatal NPCs suggesting that depolarization-induced CREB activation is a neuronal specific effect. This is possibly due to the difference in Ca^{2+} mobilization observed following depolarization between neurons and non-neurons. I found that although both neurons and non-neurons displayed Ca^{2+} influx through VGCC following depolarization, the amplitude of the Ca^{2+} response was higher in neurons than in non-neurons (as discussed in section 4.1). Analysis of conditional CREB knockout mice on Crem knockout background showed that ablation of CREB was not necessary for depolarization-induced GABA expression and neurite outgrowth. Thus, depolarization does not require CREB activation to accelerate neuronal differentiation in striatal NPCs. Previous studies have identified other important roles for CREB in neurogenesis. Transient CREB activation occurs in adult SVZ neuroblasts during later stages of tangential migration towards the OB and is critical for the differentiation and survival of OB neurons differentiating from SVZ neuroblasts (Giachino C 2005). In the adult dentate gyrus, CREB activation has been shown to increase cell

proliferation and CREB downregulation has an opposite effect (Nakagawa S 2002). Furthermore, CREB was shown to be activated following cerebral ischemia in adult dentate gyrus and increased the survival of NPCs (Zhu DY 2004). Any possible role of CREB in striatal NPC proliferation and survival remains to be tested in long term experiments.

Furthermore, analysis of GAD 65 and GAD 67 mRNA levels by RT-PCR showed that depolarization-induced GABA expression did not involve transcriptional regulation of GAD. My experiments with transcription and translation blockers showed that depolarization-induced GABA expression is independent of transcription and translation, suggesting a post-translational mechanism for the regulation of depolarization-induced GABA expression. Hence, my results point towards a novel post-translational regulation of neuronal differentiation by neural activity.

4.4: Regulation of GABA expression by depolarization-induced Ca^{2+} influx in neurons differentiating from striatal NPCs

4.4.1: A brief VGCC-dependent Ca^{2+}-influx, but not the frequency of Ca^{2+} transients, regulates GABA expression

A previous study had established a correlation between depolarization-induced Ca^{2+} influx and an increase in GABA acquisition following depolarization (Ciccolini F 2003). I found that experiments performed in the absence of extracellular Ca^{2+} showed that the removal of extracellular Ca^{2+} prevented depolarization from promoting GABA expression, directly showing that depolarization requires Ca^{2+} influx to promote GABA expression in striatal NPCs. Since L-type VGCCs were the source of most of the spontaneous and depolarization-induced Ca^{2+} transients, I tested the role of L-type VGCCs in

regulating GABA expression in neurons differentiating from striatal NPCs. I found that activation of L-type VGCCs promoted GABA acquisition similar to depolarization whereas blockade of L-type VGCCs (and/or N and P/Q-type and T-type VGCCs either alone or in combination) did not prevent prolonged depolarization (6 hours) from promoting GABA expression. The inability of VGCC blockers to prevent depolarization-induced Ca^{2+} influx and hence induce early GABA expression, suggested that during prolonged depolarization any marginal, unblocked Ca^{2+} influx is perhaps sufficient to trigger changes in GABA expression. Indeed, this turned out to be the case. Exposing differentiating NPCs to short pulses of depolarization instead of prolonged exposure showed that a single event of depolarization was sufficient to promote GABA acquisition, although it required 1 hour of minimum incubation time after the pulse (i.e. washout of KCl). When NPCs were exposed to a single depolarizing pulse in the presence of L-type, T-type, N and P/Q-type VGCCs blockers, the effect of depolarization in promoting GABA acquisition was blocked. These results show that a single event of depolarization-induced Ca^{2+} influx through VGCCs is sufficient to induce promote GABA acquisition in striatal NPCs. Hence, during prolonged depolarization in the presence of VGCC blockers, any marginal unblocked/leakage Ca^{2+} influx is sufficient to induce early GABA acquisition. Thus, although depolarization increases the frequency of Ca^{2+} transients through VGCCs, it is not the frequency of Ca^{2+} transients that regulates GABA expression rather it is single events of VGCC-mediated Ca^{2+} influx. Since regulation of GAD transcription is correlated with the frequency of Ca^{2+} transients, this also explains why depolarization-induced GABA acquisition does not involve regulation of GAD gene-transcription (Spitzer NC 2000; Watt SD 2000). It is conceivable that signaling cascades that are located in the vicinity of VGCCs are immediately activated by Ca^{2+} influx

through VGCCs and these signaling molecules in-turn activate downstream targets, kinases, phosphatases etc. that can modulate GABA expression. It is also possible that a single event of Ca^{2+} influx through VGCCs triggers Ca^{2+}-induced-Ca^{2+}-release from the internal stores causing cytosolic Ca^{2+} concentration to rise significantly above resting levels and activate down-stream signaling cascades that modulate GABA expression. These rapid changes allow the young neurons to differentiate faster by acquiring neurotransmitter and hence, prime them to become functional and integrate in the network.

4.4.2: BDNF increases GABA expression through a mechanism distinct from depolarization

Secreted factors such as neurotransmitters and neurotrophins can induce Ca^{2+} influx. For example, glutamate and GABA have been shown to regulate neurogenesis of NPCs by promoting Ca^{2+} influx through VGCCs (LoTurco JJ 1995; Ciccolini F 2003; Tozuka Y 2005). Since, Ca^{2+} influx regulates GABA expression in striatal NPCs; I tested whether neurotransmitters and neurotrophins had an effect on GABA expression. Experiments where striatal NPCs were exposed to bath application of glutamate, GABA and a diacylglycerol analogue that activates TRP channels, OAG, showed that none of these affected GABA expression in neurons arising from striatal NPCs. This suggests that Ca^{2+} entry induced by neurotransmitters and TRPCs does not lead to VGCC activation or at least sufficient VGCC activation to promote GABA expression. Similarly, neurotrophins such as BDNF have been shown to induce Ca^{2+} influx in visual cortex neurons (Mizoguchi Y 2003). I found that BDNF application, but not NT-3 and NT-4, increased GABA expression in

differentiating striatal NPC cultures. However, analysis of striatal NPCs from TrkB knockout mice showed that ablation of BDNF signaling did not prevent depolarization from promoting GABA expression clearly demonstrating that depolarization and BDNF effect GABA expression by distinct mechanisms.

4.5: Specificity and mechanism of depolarization-induced GABA expression

4.5.1: PKA and PKC regulate GABA expression in neurons arising from striatal NPCs

As discussed in section 4.3.2, my results demonstrate that regulation of GABA expression by depolarization is achieved by a post-translational mechanism. Experiments in which PKA and PKC were inhibited using specific inhibitors showed increase of GABA expression in unstimulated cultures. In cultures exposed to a KCl pulse, however, inhibition of PKA and PKC blocked depolarization-induced GABA expression suggesting that KCl requires PKA and PKC activity to promote GABA expression. Enhancing PKA activity with the adenylate cyclase activator, forskolin, also caused increases in GABA expression. Since these results suggest that PKA and PKC activity have opposite effects under unstimulated and depolarizing conditions, it is conceivable that they phosphorylate distinct targets under these conditions. Thus in the dual-regulation model of GABA expression by PKA and PKC, one of the targets (that regulates GABA 1) is modulated by basal kinase activity and the other is modulated upon increased kinase activity (that regulates GABA 2) (Fig 4.3). GAD 65 and GAD 67 could be the targets that are differentially regulated by PKA and PKC. Previous work has shown that Ca^{2+}-dependent kinases and phosphatases regulate GAD enzymatic activity. GAD isoforms,

GAD 67 and GAD 65 are phosphorylated by protein kinases such as PKA and PKC and dephosphorylated by phosphatases such as PP1, PP2A and PP2B, respectively (Bao J 1994; Bao J 1995; Wei J 2004). Moreover, in *drosophila* neurons, intracellular Ca^{2+} elevation was shown to regulate GABA expression by a mechanism down-stream of GAD translation (Küppers B 2003). GAD 67 is activated upon dephosphorylation, whereas GAD 65 is activated upon phosphorylation (Wei J 2004). GAD 65 is membrane and vesicle associated and is responsible for vesicular GABA release, whereas GAD 67 is cytoplasmic and maintains a cytosolic pool of GABA (Waagepeterson HS 2001). Thus, the dual-regulation hypothesis for regulation for GABA expression by PKA and PKC in striatal NPC cultures could be as follows: basal activity of PKA and PKC under normal physiological conditions, presumably regulated by the spontaneous VGCC-mediated Ca^{2+} influx, phosphorylates and inactivates GAD 67 (Fig 4.3). This prevents GABA production by GAD 67 and pre-mature GABA expression in neurons arising from striatal NPCs. PKA and PKC inhibitors remove PKA and PKC mediated inhibition and increase active GAD 67 that increases GABA expression (referred to as GABA 1) (Fig 4.3). Increases in active PKA and PKC achieved by either forskolin or depolarization on the other hand phosphorylates and activates GAD 65 that in-turn increases GABA (referred as GABA 2) (Fig 4.3)

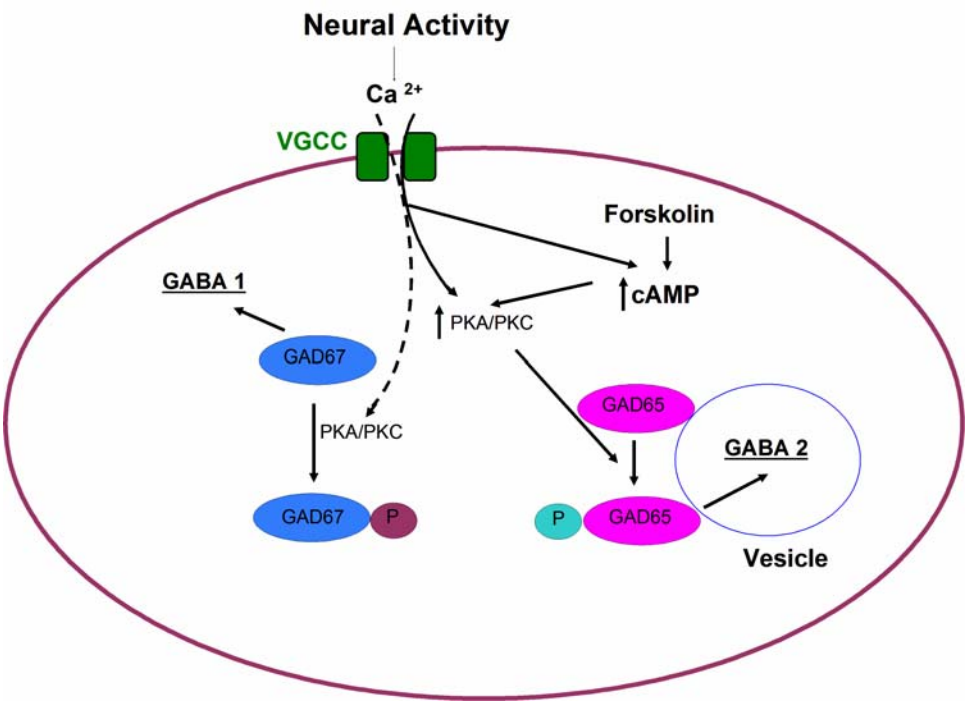

Figure 4.3: Proposed dual regulation of GAD 65 and GAD 67 by PKA and PKC

The cartoon demonstrates the mechanism of dual regulation of GABA expression under control and depolarizing conditions. Under normal physiological conditions, basal PKA/PKC activity that might be regulated by spontaneous VGCC-mediated Ca^{2+} influx (dashed arrow for small Ca^{2+} influx), phosphorylates and inactivates GAD 67 that prevents pre-mature expression of cytosolic GABA (GABA 1). On the contrary, depolarization-mediated Ca^{2+} influx (solid arrow for large Ca^{2+} influx) and forskolin, increase active PKA and PKC levels that now phosphorylate and activate GAD 65 leading to increase in vesicular GABA pool (GABA 2).

4.5.2: Depolarization promotes GABA expression only in neurons committed to GABAergic fate

In an attempt to determine the specificity of depolarization-induced GABA expression, I found that the percentage of GABA positive neurons following depolarization was comparable to the percentage of neurons that acquire

GABA at later stages of differentiation in striatal and cortical NPCs. Thus, depolarization does not alter the final percentage of GABAergic neurons arising from differentiation of NPCs, and acts specifically to accelerate GABA expression. These results were contrary to the recent findings in *Xenopus*, where during neural tube development modulation of the frequency of Ca^{2+} transients by neuronal activity caused neurons to express inappropriate neurotransmitters without altering the expression of cell surface markers (Borodinsky LN 2004). Increasing the frequency of Ca^{2+} transients caused neurons to acquire inhibitory neurotransmitters (GABA and glycine), whereas decreasing the frequency of Ca^{2+} transients had an opposing effect causing neurons to acquire excitatory neurotransmitters (glutamate and acetylcholine) (Borodinsky LN 2004). The adult mammalian brain receives various excitatory and inhibitory signals at all times. My results suggest that the neural activity in the brain regulates differentiation of the neurons, however it does not alter the neurotransmitter type expressed. This is important because regulation of neuronal differentiation by neural activity allows the NPCs to differentiate into mature neurons and integrate into neuronal networks. However, if neural activity would alter the identity of neurons differentiating from NPCs by changing the neurotransmitter they express, the function of these newly born neurons will be altered and they will continue to function abnormally even after withdrawal of the stimuli, most likely leading to malfunctioning of the mammalian brain.

Chapter 5 : Outlook

5.1: Dissecting the signaling pathway that promotes neurite outgrowth following depolarization

The present study aimed at exploring the role of neural activity in regulating neuronal differentiation of NPCs. Depolarization enhanced differentiation of neurons by promoting GABA expression and neurite outgrowth. Interestingly, GABA expression and neurite outgrowth were found to be regulated by distinct signaling pathways. Depolarization enhanced neurite outgrowth via activation of MAPK and CaMK pathways and also involved sAPP. A model based on these results for the regulation of neurite outgrowth by depolarization is proposed in section 4.3.1. and Fig 4.2. Although the present study, as well as previous work, has shown that the neurite outgrowth-promoting effect of depolarization requires NMDAR, MAPK and CaMK activation and is blocked when sAPP or its production is blocked, it is not clear whether MAPK/CaMK are upstream of sAPP or downstream. Further experiments with pharmacological modulators will help investigate this in more detail.

5.2. Functional significance of L-type VGCC-mediated Ca^{2+} transients

Neurons differentiating from NPCs showed L-type VGCC-mediated Ca^{2+} transients that increased with depolarization. Depolarization also promoted GABA expression, an effect that was triggered by a single pulse of Ca^{2+} influx through VGCCs. Therefore, the increase in GABA expression was not related to the frequency of L-type VGCC-mediated Ca^{2+} transients. Hence, the functional significance of spontaneous and evoked L-type VGCC-mediated Ca^{2+} transients remains unclear. However, as shown by experiments performed in Ca^{2+} free medium, extracellular Ca^{2+} is essential for normal differentiation of striatal

NPCs and might regulate acquisition of GABA phenotype under normal physiological conditions. Thus, it is possible that spontaneous Ca^{2+} influx through L-type VGCCs might be involved in regulating striatal NPC neurogenesis at several stages such as proliferation, survival and differentiation as found in cortical and hippocampal NPCs (Deisseroth K 2004; D'Ascenzo M 2006). This can be investigated in long-term experiments where proliferating and/or differentiating neural precursors should be exposed to L-type VGCC agonists and antagonists.

5.3: Confirmation of dual-regulation model for GABA expression

Here I have shown that membrane depolarization induces Ca^{2+} influx through VGCCs that triggers rapid post-translational changes that in-turn promote GABA expression. The pharmacological modulation of signaling pathways performed in this study provide evidence that PKA and PKC regulate GABA expression in an opposite manner under normal physiological conditions and when exposed to depolarization stimuli, suggesting that they act on distinct targets under unstimulated and depolarization conditions. These results are in-line with the literature where it has been shown that PKA and PKC regulate GABA expression by modulating activity of two GABA-synthesizing enzymes, GAD 65 and GAD 67 (Wei J 2004). GAD 65 and GAD 67 are differentially localized within the cell and are responsible for synthesizing distinct pools of GABA. GAD 65 is membrane associated and maintains vesicular pool of GABA (referred as GABA 2 in Fig 4.3), whereas GAD 67 is cytosolic and maintains cytosolic pool of GABA (referred as GABA 1 in Fig 4.3) (Wei J 2004). Taken together, my results and data from the literature point towards the dual-regulation hypothesis for GABA expression as discussed in section 4.5.1 and

Fig 4.3. This hypothesis can be confirmed by performing experiments designed to look at GAD 65 and GAD 67 individually. One way to look at this is by electron microscopy. Electron microscopy will allow one to visualize any changes in vesicular GABA (increase or decrease in the number of vesicles) following depolarizing stimuli. It is known that depolarizing the cells in the presence of tiagabine, a nontransportable inhibitor of plasma membrane GABA carriers, selectively induces release of the vesicular GABA pool and treatment with NMDA in the presence of AMPA causes reversal of GABA carrier and release of cytosolic GABA (Waagepeterson HS 2001). Experiments designed to selectively release vesicular or cytosolic GABA in the presence of antagonists or agonist of PKA and PKC will provide further insight into the mechanism of dual-regulation of GABA expression by these kinases.

References:

Alvarez-Buylla A, Garcia-Verdugo JM,Tramontin AD (2001). "A unified hypothesis on the lineage of neural stem cells." Nature Reviews Neuroscience 2(April): 287-29

Bading H (2000). "Transcription-dependent neuronal plasticity: The nuclear calcium hypothesis." European J. Biochem. 267: 5280-5283.

Bao J, Cheung WY, Wu JY (1995). "Brain L-glutamate decarboxylase. Inhibition by phosphorylation and activation by dephosphorylation." J. Biol. Chem. 270: 6464-6467.

Bao J, Nathan B, Hsu CC, Zhang Y, Wu R, Wu JY (1994). "Role of protein phosphorylation in regulation of brain L-glutamate decarboxylase activity." J. Biomed. Sci 1: 237-244.

Behar TN, Schaffner AD, Scott CA, Greene CL, Barker JL (2000). "GABA receptor antagonists modulate postmitotic cell migration in slice cultures of embryonic rat cortex." Cereb Cortex 10: 899-909.

Behar TN, Smith SV, Kennedy RT, Mckenzie JM, Maric I, Barker JL (2001). "$GABA_B$ receptors mediate motility signals for migrating embryonic cortical cells." Cereb Cortex 11: 744-753.

Berridge MJ, Bootman MD, Lipp P (1998). "Calcium- a life and death signal." Nature 395: 645-648.

Berridge MJ, Bootman MD, Roderick HL (2003). "Calcium signalling:dynamics, homeostasis and remodelling." Nature Reviews Molecular Cell Biology 4(July): 517-529.

Borodinsky LN, Root C, Cronin JA, Sann SB, Gu X, Spitzer NC (2004). "Activity-dependent homeostatic specification of transmitter expression in embryonic neurons." Nature 429(June): 523-530.

Caille I, Allinquant B, Dupont E, Bouillot C, Langer A, Müller U, Prochiantz A (2004). "Soluble form of amyloid precursor protein regulates proliferation of progenitors in the adult subventricular zone." Development and disease 131: 2173-2181.

Cameron HA, McEwen B, Gould E (1995). "Regulation of Adult Neurogenesis by Excitatory Input and NMDA Receptor Activation in the Dentate Gyrus." J Neuroscience June(15(6)): 4687-4692.

Carey MB, Matsumoto SG (1999). "Spontaneous calcium transients are required for neuronal differentiation of murine neural crest." Developmental Biology 215: 289-313.

Catterall WA (2000). "Structure and regulation of voltage-gated Ca^{2+} channels." Ann. Rev Cell Dev Biol 16: 521-555.

Ciccolini F, Collins TJ, Sudhoelter J, Lipp P, Berridge MJ, Bootman MD (2003). "Local and Global Spontaneous Calcium Events Regulate Neurite Outgrowth and Onset of GABAergic Phenotype during Neural Precursor Differentiation." The Journal of Neuroscience 23(1): 103-111.

Ciccolini F, Svendsen CN (1998). "Fibroblast growth factor 2 (FGF-2) promotes acquisition of epidermal growth factor (EGF) responsiveness in mouse striatal precursor cells: identification of neural precursors responding to both EGF and FGF-2." Journal of Neuroscience 18: 7869-7880.

D'Ascenzo M, Piacentini R, Casalbore P, Budoni M, Pallini R, Azzena GB, Grassi Claudio (2006). "Role of L-type Ca^{2+} channels in neural stem/progenitor cell differentiation." European Journal of Neuroscience 23: 935-944.

Deisseroth K, Singla S, Toda H, Monje M, Palmer TD, Malenka RC (2004). "Excitation-Neurogenesis Coupling in Adult Neural Stem/Progenitor Cells." Neuron 42(May): 535-552.

Doetsch F, Caille I, Lim DA, Garcia-Verdugo JM, Alvarez-Buylla A, (1999). "Subventricular zone astrocytes are neural stem cells in the adult mammalian brain." Cell 97: 703-716.

Finkbeiner S, Greenberg M (1998). "Ca^{2+} channel-regulated neuronal gene expression." J Neurobiology 37: 171-189.

Gage FH (2000). "Mammalian neural stem cells." Science February(287(5457)): 1433-1438.

Giachino C, De Marchis S, Giampietro C, Parlato R, Perroteau I, Schütz G, Fasolo A, Peretto P (2005). "cAMP Response Element Binding Protein regulates differentiation and survival of newborn neurons in the olfactory bulb." Journal of Neuroscience 25(44): 10105-10118.

Gould E, Tanapat P, Rydel T, Hastings N (2000). "Regulation of hippocampal neurogenesis in adulthood." Biol. Psychiatry 48: 715-720.

Gu X, Spitzer NC (1995). " Distinct aspects of neuronal differentiation encoded by frequency of spontaneous Ca^{2+} transients." Nature 375(June): 784-787.

Hansen TVO, Rehfeld J, Nielsen FC (2003). "KCl potentiates forskolin-induced PC12 cell neurite outgrowth via protein kinase A and extracellular signal-regulated kinase signaling pathways." Neuroscience Letters 347(August): 57-61.

Hayashi Y, Kashiwagi K, Ohta J, Nakajima M, , Kawashima T, Yoshikawa K (1994). "Alzheimer amyloid protein precursor enhances proliferation of neural stem cells from fetal rat brain." Biochem. Biophys. Res. Commun. 205: 936-943.

Hung AY, Koo EH, Haass C, Selkoe DJ (1992). "Increased expression of beta-amyloid precursor protein during neuronal differentiation is not accompanied by secretory cleavage." PNAS 89: 9439-9443.

Kempermann G, Wiskott L, Gage FH (2004). "Functional significance of adult neurogenesis." Curr. Opin. Neurobiol. 14: 186-191.

Kintner C. (2002). "Neurogenesis in embryos and in adult neural stem cells." Journal of Neuroscience 22(3): 639-643.

Küppers B, Sanchez-Soriana N, Letzkus J, Technau GM, Prokop A (2003). "In developing *Drosophila* neurones the production of γ-aminobutyric acid is tightly regulated downstream of glutamate decarboxylase translation and can be influenced by calcium." Journal of Neurochemistry 84: 939-951.

Kwak YD, Brannen CL, Qu T, Kim HM, Dong Y, Soba P, Majumdar A, Kaplan A, Beyreuther K, and Sugaya K (2006). "Amyloid precursor protein regulates differentiation of human neural stem cells." Stem cells and development 15: 381-389.

Lai HC, Jan LY (2006). "The distribution and targeting of neuronal voltage-gated ion channels." Nature 7(July): 548-562.

Lankford KL and Letourneau PC (1989). "Evidence that calcium may control neurite outgrowth by regulating the stability of actin filaments." J Cell Biology 109.

Leissring M, Murphy M, Mead TR, Akbari Y, Sugarman C, Jannatipour M, Anliker B, Müller U, Saftig P, Strooper BD, Wolfe MS, Golde TE, LaFerla FM "A physiologic signaling role for g-secretase-derived intracellular fragment of APP." PNAS 99: 4697-4702.

Li Y, Jia YC, Cui K, Li N, Zheng ZY, Wang YZ, Yuan XB (2005). "Essential role of TRPC channels in the guidance of nerve growth cones by brain-derived neurotrophic factor." Nature 434: 894-898.

Lledo PM, Alonso M, Grubb MS (2006). "Adult neurogenesis and functional plasticity in neuronal circuits." Nature Reviews Neuroscience 7(March 6): 179-190.

Lois C and Alvarez-Buylla (1994). "A long-distance neuronal migration in the adult mammalian brain." Science 264: 1145-1148.

LoTurco JJ, Owens DF, Heath MJS, Davis MBE, Kriegstein AR (1995). "GABA and Glutamate depolarize cortical progenitor cells and inhibit DNA synthesis." Neuron 15: 1287-1298.

Malatesta P, Hartfuss E, Gotz M (2000). "Isolation of radial glial cells by fluorescent-activated cell sorting reveals a neuronal lineage." Development Dec(127(24)): 5253-63.

Mantamadiotis T, Lemberger T, Bleckmann SC, Kern H, Kretz O, Villalba AM, Tronche F, Kellendonk C, Gau D, Kapfhammer J, Otto C, Schimd W, Schütz G (2002). "Disruption of CREB function in brain leads to neurodegeneration." Nature Genetics 31(May 2002): 47-54.

Mattson MP (1997). "Cellular Actions of b-Amyloid Precursor Protein and Its Soluble and Fibrillogenic Derivatives." Physiol Rev October(77): 1081-1115.

Mattson MP (2004). "Pathways towards and away from Alzheimer's disease." Nature 430(August): 631-639.

Mills J, Reiner PB (1999). "Regulation of amyloid precursor protein cleavage." J Neurochem 72: 443-460.

Mizoguchi Y, Nabekura J (2003). "Sustained intracellular Ca^{2+} elevation induced by a brief BDNF application in rat visual cortex neurons." Neuroreport 6: 1481-1483.

Mizuguchi R, Sugimori M, Takebayashi H, Kosako H, Nagao M, Yoshida S, Nabeshima Y, Shimamura K, Nakafuku M (2001). "Combinatorial roles of olig 2 and neurogenin 2 in the coordinated induction of pan-neuronal and subtype-specific properties of motor neurons." Neuron 31: 757-771.

Morshead CM (2004). "Adult neural stem cells: attempting to solve the identity crisis." Dev Neuroscience 26: 93-100.

Nakagawa S, Kim JE, Malberg JE, Chen J, Steffen C, Zhang YJ, Nestler EJ, Duman RS (2002). "Regulation of Neurogenesis in adult mouse hippocampus by cAMP and the cAMP response element-binding protein." J Neuroscience 22(9): 3673-3682.

Nitsch R, Farber S, Growdon J, Wurtman R (1993). "Release of amyloid b-precursor derivatives by electrical depolarization of rat hippocampal slices." PNAS 90: 5191-5193.

Noctor SC, Flint AC, Weissman TA, Dammerman RS, Kriegstein AR (2001). "Neurons derived from radial glial cells establish radial units in neocortex." Nature Feb(409(6821)): 714-20.

Noctor SC, F. A., Weissman TA, Wong WS, Clinton BK, Kriegstein AR (2002). "Dividing precursor cells of the embryonic cortical ventricular zone have morphological and molecular characteristics of radial glia." J Neuroscience April(22(8)): 3161-3173.

Noctor SC, Martinez-Cerdeno V, Ivic L, Kriegstein AR (2004). "Cortical neurons arise in symmetric and asymmetric division zones and migrate through specific phases." Nature Neuroscience 7: 136-144.

Novitch BG, Chen AI, Jessell TM (2001). "Coordinate regulation of motor neuron subtype identity and pan-neuronal properties by the bHLH repressor Olig2." Neuron 31: 773-789.

Ohsawa I, Takamura C, Morimoto T, Ishiguro M, Kohsaka S (1999). "Amino-terminal region of secreted form of amyloid precursor protein stimulates proliferation of neural stem cells." European J. Neuroscience 11: 1907-1913.

Owens DF and Kriegstein AR (2002). "Is there more to GABA than synaptic inhibition?" Nature Reviews Molecular Cell Biology 3(September): 715-727.

Owens DF, Krigstein AR (1998). "Patters of intracellular calcium fluctuation in precursor cells of the neocortical ventricular zone." Journal of Neuroscience 18: 5374-5388.

Perron JC, Bixby JL (1999). "Distinct Neurite Outgrowth Signaling Pathways Converge of ERK Activation." Molecular & Cellular Neuroscience 13(May): 362-378.

Pla AF, Maric D, Brazer SC, Giacobini P, Chang YH, Ambudkar IS, Barker JL (2005). "Canonical transient receptor potential 1 plays a role in basic fibroblast growth factor (bFGF)/FGFR receptor-1-induced Ca^{2+} entry and embryonic rat neural stem cell proliferation." J Neuroscience May(25(10)): 2687-2701.

Redmond L, Kashani A, Ghosh A (2002). "Calcium regulation of dendritic growth via CaM kinase IV and CREB-mediated transcription." Neuron 34: 999-1010.

Reynolds BA, Weiss S (1992). " Generation of neurons and astrocytes from isolated cells of the adult mammalian central nervous system." Science 255: 1707-1710.

Reynolds BA, Weiss S (1996). "Clonal and population analyses demonstrate that an EGF-responsive mammalian embryonic CNS precursor is a stem cell." Dev Biol 175: 1-13.

Rossjohn J, Cappai R, Feil SC, Henry A, McKinstry WJ, Galatis D, Hesse L, Multhaup G, Beyreuther K, Masters CL (1999). "Crystal structure of the N-terminal growth factor-like domain of Alzheimer amyloid precursor protein." Nature Structural Biology(6): 327-331.

Salbaum JM, Ruddle FH (1994). "Embryonic expression pattern of amyloid protein precursor protein suggests a role in differentiation of specific subsets of neurons." J. Exp. Zool. 269: 116-127.

Schober A, Minichiello L, Keller M, Huber K, Layer PG, Roig-López JL, García-Arrarás JE, Klein R, Unsicker K (1997). "Reduced Acetylcholinesterase (AChE) Activity of Adrenal Medulla and Loss of Sympathetic Preganglionic Neurons In TrkA-Deficient, But Not TrkB-Deficient, Mice." Journal of Neuroscience February(17): 891-903.

Shaywitz AJ, Greenberg M (1999). "CREB: a stimulus-induced transcription factor activated by diverse array of extracellular signals." Annu Rev Biochem 68: 821-861.

Small D, Nurcombe V, Reed G, Clarris H, Moir R, Beyreuther K, Masters C (1994). "A heparin-binding domain in the amyloid precursor of Alzheimer's disease is involved in the regulation of neurite outgrowth." Journal of Neuroscience14: 2117-2127.

Soghomonian J, Martin DL (1998). "Two isoforms of glutamate decarboxylase: why?" TiPS 19: 500-505.

Spitzer NC, Lautermilch NJ, Smith RD, Gomez TM (2000). "Coding of neuronal differentiation by calcium transients." BioEssays 22: 811-817.

Temple S (2001). "The development of neural stem cells." Nature 414(November): 112-117.

Tozuka Y, Fukuda S, Namba T, Seki T, Hisatsune T (2005). "GABAergic Excitation Promotes Neuronal Differentiation in Adult Hippocampal Progenitor Cells." Neuron 47(September): 803-815.

Tucker KL, Martin M, Barde YA (2001). "Neurotrophins are required for nerve growth during development." Nature Neuroscience 4(January 1): 29-37.

Vaillant AR, Zanassi P, Walsh GS, Aumont A, Alonso A, Miller FD (2002). "Signaling mechanisms underlying reversible, activity-dependent dendrite formation." Neuron June: 985-98.

Waagepeterson HS, Sonnewald U, Gegelashvilli G, Larsson OM, Schousboe A (2001). "Metabolic distinction between vesicular and cytosolic GABA in cultured GABAergic neurons using ^{13}C magnetic resonance spectroscopy." Journal of Neuroscience Research 63: 347-355.

Wang GX, Poo MM (2005). "Requirement of TRPC channels in netrin-1-induced chemotropic turning of nerve growth cones." Nature 434: 898-904.

Watt SD, Gu X, Smith RD, Spitzer NC (2000). "Specific frequencies of spontaneous Ca^{2+} transients upregulate GAD 67 transcripts in embryonic spinal neurons." Molecular & Cellular Neuroscience 16: 376-387.

Wayman GA, Kaech S, Grant WF, Davare M, Impey S, Tokumitsu H, Nozaki N, Banker G, Soderling TR (2004). "Regulation of axonal extension and growth cone motility by calmodulin-dependent protein kinase I." Journal of Neuroscience April: 3786-3794.

Wei J, Davis KM, Wu H, Wu JY (2004). "Protein Phosphorylation of Human Brain Glutamic Acid Decarboxylase (GAD) 65 and GAD67 and Its Physiological Implications." Biochemistry 43: 6182-6189.

Weissman TA, Riquelme PA, Ivic L, Flint AC, Krigstein AR (2004). "Calcium Waves Propagate through Radial Glial Cells and Modulate Proliferation in the Developing Neocortex." Neuron 43(September): 647-661.

West AE, Chen WG, Dalva MB, Dolmetsch RE, Kornhauser JM, Shaywitz AJ, Takasu MA, Tao Y, Greenberg ME (2001). "Calcium regulation of neuronal gene expression." PNAS 98(20): 11024-11031.

Xing J, Ginty DD, Greenberg ME (1996). "Coupling of the RAS-MAPK pathway to gene activation by RSK2, a growth factor-regulated CREB kinase." Science 273: 959-963.

Yang B, Gu Q (2005). "Contribution of glutamate receptors to brain-derived neurotrophic factor-induced elevation of intracellular Ca^{2+} levels." Neuroreport 16(9): 977-980.

Zhu DY, Lau L, Liu SH, Wei JS, Lu YM (2004). "Activation of cAMP-response-element-binding protein (CREB) after focal cerebral ischemia stimulates neurogenesis in the adult dentate gyrus." PNAS 101(25): 9453-9457.

Abbreviations:

APP	amyloid precursor protein
APS	ammonium persulfate
Aβ	amyloid β peptide
sAPPα	soluble amyloid precursor protein α
sAPPβ	soluble amyloid precursor protein β
BDNF	brain-derived neurotrophic factor
Ca^{2+}	divalent calcium ion
CaMK	calcium calmodulin dependent kinase
CREB	cAMP response element-binding protein
DAP	days after plating
DAPI	4'-6-Diamidino-2-phenylindole
ERK	extracellular signal-regulated kinase
GABA	γ-amino butyric acid
GAD	glutamic acid decarboxylase
GFAP	glial fibrillary acidic protein
Glu	glutamate
KCl	potassium chloride
KN-62	1-[N,O-*bis*-(5-Isoquinolinesulfonyl)-N-methyl-L-tyrosyl]-4-phenylpiperazine
Mg^{2+}	divalent magnesium ion
NEC	neuroepithelial cell
NMDAR	N-methyl-D-aspartic acid receptor
NPC	neural precursor cell
NSC	neural stem cell
NT-3	neurotrophin 3

NT-4	neurotrophin 4
OAG	1-oleoyl-2-acetyl-sn-glycerol
PKA	cAMP-dependent protein kinase
PKC	calcium and phospholipid-dependent protein kinase
PI	propylene iodide
SDS	sodiumdodecylsulfate
SVZ	subvertricular zone
Tris	(hydroxymethyl) aminomethane
Tuj1	type III tubulin
VGCC	voltage gated calcium channel
VZ	ventricular zone

Acknowledgements:

I would like to express sincere appreciation for my advisor, Dr. Francesca Ciccolini, for her kind support and guidance throughout this study. I thank her for scientific discussions during the research work and preparation of this thesis. I thank Dr. Peter Bengtson, Dr. Tiziana Cesseti and Ms. Kirsten Obernier for helping me initially with imaging experiments and for enlightening scientific discussions. It would have not been possible without the help and encouragement of all the wonderful lab members to complete this dissertation, thanks!! I would also like to thank Dr. K. Tucker, Dr. R. Parlato and Prof. G. Schütz for kindly providing transgenic mice for this study. Also many thanks to Prof. Dr. Hilmar Bading and Prof. Dr. Klaus Unsicker for supervising this dissertation. Last but not the least; I sincerely thank GK 791 for the funding.

I wish to express my heartfelt gratitude towards my parents for all their love and encouragement that gave me strength to pursue my education so far from home and family. I lack words to thank my brother for always being there for me, I am glad to have you near me. My future, my fiancé, thanks for being what you are; most loving, supportive and unimaginably amazing!! I also want to remember all my great pals in Heidelberg, who made my stay and work here enjoyable. Thank you Devraj, Vicky and Carmen for all the good times.

Above all, I thank God for blessing me with a wonderful life.